Disruption of Intestinal Th17 Signaling & the Microbiome Exacerbates Extra-Intestinal Pathologies

by

Patricia Andrea Concepcion Castillo

Bachelor of Science, University of Maryland, Baltimore County, 2012

Submitted to the Graduate Faculty of

School of Medicine in partial fulfillment

of the requirements for the degree of

Doctor of Philosophy

University of Pittsburgh

2019

UNIVERSITY OF PITTSBURGH

SCHOOL OF MEDICINE

This dissertation was presented

by

Patricia Andrea Concepcion Castillo

It was defended on

August 14, 2019

and approved by

Jennifer Bomberger, Associate Professor, Microbiology & Molecular Genetics

Timothy W. Hand, Assistant Professor, Pediatrics and Immunology

Mandy J. McGeachy, Associate Professor, Medicine and Immunology

Anuradha Ray, Professor, Immunology

Dissertation Director: Jay K. Kolls, Professor, Medicine and Pediatrics

Disruption of Intestinal Th17 Signaling & the Microbiome Exacerbates Extra-Intestinal Pathologies

Patricia Andrea Concepcion Castillo, PhD

University of Pittsburgh, 2019

IL-17 signaling to the intestinal epithelium is a critical regulator of the intestinal microbiome. There is a growing body of research linking alterations in both Th17 cells and the intestinal microbiome to extra-intestinal pathologies including hepatitis and neuroinflammation. For example, many patients with autoimmune, fulminant, and viral hepatitis exhibit increased systemic IL-17, and *Il17ra*$^{-/-}$ mice are protected in concanavalin A (Con A)-induced hepatitis, a murine model of immune-mediated hepatitis. In Multiple Sclerosis (MS), elevated IL-17 was found in CNS lesions, and disrupted Th17 differentiation in mice ameliorates disease in the experimental autoimmune encephalomyelitis (EAE) mouse model of MS. In addition, many patients with hepatitis and MS display an altered intestinal microbiome, and germ-free mice as well antibiotic-treated mice have decreased disease in Con A hepatitis and EAE. Despite these data, few studies have investigated how the relationship between enteric Th17 cells and the microbiome influences extra-intestinal pathologies.

Based on these reported links, we hypothesized that intestinal IL-17R signaling plays a critical role in mitigating hepatic and neuroinflammation. To test this, we generated intestinal epithelial specific IL-17RA knockout mice (*Il17ra*$^{fl/fl}$ x *villin cre*$^{+}$ mice). Because enteric Th17 signaling regulates the commensal microbiota, these mice exhibited an altered intestinal microbiome along with a subsequent expansion of intestinal Th17 cells. We then tested these mice in the Con A hepatitis model and EAE neuroinflammation model.

Our results showed that perturbation of intestinal IL-17RA signaling was sufficient to exacerbate both liver and neuroinflammation in a microbiome-dependent manner. Abrogation of intestinal IL-17RA disrupted the intestinal microbiota and promoted translocation of bacterial products to the liver. Together, this induced IL-18 production and subsequent lymphocyte activation and cell death to worsen hepatitis. In EAE, intestinal IL-17RA deficiency induced intestinal dysbiosis and increased intestinal *Il17* and *Csf2* and systemic responses in both cytokines. Preliminary data suggested a potential increase of inflammatory monocyte infiltration into the CNS, together exacerbating disease. These dissertation studies elucidate the differential role of enteric Th17 cells and the microbiome in extra-intestinal pathologies and more broadly in mucosal immunology. Moreover, it provides insight into novel therapeutic strategies that target the gut-liver and gut-brain axes.

Table of Contents

Preface xiv

1.0 Introduction 1

1.1 Intestinal Th17 Signaling 2

1.1.1 Interleukin 17 (IL-17) and IL-17 Receptor 2

1.1.2 Pathogenic and Non-Pathogenic Th17 Cells 4

1.1.3 Th17 Cells and Maintenance of Intestinal Homeostasis 5

1.2 Intestinal Microbiome 10

1.2.1 Immunogenic Commensal Bacteria 10

1.2.2 Bacterial Mechanisms to Influence Host Immune Responses 11

1.3 Disruption of Th17 Signaling & the Intestinal Microbiome In Disease 14

1.3.1 Intestinal Diseases 14

1.3.2 Extra-Intestinal Diseases 15

2.0 Gut-Liver Axis: Intestinal IL-17R signaling constrains IL-18 driven liver inflammation by the regulation of microbiome-derived products 20

2.1 Introduction 20

2.1.1 Liver Anatomy and Physiology 20

2.1.1.1 Structure and Blood Supply 20

2.1.1.2 Hepatic Portal System 22

2.1.1.3 Function 23

2.1.2 Hepatic Response to Intestinal-Derived Factors 24

2.1.2.1 Initial Cell Responders at the Liver Sinusoids 24

2.1.2.2 Effects of Bacterial Translocation 26

2.1.3 The Intestinal Microbiome & Bacterial Translocation in Liver Disease 30

2.1.4 Th17 Cells in Liver Disease 32

2.1.5 Study Overview 33

2.2 Methods 34

2.2.1 Experimental Model and Subject Details 34

2.2.2 Method Details 35

2.2.3 Quantification and Statistical Analysis 43

2.2.4 Data and Software Availability 46

2.3 Results 46

2.3.1 Deletion of IL-17RA in intestinal epithelium exacerbates Concanavalin A hepatitis. 46

2.3.2 Exacerbated liver injury is dependent on the intestinal microbiota. 49

2.3.3 Intestinal IL-17RA constrains TLR9-induced Type I immune responses in the liver.55

2.3.4 Intestinal IL-17RA constrains hepatic and intestinal IL-18. 63

2.3.5 IL-18-induced FasL exacerbates liver inflammation. 66

2.3.6 Anti-IL18 mitigates liver injury in intestinal IL-17RA-deficient mice. 69

2.4 Discussion 70

2.5 Working Model 80

3.0 Gut-Central Nervous System Axis: Disruption of Intestinal Th17 Signaling and the Microbiome Exacerbate Autoimmune Neuroinflammation 81

3.1 Introduction 81

3.1.1 Overview of Multiple Sclerosis 82

3.1.1.1 Epidemiology 82

3.1.1.2 Disease Manifestations 83

3.1.1.3 Diagnosis 84

3.1.1.4 Prognosis 84

3.1.1.5 Treatment 85

3.1.2 Th17 Cells and the Microbiome in Multiple Sclerosis 87

3.1.2.1 Barriers of the CNS 87

3.1.2.2 Th17 Cells in Multiple Sclerosis 91

3.1.2.3 Intestinal Microbiome in Multiple Sclerosis 93

3.1.3 Study Overview 94

3.2 Methods 95

3.2.1 Experimental Model and Subject Details 95

3.2.2 Method Details 97

3.2.3 Quantification and Statistical Analysis 101

3.2.4 Data and Software Availability 103

3.3 Results 103

3.3.1 Disruption of enteric IL-17RA signaling exacerbates neuroinflammation. 103

3.3.2 Disease in *Il17ra*$^{fl/fl}$ *x villin cre*$^{+}$ mice is microbiome-dependent. 107

3.3.3 *Il17ra*$^{fl/fl}$ *x villin cre*$^{+}$ mice exhibit increased splenic IL-17 responses and increased antigen-specific GM-CSF responses 108

3.3.4 *Il17ra*$^{fl/fl}$ *x villin cre*$^{+}$ disease exacerbation is IL-1β-independent. 111

3.3.5 *Il17ra*$^{fl/fl}$ *x villin cre*$^{+}$ mice have increased intestinal *Ccr2* and *Ccr6* and spinal cord *Nos2* prior to EAE onset. 113

3.4 Discussion 116

3.5 Working Model 125

4.0 Overall Conclusions & Future Directions 126

Bibliography 135

List of Tables

Table 1-1. Experimental Assays Used to Measure Th17 Responses in Current Dissertation Studies 4

Table 1-2. Pathogenic & Non-Pathogenic Th17 Differentiation 5

Table 1-3. Experimental Assays Used to Assess the Microbiome in Current Dissertation Studies 14

Table 2-1. Single Cell RNAseq Cluster Gene Lists. 56

Table 3-1. 2017 McDonald Criteria 84

Table 3-2. Disease-Modifying Therapies Approved for MS 86

List of Figures

Figure 1-1. Intestinal Th17 Cells Contribute to the Mucosal Firewall. 7

Figure 1-2. Diseases w/ Evidence Implicating Th17 cells & the Intestinal Micrbiome 16

Figure 2-1. Liver Anatomy 21

Figure 2-2. Deletion of IL-17RA in intestinal epithelium exacerbates Concanavalin A hepatitis. 48

Figure 2-3. Exacerbated liver injury is dependent on the intestinal microbiota. 50

Figure 2-4. *Il17ra*$^{fl/fl}$ *x villin cre*$^{+}$ mice have an increased fecal bacterial burden, enriched with neomycin-sensitive, IgA-unbound bacteira. 52

Figure 2-5. *Il17ra*$^{fl/fl}$ *x villin cre*$^{+}$ mice do not have elevated serum or liver LPS. 54

Figure 2-6. CpG DNA promotes fatal Con A hepatitis. 54

Figure 2-7. Intestinal IL-17RA constrains TLR9-induced Type I immune responses in the liver. 58

Figure 2-8. Cohousing eliminates differences in liver IFNγ between *Il17ra*$^{fl/fl}$ *x villin cre*$^{+}$ mice and floxed controls. 60

Figure 2-9. CD4 and CD8 T cells comprise the majority of IFNγ+ cells following CpG DNA stimulation. 62

Figure 2-10. Intestinal IL-17RA constrains hepatic and intestinal IL-18. 64

Figure 2-11. IFNγ blockade did not ameliorate hepatitis in *Il17ra*$^{fl/fl}$ *x villin cre*$^{+}$ mice. 66

Figure 2-12. *Fasl* is expresed by liver T cells, NK cells, and NKT cells. 67

Figure 2-13. IL-18-induced Fasl exacerbates liver inflammation. 68

Figure 2-14. Cohousing eliminated liver FasL differences between *Il17ra*$^{fl/fl}$ *x villin cre*$^{+}$ mice and floxed controls. 69

Figure 2-15. Anti-IL18 mitigates liver injury in intestinal Il17RA deficient mice. 70

Figure 2-16. Liver IL-17 is not increased in *Il17ra*$^{fl/fl}$ *x villin cre*$^{+}$ mice at the naïve state or 5h-post Con A. 72

Figure 2-17. Naïve *Il17ra*$^{fl/fl}$ *x villin cre*$^{+}$ mice do not exhibit baseline intestinal barrier defects. 74

Figure 2-18. TLR9 ligands in *Il17ra*$^{fl/fl}$ and *Il17ra*$^{fl/fl}$ *x villin cre*$^{+}$ liver homogenate are DNase-resistant. 75

Figure 2-19. Excess intestinal IL-18 partnered with decreased systemic IL-18 control exacerbate hepatitis. 76

Figure 2-20. Liver mononuclear cells from naïve *Il17ra*$^{fl/fl}$ *x villin cre*$^{+}$ exhibit increased IFNγ upon *ex vivo* stimulation. 78

Figure 2-21. Working Model 80

Figure 3-1. CNS Barriers 89

Figure 3-2 Disruption of enteric IL-17RA signaling exacerbates neuroinflammation. 105

Figure 3-3. Moderately exacerbated EAE in *Il17rc*$^{fl/fl}$ *x villin cre*$^{+}$ mice is microbiome-dependent. 106

Figure 3-4. Disease in *Il17ra*$^{fl/fl}$ *x villin cre*$^{+}$ mice is microbiome-dependent. 108

Figure 3-5 *Il17ra*$^{fl/fl}$ *x villin cre*$^{+}$ mice exhibit increased splenic IL-17 responses and increased antigen-specific GM-CSF responses..... 110

Figure 3-6 *Il17ra*$^{fl/fl}$ *x villin cre*$^{+}$ disease exacerbation is IL-1β-independent. 112

Figure 3-7 *Il17ra*$^{fl/fl}$ *x villin cre*$^{+}$ mice have increased intestinal *Ccr2* and *Ccr6* and spinal cord *Nos2* prior to EAE onset. 115

Figure 3-8. *Il22ra2*$^{-/-}$ mice are protected from EAE. 119

Figure 3-9. Terminal ileum tight junction protein gene expression at day 9 post EAE immunization. 123

Figure 3-10. Working Model 125

Preface

These past four years have undoubtedly been a trying but immensely rewarding journey. As the saying goes, it takes a village. Therefore, to start this dissertation, I first want to acknowledge all the individuals who brought me to where I am today.

I would first like to thank my mentor, Dr. Jay Kolls for his guidance, support, and overall scientific brilliance that he has shared and offered to me throughout my PhD training. This partnered with our weekly in-depth discussions of the science and data allowed me to develop my skills as an independent researcher. Though I rarely vocalized this, I always counted it as a "win" when I came to the same experimental ideas and next steps as Dr. Kolls. While he would often come to these conclusions 1000x faster, I was gratified to know my scientific thinking was progressing toward that of a successful physician-scientist like himself. He has been a great role model for what a career as a successful physician-scientist can look like. Even through the move of the Kolls lab to Tulane, Dr. Kolls maintained his unwavering support and commitment to my training, and for all of this I am truly grateful.

I would also like to thank my second mentor, Dr. Timothy Hand, who kindly adopted me into the Hand Lab for the past two years. My thesis work falls at the intersection of Th17 immunology and the intestinal microbiome. As such, moving into the Hand Lab was a great fit. Dr. Hand's expertise in the field, valuable mentorship advice, enthusiasm for the work, and daily support have greatly benefited my research and development as a young scientist. Therefore, far from being a detriment to my training, being in both the Kolls and Hand labs has afforded me the opportunity to learn from two outstanding mentors and learn in incredibly rich and welcoming laboratory environments.

I would like to acknowledge laboratory members of the Kolls and Hand labs as well. Dr. Taylor Eddens and Dr. Waleed Elsegeiny were former graduate students in the Kolls lab that were always willing to assist and answer the many questions I had as a new (and not so new) PhD student. I sincerely thank them for their patience and friendship. I would also like to thank Dr. Pawan Kumar, who helped develop the groundwork for the projects detailed within this dissertation, as well as Dr. Kong Chen and Dr. Giraldina Trevejo for their invaluable support in my training. A big thank you the other past and present members of the Kolls lab including Kara Kracinovski and William Horne who always offered a helping hand, and Alanna Wanek who contributed largely to the sequencing studies described in this work. To the members of the Hand Lab—Ansen Burr, Dr. Abby Overacre-Delgoffe, Dr. Kathy Gopalakrishna, Justin Tometich, and Dr. Amrita Bhattacharjee, thank you for warmly welcoming me into the lab with huge smiles and an equal if not greater passion for all things related to mouse stool. The lab environment fostered by these two groups over the years was indispensable to my scientific training, sanity, and overall joy throughout my PhD.

In addition to the Kolls and Hand labs, I would like to thank the other members of my thesis committee—Dr. Jennifer Bomberger, Dr. Mandy McGeachy, and Dr. Anuradha Ray. Their insightful suggestions regarding my thesis work have advanced and shaped this dissertation immensely. Beyond that, all of them are models of successful women in science. In a field still predominantly male, I believe it is important for trainees to see individuals who look like them accomplish similar future goals. A big thank you to the neighboring labs in Rangos as well—the Campfield, Canna, and Poholek Labs, all of whom contributed to building an enriching lab environment. I would also like to thank the Pitt-CMU MSTP and Dr. Steinman for the ongoing support as well as giving me the privilege to pursue my MD/PhD at this institution. I would also

like to acknowledge the Meyerhoff Program at the University of Maryland, Baltimore County, though which I attained the research experiences and encouragement that shaped my desire to pursue an MD/PhD.

Last but definitely not least, I would like to thank all of my family and friends who were essential to my success. I would like to specifically acknowledge my parents, Antonio and Leila Castillo, for their constant love, support, and prayers throughout this journey. I would truly not be where I am today without the examples they set for me, the belief they have in my capabilities, and their constant encouragement to be better and seize the opportunities we came to the United States for. Finally, I would like to thank my husband, Kc dela Cruz. In the midst of all the uncertainty research brings and more broadly in this career path I have chosen, he has been a constant source of love, support, and laughs throughout these many years. I cannot express my thanks enough.

1.0 Introduction

Parts of this introduction have been adapted from the publication:

Castillo, P. A. C., and T. W. Hand. 2018. A little fiber goes a long way. Immunity 48: 844–846.

One of the underlying drivers of this work was the idea that the immunologic interaction between different organ systems and how this impacts health and disease is an understudied but critical avenue by which to advance science. As such, the projects detailed within this dissertation investigate the gut-liver and gut-central nervous system axes in the context of liver and neuro-inflammation. This focus stemmed from the rapidly growing body of literature describing how the intestinal microbiome had implications beyond the gut. In addition, ongoing research in laboratories including the Kolls lab were showing that the intestinal microbiome actually had a reciprocal regulatory relationship with T helper 17 (Th17) cells, a subset of T helper cells implicated in a wide range of diseases. The synthesis of these findings led to the overarching hypothesis of this thesis—Disruption of intestinal Th17 signaling and subsequent effects on the microbiome contribute to extra-intestinal pathologies.

1.1 Intestinal Th17 Signaling

1.1.1 Interleukin 17 (IL-17) and IL-17 Receptor

IL-17 and IL-17 receptor A (IL-17RA) were first cloned over two decades ago by Rouvier et al. and Yao et al., respectively (1, 2). This ultimately led to the identification of a new class of T helper (Th) cells, Th17 cells, that was separate from the established Th1/Th2 lineages (3). Identification of Th17 cells as a distinct subset was prompted by the observation that the Th1/Th2 dichotomy could not fully explain inconsistencies observed in some autoimmune and infectious pathologies (3). Almost 10 years since the discovery of IL-17, data from multiple labs showed that specific cytokines including IL-23, TGFβ, IL-21, and IL-6 could promote Th17 differentiation (4–10). Concurrently, Th17 master transcription factor retinoic acid-related orphan receptor gamma T (Rorγt) was identified and found to be mediated by STAT3 (11–14). Since the initial discovery of the founding ligand: receptor relationship, five IL-17R family members (IL-17RA-E) and six ligands (IL-17A-F) have been identified (15). The first ligand and receptor cloned, IL-17A and IL-17RA, are the most well described and are a larger focus of these studies.

IL-17RA is a type I transmembrane protein with a 293 amino acid extracellular domain, 21 amino acid transmembrane domain, and a 525 amino acid cytoplasmic tail (2). It functions in multimeric complexes, such as a multimeric complex with IL-17RC and itself and a dimeric complex with IL-17RB or IL-17RD (15). It remains undetermined whether these receptors reside on the surface as monomers and form complexes in a ligand-dependent manner or if they reside on the surface as preformed complexes independent of ligand (15). IL-17RA is ubiquitously expressed in many tissues. mRNA expression was identified in the intestine, lung, spleen, and kidney (12). At the cellular level, expression was observed in leukocytes, epithelium, endothelium,

fibroblasts, and some myeloid cells (2, 12, 13). While *Il17ra* expression is observed in hematopoietic cells, most functional effects of IL-17A and IL-17F through IL-17RA have largely been documented in non-hematopoietic cells such as the epithelium (15, 16). This is indeed one reason why the following dissertation studies targeted IL-17R signaling specifically in the intestinal epithelium as a means to investigate role of IL-17R signaling in the intestine.

IL-17A is a 155 amino acid, disulfide-linked homodimeric glycoprotein (2). It is capable of signaling through IL-17RA and IL-17RC as a homodimer or heterodimer with IL-17F, which shares over 40% homology with IL-17A (12, 15). However, the affinity of the IL-17A homodimer for the IL-17R receptor is greater than that of the IL-17A-F heterodimer or IL-17F homodimer (17). Similar to the receptor, *Il17a* is expressed by multiple cell types including T cells, NK cells, innate lymphoid cells, and lymphoid tissue inducer cells (15, 18).

Activation of the IL-17R by IL-17 induces the NFκβ pathway and alternatively, the C/EBPβ and C/EBPδ pathways (16). Signaling results in transcriptional regulation, such as the induction of *Lcn2* (19), and mRNA stability regulation as with *Cxcl1* and *Cxcl5* (20–22). As such, IL-17 signaling can result in a wide range of downstream inflammatory processes. With this in mind, the general consequences of IL-17 can largely be broken down into five categories: 1. Proinflammatory chemokine release (CXCL9, CXCL10, CCL2, CCL20), 2. Hematopoietic cytokine production (IL-6, TNF, G-CSF, GM-CSF, etc.), 3. Upregulation of acute phase response genes (Serum amyloid A, CRP, Lipocalin), 4. Induction of anti-microbial factors (Defensins, S100 proteins, sIgA, etc.), and 5. Proliferation of epithelial and lymph node stromal cells (16, 23). As expected, these effects can have massive consequences on the immune system and therefore must be regulated.

Table 1-1. Experimental Assays Used to Measure Th17 Responses in Current Dissertation Studies

RNA-based Assays	Protein-based Assays
Quantitative Real Time Polymerase Chain Reaction (qRT-PCR)	Enzyme-linked Immunosorbent Assay (ELISA)
Single Cell RNA sequencing	Luminex
	Flow Cytometry

There are a number of factors upstream of Th17 signaling that help regulate Th17 responses (18). For example, IL-27 has been shown to inhibit IL-17 release and protect against autoimmunity (24, 25). Conversely, IL-21 is a cytokine produced by Th17 cells that promotes Th17 generation in an autocrine fashion (6). IL-23 is required for maintenance of Th17 responses *in vivo* (26), but can also favor more pathogenic Th17 responses as described in the next section (27–29).

1.1.2 Pathogenic and Non-Pathogenic Th17 Cells

More recent work has suggested that Th17 cells can be subcategorized as pathogenic versus non-pathogenic based on cytokine production. While IL-17 is a hallmark cytokine of Th17 cells, these cells also secrete other cytokines such as IL-21, IL-22, IFNγ, and GM-CSF. The more "pathogenic" Th17 cells are characterized by their ability to double produce IL-17 and IFNγ or IL-17 and GM-CSF (28). Different inflammatory milieus support the differentiation of pathogenic and non-pathogenic Th17 cells as seen in Table 1-2 (30).

Table 1-2. Pathogenic & Non-Pathogenic Th17 Differentiation

	Cytokines that promote differentiation of Th17 Cells
Non-Pathogenic	TGFβ1 and IL-6
Pathogenic	1. TGFβ1, IL-6, IL-23 2. TGFβ3, IL-6 3. IL-1β, IL-6, IL-23

TGFβ1 and IL-6 together induce a non-pathogenic Th17 cell while three different combinations have been shown to induce pathogenic Th17 cells: [l] TGFβ1, IL-6, IL-23; [2] TGFβ3, IL-6; [3] IL-1β, IL-6, IL-23(30). These categories have been defined by *in vivo* functional studies where pathogenic Th17 cells were shown to exacerbate disease in the experimental autoimmune encephalomyelitis (EAE) model of MS (30). More specifically, adoptive transfer of naïve myelin oligodendrocyte glycoprotein-specific cells differentiated in the "pathogenic" conditions listed in Table 1-2 resulted in exacerbated disease as compared to disease induction by cells differentiated in non-pathogenic conditions (28). There are now ongoing studies in other diseases such as rheumatoid arthritis investigating the potential role of these "pathogenic" Th17 cells (31). However, these studies are partially biased by the use of systems that are inherently self-reactive. If these cells bore an anti-pathogen specific TCR, it may be the case that "pathogenic" Th17 may be more effective in host defense.

1.1.3 Th17 Cells and Maintenance of Intestinal Homeostasis

It is important to note that while Th17 cells have been subcategorized as pathogenic and non-pathogenic, consequences of Th17 cell activation are contextual and can be detrimental or

beneficial depending on the circumstance. This is because Th17 cell signaling has a wide variety of immune consequences including neutrophil recruitment, chemokine release, and more. In the context of these studies, a major interest in its function lies in the role of Th17 cells in maintaining intestinal homeostasis.

The intestine is a very complex dynamic environment that must be able to balance tolerogenic and inflammatory responses to an array of antigens, both external and otherwise. There is constant exposure to food antigens, external pathogens, and the intestinal microbiota, comprising of the more than 10^{14} microbes inhabiting the intestine (32). While the microbiome will be discussed in more detail later, it is important to note that the microbiota are key drivers of T cell development in the intestinal lamina propria. Indeed, germ-free mice exhibit decreased lamina propria lymphocytes (33). However, left uncontrolled, the microbiota can have detrimental effects. Therefore, the body has built a "mucosal firewall" to help regulate and contain the microbiota and aforementioned factors to promote intestinal homeostasis (Figure 1-1) (34). Evidence suggests that the most immunogenic bacteria are those that gain access to the epithelial layer (35). Indeed, known immunogenic bacteria segmented filamentous bacteria (Sfb) actually require adhesion to the intestinal epithelium to exert its effects (36). The mucosal firewall helps prevent access to the host through the physical intestinal epithelium as well as the overlying mucus layer, antimicrobial peptides, and secretory IgA (34). Actions of IL-17 and IL-22, another hallmark Th17 cytokine, on the intestinal epithelium contribute largely to these elements.

IL-22 is an IL-10 family member produced by numerous cells types including T cells, NK cells, and ILCs (37). It signals through a dimeric receptor complex comprised of IL-22RA1 and IL-10R2 (38). While IL-22RA1 is localized on other cell types such as hepatocytes, within the

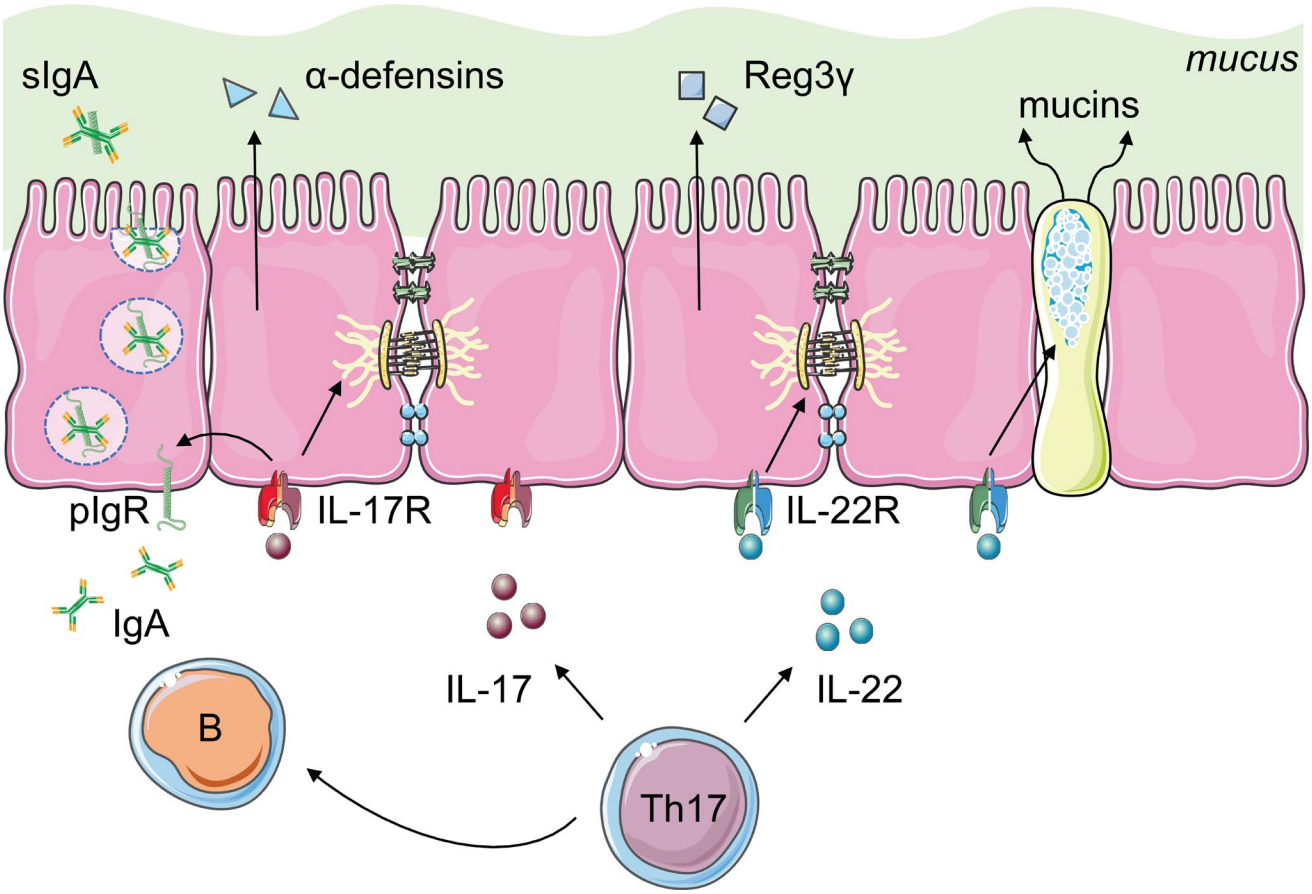

Figure 1-1. Intestinal Th17 Cells Contribute to the Mucosal Firewall.

Intestinal T helper 17 (Th17) cells contribute to the mucosal firewall in multiple ways. Production of interleukin 17 (IL-17) and binding of IL-17 to the IL-17 receptor (IL-17R) promote polymeric immunoglobulin receptor (pIgR) expression, which transports dimeric IgA from B cells across the intestinal epithelium to be secreted into the intestinal lumen as secretory IgA (sIgA). Interleukin 22 (IL-22), another hallmark Th17 cytokine, binds to the IL-22 receptor (IL-22R) on the intestinal epithelium to promote mucin production by goblet cells. In addition, both IL-17 and IL-22 affect tight junction proteins between enterocytes and promote antimicrobial peptide release, specific examples including alpha defensins (α-defensins) and Regenerating islet-derived 3 gamma (Reg3γ), respectively. **Images adapted from Servier Medical Art by Servier. Original images are licensed under a Creative Commons Attribution 3.0 Unported License (https://creativecommons.org/licenses/by/3.0/legalcode).*

intestine, the IL-22RA1 subunit is limited to the epithelial cells, restricting the consequences of enteric IL-22 signaling to the intestinal epithelium (39).

There are data *in vivo* and *in vitro* demonstrating that IL-17 and IL-22 regulate intestinal barrier integrity. IL-17 affects tight junction complexes between enterocytes through alterations of tight junction proteins such as occludens (40). Specifically, in a mouse model of acute intestinal injury, IL-17 from gamma delta T cells contributed to barrier integrity in an IL-23-independent manner (40). Conversely, IL-22 has been shown to alter intestinal permeability by promoting *Claudin 2* expression in the intestinal epithelium through the JAK/STAT pathway (41). *In vitro* treatment of Caco2 cells with IL-22 in a transwell system reduced transepithelial resistance, suggesting that IL-22 enhances permeability of colonic epithelial cells (41). In addition to affecting tight junctions, there is also evidence in a mouse model of colitis showing that IL-22 enhances mucus production from goblet cells, thereby fortifying the mucus barrier above the enterocytes (42). Moreover, IL-22 supports intestinal epithelial stemness independent of Paneth cells to induce epithelial regeneration and maintain barrier integrity (43).

Beyond the physical intestinal barrier, IL-17 and IL-22 induce strong antimicrobial peptide (AMP) responses. Antimicrobial peptides promote bacterial killing by both enzymatically and non-enzymatically targeting cell wall structures and synthesis, as well as assisting with detection and response by the immune system (44). Alpha defensins are a subset of AMPs expressed by small intestinal Paneth cells (44). In mice, they are produced as pro-alpha defensins and stored in intracellular secretory granules where they are cleaved to active alpha-defensins exclusively by matrix metalloproteinase 7 (45). Following exocytosis, alpha-defensins target the bacterial membrane and are critical in maintaining the intestinal microbiota and protecting against bacterial invasion (44). For example, transgenic mice expressing human alpha defensin 5 exhibit baseline

changes in the composition of the intestinal microbiota and are protected against oral Salmonella infection (46, 47). Kumar et al. showed that global knockout of IL-17A and global or intestinal-specific knockout of IL-17RA dramatically decreased alpha defensins in the intestine (48), suggesting that IL-17 regulates intestinal AMPs. Regenerating islet-derived 3 gamma (Reg3γ), another type of intestinal AMP, is a soluble lectin induced by IL-22 (49, 50). Colonization of bacteria into germ-free mice actually induced secretion of Reg3γ into the intestinal lumen where it bound gram-positive bacteria, demonstrating a regulatory relationship between bacteria and host (51). This relationship has implications beyond the intestine as well; McAleer et al. showed that oral supplementation of Reg3γ in *Il22*$^{-/-}$ mice protected them from pulmonary inflammation induced by *Aspergillus fumigatus* (52).

Along with AMPs, immunoglobulin A (IgA) plays a large role in regulating the intestinal microbiota. IgA is secreted into the intestinal lumen through the polymeric immunoglobulin receptor (pIgR) (53). More specifically, dimeric IgA from plasma cells is transported across intestinal epithelial cells through pIgR. Cleavage of pIgR near the apical membrane releases both the secretory component of pIgR and the bound dimeric IgA into the lumen, together forming secretory IgA (sIgA) (53). pIgR is upregulated by Th17 cells *in vivo* (54). Indeed, both global and intestinal-specific knockout of IL-17R resulted in decreased levels of intestinal pIgR and sIgA (48, 54). Moreover, both IgA deficient mice and pIgR knockout mice exhibited an altered commensal microbiome (55, 56). These data suggest that IL-17 also regulates the intestinal microbiome through its role in pIgR expression and sIgA release.

Taken together, these studies demonstrate that intestinal homeostasis is maintained in large part by Th17 hallmark cytokines that reinforce the mucosal firewall. Given this role, it is not surprising that Th17 cell signaling is predominantly involved in constraining microbes residing

close to the intestinal epithelium, thus playing a prominent role in regulating the intestinal microbiome.

1.2 Intestinal Microbiome

As previously mentioned, there are over 10^{14} bacteria residing in the intestine, with increasing bacterial concentrations from the duodenum to the colon (32). The outdated view of the intestinal microbiota was that there were pathogenic and nonpathogenic bacteria. While there are indeed certain pathogens whose presence in the intestine will undoubtedly cause illness, the understanding of the field has moved from a dichotomy of "good versus bad" bacteria to the idea that a "healthy" microbiota is more about balance. Indeed, bacterial diversity indices are common descriptive measures used in microbiome studies with increased diversity often, but not always, correlating with health (57–59). More research is also emerging detailing regulatory mechanisms between the host and microbiome. For example, Sfb induces Th17 cells, which then work to constrain the Sfb population (36, 48, 60). In these ways, balance in terms of both the composition of the microbiota and in host-microbiome interactions is required to maintain intestinal homeostasis.

1.2.1 Immunogenic Commensal Bacteria

There are multiple commensals identified that induce intestinal immune responses. For example, *Clostridia spp.* and *Bacteroides fragilis* have been shown to promote colonic Treg responses (61–64), and Sfb induces small intestinal Th17 responses (48, 60). The resulting effects

of a particular bacterium, however, are often contextual, not only in terms how its immune consequences align with the current health/disease state, but there is also emerging evidence that the immune sequelae of a specific bacterium may actually differ depending on the environment it is in. To illustrate the first point, Sfb colonization of the intestine and subsequent enteric Th17 responses (60) were detrimental in neuroinflammation during EAE (48) but associated with protection against spontaneous diabetes in nonobese mice (65). Toward the second point, there is literature showing that *Helicobacter hepaticus* induces strong Th1-Th17 responses in an *Il10*$^{-/-}$ model of colitis, but induces T regulatory responses during colitis in IL-10 sufficient mice (66). In addition, the commensal *Akkermansia muciniphila* induced T follicular helper responses in mice with an altered Schaedler flora and a complex microbiota, but only induced proinflammatory T effector responses in the latter environment (67). Together, these data illustrate how immune and bacterial signals present in the gut can dictate the resulting responses to bacteria.

1.2.2 Bacterial Mechanisms to Influence Host Immune Responses

Bacteria exert their effects on the host through direct and indirect mechanisms. As mentioned above, many known immunogenic bacteria are located close or adhere to the intestinal epithelium. In addition to Sfb, *Citrobacter rodentium* and *Escherichia coli O157* are examples of microbes that require adhesion to trigger Th17 immune responses. Atarashi et al. showed that these bacteria adhere to the intestinal epithelium and induce immune responses, whereas mutants lacking the ability to adhere could not induce enteric Th17 responses (36). Direct access to the intestinal epithelium allows the bacteria to prompt inflammation through utilization of their own virulence factors such as the type three secretion system in *Salmonella* (68), or via pattern recognition

receptor signaling pathways including those of toll like receptors (TLRs) and the NOD-like receptors (NLRs) (69).

Pattern recognition receptors can also be engaged more distantly from the bacteria due to release of bacterial products such as lipopolysaccharide (LPS) and unmethylated CpG DNA. These products are released during normal bacterial growth, division, and lysis (70, 71). These and other inflammatory mediators can also be released via extracellular vesicles. For example, outer membrane vesicles (OMVs) are a type of bacterial extracellular vesicle produced by gram-negative bacteria through the budding of the bacterial outer membrane along with periplasmic content (72). Bacterial OMVs can carry cargo from the bacteria to more distant sites in the body (72). Data has shown that there are not only differences in the types of cargo encased in these vesicles, but that selection of the cargo is a regulated process (72). As such, OMVs from one bacterium do not necessarily exert the same effects as that of another bacterium. For example, OMVs isolated from *Akkermansia muciniphila,* but not *E. coli*, increased intestinal barrier integrity in Caco2 cells (73). Differential effects in bacterial OMVs have been documented in disease as well—OMVs from *B. fragilis* were protective in experimental colitis (74), while OMVs from *B. theta* were detrimental (75).

Another major mechanism through which bacteria indirectly affect host health and disease is bacterial metabolites. Research over the past decade has shown that short-chain fatty acids (SCFAs) derived from bacterial fermentation of dietary fiber have anti-inflammatory properties (76, 77). Three prominent examples of these SCFAs are acetate, propionate, and butyrate (76). These compounds exert their effects through multiple mechanisms, including the binding of G-coupled Protein receptors, inhibition of Histone deacetylases, and effects on cell metabolism (78). SCFAs are capable of signaling to a variety of immune cells including T cells, neutrophils, and

macrophages. For example, butyrate has been shown to induce colonic Tregs (79). There are also data showing that a high fiber diet and subsequent SCFAs increased $CD8^+$ T cell effector function and altered bone marrow hematopoiesis to increase the differentiation of $Ly6C^{neg}$ patrolling monocytes and alternatively activated macrophages (80–82). In addition, SCFAs have been associated with a reduction in neutrophil and macrophage activation (76, 78). Interestingly, ingestion of dietary fiber also influences bacterial composition and how bacteria can affect health and disease. Data has shown that a fiber-deficient diet caused bacteria within the colon to feed on the mucus glycoproteins as opposed to the nutrients normally attained from dietary fiber (83). As a result, the protective mucus layer was degraded. This changed the bacterial environment and indeed altered the composition of the intestinal microbiota to favor mucophilic bacteria (83). It also provided greater access to the intestinal epithelium, affording commensal bacteria and invading pathogens an additional opportunity by which to directly interact with the host and induce immune responses.

Bile acid metabolism is another arena where bacteria influences human health. Bile acids, which are required for lipid metabolism, are made in the liver and stored in the gallbladder. Consuming food triggers the release of bile through the bile ducts into the duodenum where it facilitates breakdown of lipids. Most bile acids are then recycled back up and stored in the gallbladder (84, 85). Bile acids not reabsorbed are metabolized from primary bile acids to secondary bile acids by specific intestinal bacteria able to facilitate this conversion (86, 87). This switch in bile acid structure allows secondary bile acids to passively diffuse through the colon to re-enter the enterohepatic circulation. In addition, secondary bile acids can also affect host metabolism though various signaling pathways including through the Farnesoid-X-Receptor

(FXR) and TGR5 bile-acid responsive receptors (85, 87, 88). In this way, bile acid metabolism allows the intestinal microbiota to indirectly influence host health and metabolism (87).

As with other aspects of the microbiota previously discussed, there is a host to microbiome regulation in bile acid metabolism as well. Changes in bile acid type and amount can favor certain bacterial species over others, altering the composition of the intestinal microbiota (87). For example, there is evidence that deoxycholate, a bacterial-derived metabolite of bile, promotes germination of *C. difficile* spores (89). Considering the bidirectionality of this and many other host-microbiome interactions, disruption of either can often lead to disease.

Table 1-3. Experimental Assays Used to Assess the Microbiome in Current Dissertation Studies

Assay:	**Utility in Current Studies:**
Quantitative Real Time Polymerase Chain Reaction (qRT-PCR)	To measure bacterial DNA signal in intestinal content and tissues
16S rRNA Sequencing	To describe the relative abundances of bacterial communities in a given sample
Bacterial Culture	To assess live bacteria in organs
Flow Cytometry	To quantify fecal bacterial burden
Mouse Toll Like Receptor (TLR) Reporter Cell Lines	To quantify the amount of TLR ligands in a given biological sample

1.3 Disruption of Th17 Signaling & the Intestinal Microbiome In Disease

1.3.1 Intestinal Diseases

Th17 signaling and the microbiome play an extensive role in intestinal homeostasis. As such, perturbations in these factors have been documented in many diseases. In the intestine, these factors have been implicated separately in diseases such as inflammatory bowel disease (IBD) and colon cancer. In IBD patients, there was an increase in Th17 cells within inflamed tissue biopsies

(90). In mouse models of IBD, IL-21 or IL-23 deficiency was protective, though IL-17A deficiency was not (90). In models of colorectal cancer (CRC), IL-17 promoted tumor progression, and in CRC patients, increased *Il17a* expression was associated with worse disease outcomes (90). Data in CRC also implicates the "Pathogenic" Th17 cell co-expressing IFNγ and IL-17A (91). The microbiome composition is also altered in both of these diseases (92, 93). Mouse models supported the role of the microbiome in disease pathogenesis as germ free mice were highly susceptible to the DSS-colitis model of IBD (94), but were protected in a colitis-associated CRC model (95). These are only two examples of how Th17 cells and the intestinal microbiome have been implicated in intestinal pathology. Yet within these two examples alone, the contrasting effects of IL-17 and the microbiome illustrate the complexity of these two components in disease and further reaffirm the contextual nature of their consequences.

1.3.2 Extra-Intestinal Diseases

Beyond the intestine, Th17 cells have been linked to a wide range of diseases throughout the body. More recently, the microbiome has been associated with extra-intestinal pathologies as well. What is especially interesting in the context of these dissertation studies are that many of these extra-intestinal diseases that the microbiome has been implicated in have a previously described Th17-related component. This ranges from barrier and non-barrier tissues anatomically close to the intestine, such as liver and pancreas, to the lung, and even further to immunoprivileged sites such as the eye and central nervous system (Figure 1-2).

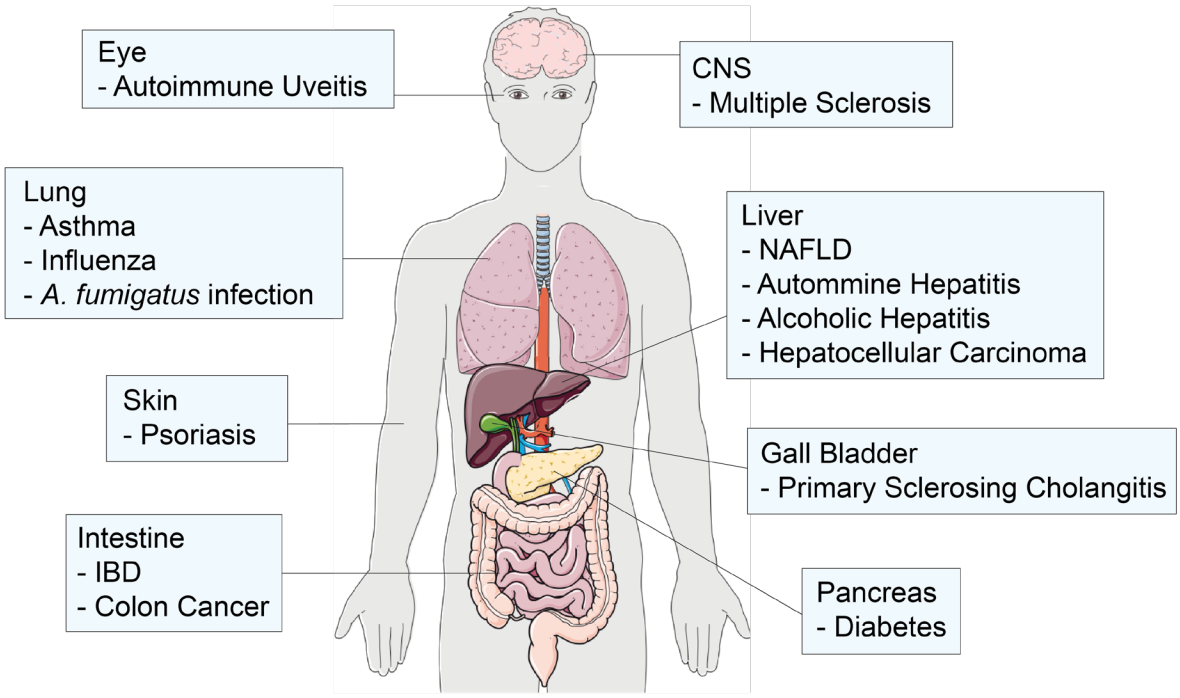

Figure 1-2. Diseases w/ Evidence Implicating Th17 cells & the Intestinal Micrbiome

**Images adapted from Servier Medical Art by Servier. Original images are licensed under a Creative Commons Attribution 3.0 Unported License (https://creativecommons.org/licenses/by/3.0/legalcode).*

Within the abdominal cavity, there have been links to both the pancreas and liver. In the pancreas, Zhao et al (2018) integrated human and mouse studies to show that a high fiber diet (HFD) selectively caused an increase in SCFA-producing bacteria that were associated with a significant reduction in symptoms associated with Type 2 Diabetes (T2D), a disease linked to Th17 cells and Th17/Treg imbalance (96, 97). In a study by Zhao et al., patients with T2D were treated with standard of care therapies supplemented with a regulated HFD and an inhibitor to increase the bioavailability of fermentable fiber to intestinal bacteria. These additional interventions improved clinical outcomes as measured by hemoglobin A1c and glucose tolerance tests. To determine the contribution of the microbiota in their results, fecal transplant from patients into

germ-free mice showed that mice receiving stool from HFD patients demonstrated the best metabolic outcomes (59). This suggested that the microbiota was the primary mediator of the effect of HFD, and that a patient's microbiota can be manipulated via dietary changes to improve metabolic health.

In the liver, there have been links to non-alcoholic fatty liver disease (NAFLD), alcoholic hepatitis, autoimmune hepatitis, hepatocellular carcinoma, and more (98, 99). In NAFLD, which includes nonalcoholic fatty liver that can progress to nonalcoholic steatohepatitis, patients exhibited increased hepatic *Il17* expression and increased Th17 cells in peripheral blood (100). In addition, studies showed disease progression in humans was associated with increased hepatic IL-17-producing $CD4^+$ lymphocytes (101). In mice, Henao-Mejia et al. showed that alterations in the inflammasome prompted changes in the composition of the intestinal microbiome, consequently exacerbating NAFLD (102). In viral and autoimmune hepatitis, patients exhibited intestinal dysbiosis (103, 104) and increased serum IL-17 (105–107). In some mouse models of these diseases, manipulation of the microbiome through antibiotics ameliorated liver inflammation (108). Finally, in hepatocellular carcinoma (HCC), the intestinal microbiota and TLR4 signaling were required for disease progression in mice (109), which aligned with the increases in bacterial translocation seen in patients (110).

Moving further to the thoracic cavity, Th17 cells and the microbiome have been linked lung pathology in asthma, influenza, and fungal infections. In a mouse model of asthma, two studies showed that dietary fiber and subsequent bacterial-derived SCFAs decreased disease severity by altering macrophage, T cell, and dendritic cell activation (82, 111). In patients, studies described a dysbiotic microbiota in both children diagnosed with asthma and at risk for asthma (112). Both mouse and patient data have implicated Th17 cells in the pathogenesis of steroid-

resistant asthma as well (113–115). More specifically, in an adoptive transfer model of allergic airway inflammation, steroid treatment was able to ameliorate both inflammation and airway hyperresponsiveness during adoptive transfer of Th2-polarized cells but not of Th17-polarized cells (116). In humans, increased IL-17 responses were observed from PBMCS of patients with steroid-resistant asthma as compared to PMBCs from patients with steroid-sensitive asthma (113, 115). With regards to infectious agents, there is data suggesting that IL-17RA mediates immunopathology during influenza (117). Microbiome involvement in influenza infection has been described as well. Marsland and colleagues found that dietary fiber and bacterial-derived SCFAs decreased immunopathology and mortality associated with influenza A viral infection by increasing $CD8^+$ T cell effector function and altering bone marrow hematopoiesis to increase the differentiation of $Ly6C^{neg}$ patrolling monocytes and alternatively activated macrophages (82). In fungal infection, a study by McAleer et al. examined how intestinal Th17 cells and the microbiome contributed to pulmonary *Aspergillus fumigatus* infection. They found that protection against this fungal pathogen was dependent on the AMP Reg3γ and Sfb, both factors intimately involved in intestinal Th17 cell signaling (52).

Finally, moving even more distally from the intestine, there are data linking Th17 cells and the intestinal microbiome to pathologies in immune privileged sites such as the eye and the central nervous system (CNS). In patients with acute uveitis associated with Vogt–Koyanagi–Harada (VKH) disease, there were increased serum IL-23 and elevated IL-17 production from stimulated PBMCs (118). In a mouse model of experimental autoimmune uveitis (EAU), neutralization of IL-17 was protective (119, 120). Interestingly, Caspi and colleagues demonstrated that the autoreactive T cells responsible for ocular pathology in EAU were actually primed in the intestine by commensal antigens, migrated to the eye via the systemic circulation, and cross-reacted with

ocular antigens (121, 122). This proposes molecular mimicry as another mechanism by which the microbiota can influence disease. As further evidence of the role of the microbiome in autoimmune uveitis, treatment with broad-spectrum antibiotics or germ-free rederivation of a spontaneous autoimmune uveitis mouse strain ameliorated disease (122).

In addition to the eye, the central nervous system is another immune privileged site in which Th17 cells and the intestinal microbiome have been implicated. Numerous studies have described the role of Th17 cells in multiple sclerosis (MS). There are increased levels of IL-17 in MS patient serum and CNS lesions (123, 124), and in mice blocking IL-17 globally via neutralizing antibodies or genetic knockout ameliorated EAE (125, 126). As further support, neuronal protease BACE1 promoted IL-17 production and increased EAE susceptibility (127). Patients with MS also exhibit commensal dysbiosis (128). Fecal transplant from MS patients into germ-free mice resulted in decreased Tregs and exacerbated EAE as compared to mice receiving normal control feces, together suggesting a role for the microbiome in disease severity (129).

Though Th17 cells and the microbiome have individually been implicated in these diseases, few studies have investigated how the extensive relationship between the two contribute to pathologies. Thus, the focus of the following chapters will be on investigating this Th17 cell-microbiome relationship in the context of extra-intestinal diseases, beginning with the gut-liver axis, then moving more distally to the gut-brain axis. A more in-depth review of the literature specific to those organ systems will be discussed in the respective chapters.

2.0 Gut-Liver Axis: Intestinal IL-17R signaling constrains IL-18 driven liver inflammation by the regulation of microbiome-derived products

2.1 Introduction

2.1.1 Liver Anatomy and Physiology

The liver is a unique organ in terms of its intimate association with the intestine. To appreciate this link, it is important to understand the basic liver anatomy and physiology that connect these two organ systems.

2.1.1.1 Structure and Blood Supply

The liver is located in the upper right quadrant of the abdominal cavity (Figure 2-1A). The human liver typically has four lobes which are comprised of the basic liver structural unit, the hepatic lobule (Figure 2-1B). Each lobule has a central vein, which drains blood from the liver and empties it into the hepatic vein to the inferior vena cava and heart. Emanating from the central vein are specialized capillaries called the liver sinusoids. Surrounding the sinusoids are the hepatocytes, which make up most of the cellular density of the liver, and other cell types that reside within the liver parenchyma and vasculature. This includes the liver sinusoidal endothelial cells and Kupffer cells, specialized macrophages of the liver. These sinusoids connect to the portal triad, which includes three components: 1. Bile duct, 2. Hepatic artery, and 3. Portal vein (Figure 2-1C). The bile duct connects the liver to the gallbladder nested at the inferior part of the liver, which stores the bile produced by the liver. The hepatic artery is a branch of the descending aorta that supplies

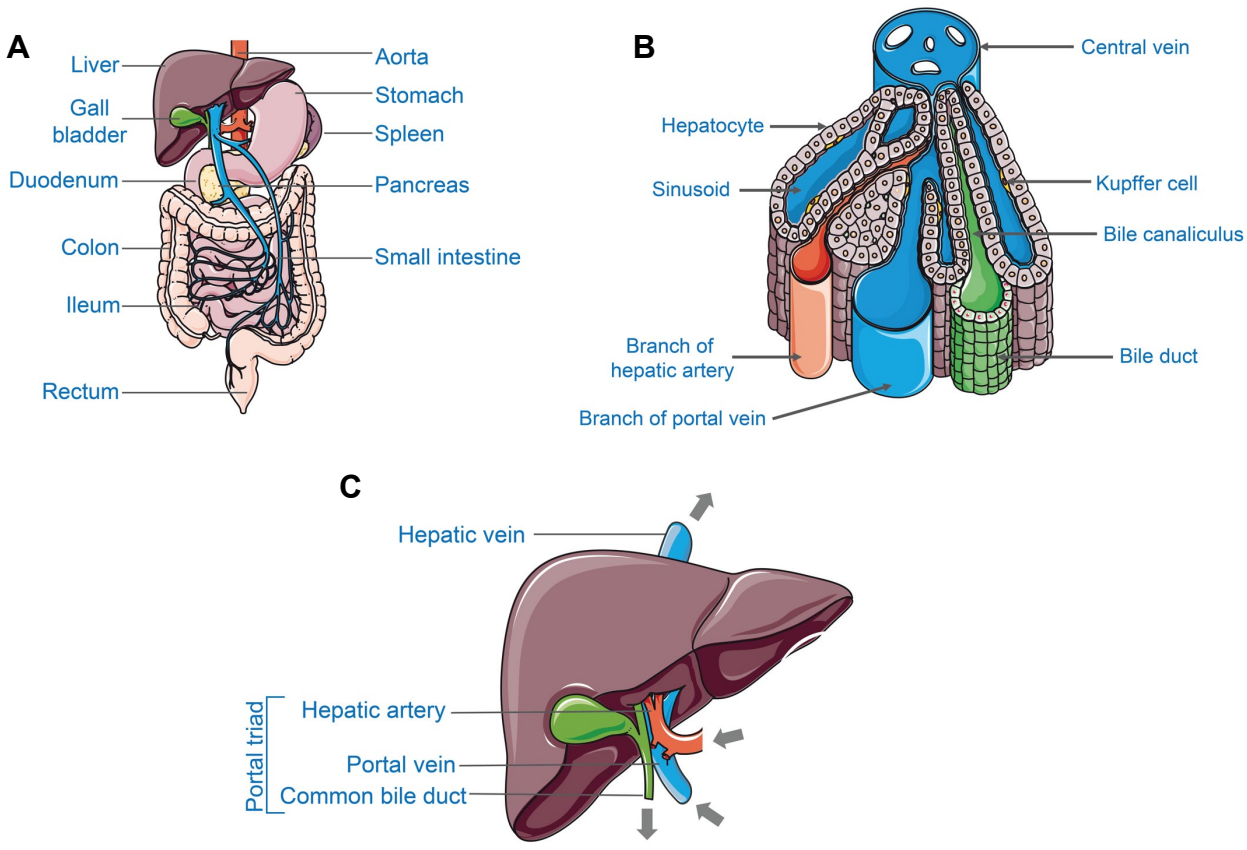

Figure 2-1. Liver Anatomy

(A) The liver is located in the upper right quadrant of the abdominal cavity. The hepatic portal circulation drains the spleen, pancreas, and gastrointestinal tract from the lower esophagus to the upper anal canal, thereby connecting other organs in the abdominal cavity to the liver. (B) Structure of the liver lobule—The hepatic lobule is the basic liver structural unit. Each lobule has a central vein, which drains into the hepatic vein, to the inferior vena cava, and then to the heart. Emanating from the central vein are specialized capillaries called the liver sinusoids. Surrounding the sinusoids are the hepatocytes and other cell types that reside within the liver parenchyma and vasculature. This includes Kupffer cells, specialized liver macrophages. The liver sinusoids connect the central vein to the portal triad—the bile duct, hepatic artery, and portal vein. (C) Inputs and outputs of liver as indicated by arrow direction—Inputs: the hepatic artery (25% percent of the liver blood supply); hepatic portal vein (~75% percent of the liver blood supply). Outputs: The hepatic vein (drains the central veins of each liver lobule); the common bile duct (releases the bile made by the liver and stored in gallbladder into the intestinal lumen).

oxygenated blood to the liver parenchyma via the sinusoids. The hepatic artery supplies about 25% of the hepatic blood supply. The remaining 75% comes from the hepatic portal vein which brings both nutrients and deoxygenated blood to the liver. This structure creates a dynamic interface at the liver lobule that's a mixture of products derived from hepatic cells, oxygenated blood, deoxygenated blood, and the nutrients and other products entering the liver through the portal vein. (88, 130, 131)

2.1.1.2 Hepatic Portal System

The portal vein is part of the hepatic portal system. A portal system differs from the traditional route of circulation in which oxygenated blood from the heart flows through arteries, arterial capillary beds, and then to the target organ. In this traditional circuit, the target tissue then utilizes the oxygen and nutrients from the arterial blood, and venous capillaries drain the deoxygenated blood from the tissue. This blood is transported to veins draining into the vena cava and then to the heart for reoxygenation and redistribution. In a portal system, the tissue-draining venous capillaries empty that blood into another venous capillary bed. In the case of the hepatic portal system, the receiving venous capillary bed drains into the hepatic portal vein and into the liver. In doing so, there is a direct connection from organ to organ without going through the heart. The hepatic portal vein drains the spleen, pancreas, and gastrointestinal tract from the lower esophagus to the upper anal canal (Figure 2-1A). As such, there is a direct mode of transportation from these organs to the liver.

2.1.1.3 Function

The extensive connections between the liver and other organ systems facilitate the liver's many functions in the body. All of the blood, nutrients, and products the liver receives through the portal and arterial inputs are filtered through the liver and also act as starting blocks for some of its functions. Examples include amino acid and protein synthesis. The liver is responsible for producing carrier proteins such as albumin and transferrin as well as numerous proteins involved in immune responses including opsonins, complement, and serum amyloid proteins. The liver is also heavily involved in carbohydrate metabolism, regulating both glucose storage and synthesis, and lipid metabolism due its role in bile acid metabolism. As mentioned above, the liver produces bile, which is stored in the gallbladder. Bile is released into the intestinal lumen via the common bile duct post-prandially to promote fat emulsification and digestion. The intestinal microbiome contributes to this process by metabolizing primary bile acids into secondary bile acids, which facilitate bile acid reabsorption into the hepatic portal system for recycling and future use. This circuit is termed the enterohepatic circulation and offers another line of communication from the gut to the liver. Another major function of the liver is detoxification. Many drugs in the blood stream are metabolized in the liver and filtered out from systemic circulation by the prominent liver macrophage population. With regards to this dissertation, the most relevant aspect of the liver in terms of its function as gatekeeper to the rest of the body is its ability to filter out bacteria and bacterial products coming from the arterial and venous inputs. Research performed as early as the 1920s showed that the liver was very effective in bacterial clearance from the vasculature (132). In these studies, a known concentration of bacteria was perfused into the liver and other organs. Bacterial concentration of the output was measured as an indicator of the efficacy of bacterial clearance. Indeed, the liver was the most efficient as compared to spleen, brain, lung, and intestine

(132). These results reflect the requirement and capability of the liver to manage the high exposure to intestinal-derived components whether it be cytokines, cells, microbes, or bacterial products. The mechanisms by which the liver manages this interaction with the intestine are described in more detail in the next section.

2.1.2 Hepatic Response to Intestinal-Derived Factors

2.1.2.1 Initial Cell Responders at the Liver Sinusoids

Numerous cell types contribute to liver management and response to intestinal-derived products. At the interface of the liver and the incoming vascular supply are liver sinusoidal endothelial cells (LSECS), hepatic stellate cells (HSCs), and Kupffer cells (KCs).

LSECS and HSCs are two types of hepatic stromal cells. Because of their location, these cells are highly exposed to the incoming components from portal and arterial supplies. The LSECs line the liver sinusoids to form a fenestrated endothelium which is unique in that it also lacks a basement membrane (88). Together, this allows for increased hepatic access of blood-borne factors including bacteria, bacterial products, proteins, lipids, and other nutrient and macromolecule transport (133). This fenestration is critical for the liver to effectively receive these substances for metabolism, detoxification, and hepatocyte maintenance. Indeed, this fenestrated structure is eliminated during some liver diseases, depriving the liver of necessary nutrients and allowing access of potentially harmful substances to the systemic circulation (133). HSCs are vitamin A-rich pericytes that reside in the space of Disse between the endothelial layer and hepatocytes. They comprise close to 10% of resident liver cells and remain largely quiescent, but can be activated and transdifferentiate into collagen-producing myofibroblasts with diverse immune consequences (134, 135).

Both LSECs and HSCs play a role in innate and adaptive immunity. LSECs and HSCs express toll like receptors (TLRs) and scavenger receptors, allowing them to filter and respond to incoming pathogen- and danger-associated molecular patterns (133, 136). The enrichment of scavenger receptors such as mannose receptor afford LSECs a high endocytic capacity (133), which has been shown to be critical in blood-borne pathogen clearance (137). In activated HSCs, TLR9 activation promoted chemokine release and Kupffer cell chemotaxis (138), while TLR3 activation enhanced γδ T cell-derived IL-17A (134). With regards to adaptive immunity, LSECs are able to present antigens to CD8+ T cells and CD4+ T cells through MHC I and MHC II, respectively (139, 140). Similarly, HSCs can act as antigen presenting cells, especially to invariant NKT cells via CD1d (141, 142). Both stromal cell types largely produce more anti-inflammatory responses. This includes production of IL-10, PD-1, and TGFβ that favor T regulatory cells and more tolerogenic responses (88). When considering the volume and diversity of potentially inflammatory agents these cells are be exposed too, it is appropriate that part of their role is limiting the overactivation of T cell responses to these substances.

The Kupffer cell (KC) is the third cell type mentioned that resides at the liver sinusoids. KCs are specialized liver-resident macrophages, which comprise the largest macrophage population in the body (88). They are developmentally distinct from monocyte-derived macrophages, because of their origin from fetal liver-derived progenitor cells (143). These cells take up a larger role in surveillance compared to the migratory infiltrating monocyte-derived macrophages. Because of the high demand of immune surveillance in the liver, it is perhaps not surprising that for every 100 hepatocytes, there are 20-40 macrophages (143). To facilitate their role in immune surveillance, KCs express TLRs, scavenger receptors, and Fc receptors like LSECs (143). High expression of these receptors partnered with their extremely high phagocytic activity

allow KCs to fulfill their critical role in eliminating bacteria and bacterial products coming from the intestine. To promote bacterial clearance, KCs coordinate with LSECs, platelets, and other cells to promote bacterial phagocytosis, lysis, and other bactericidal consequences (143). Importantly, these cells also act as antigen presenting cells, expressing MHC II (140, 142). They can activate NKT cells as well through CD1-mediated antigen presentation (142). Furthermore, they secrete various immune mediators including cytokines and reactive oxygen species (142). Therefore, the effects of KCs encompass both the regulation of incoming bacterial products as well as the interactions with other hepatic and circulating lymphocytes.

Because LSECs, HSCs, and KCs reside at the interface of the liver and intestinal vascular supply, they can induce many different effects depending on the incoming products, cells, and other immunogenic components. In the context of these dissertation studies, we focused on the effects of bacterial translocation from the intestine to the liver.

2.1.2.2 Effects of Bacterial Translocation

Translocation of bacteria and bacterial products to the liver can have a wide range of consequences. This section will broadly focus on three effects that are pertinent to these dissertation studies: immune cell recruitment, immune cell activation, and activation of death receptors.

Immune Cell Recruitment

As mentioned above, engagement of TLRs on these cells at the forefront of the gut-liver interface can prompt chemokine release and immune cell recruitment. Though they largely promote a tolerogenic environment to quell aberrant immune activation and maintain homeostasis, liver pathology and inciting stimuli can prompt these cells to contribute to a proinflammatory

environment. For example, while Kupffer cells are not a migratory macrophage population, they have the capacity to heavily recruit inflammatory monocytes. There are data showing that TLR4 activation by LPS can induce CCL2 secretion (144), which can promote recruitment of CCR2+ monocytes to the liver. Changes in adhesion molecules such as selectins on LSECs in response to bacterial products can promote T cell arrest and recruitment from the circulation (145, 146). In addition, TLR9 activation in a mouse model of hepatitis promoted recruitment of NKT cells from the periphery (147). Beyond these examples, there are also the various cytokines induced in response to bacterial products that can trigger chemokine release and further leukocyte recruitment.

Immune Cell Activation

As eluded to above, bacterial translocation can also activate other immune cells including T cells, NKT cells, and NK cells.

Because CD4+ and CD8+ T cells express TLRs only at low levels, their activation by bacterial translocation is often mediated by other cell types. As mentioned above, KCs and LSECs can act as antigen presenting cells to circulating T cells. The liver is unique compared to other solid organs due to its capability to activate naïve T cells independent of lymphoid tissues (139, 148, 149). This is facilitated by the structure and organization of the liver which allows high exposure to antigen and circulating naïve T cells in the liver sinusoids. There is also evidence of tissue resident memory T cells that patrol the liver sinusoids (150), which can be activated when exposed to cognate antigen from the incoming vascular supply. In addition to this, T cells can be activated in a bystander fashion through the cytokine milieu produced by KCs, LSECs, and HSCs.

NKT cells make up a large portion of the resident liver cell population. In mice, this can be up to 30% of the liver T lymphocytes (151). As such, these cells play large role in maintaining

liver homeostasis. Of note, the majority of liver NKT cells in mice are invariant NKTs (iNKTs). These cells specifically express Vα14-Jα18 with restricted variations in beta chains (88). iNKTs mount strong immune responses to sphingolipids found on and released by bacteria including those of the intestinal microbiome. Certain bacteria such that those in the Phylum Bacteroidetes are known highly produce these compounds (152). The stimulatory capacity of sphingolipids on iNKTs has been shown many times by administration of synthetic sphingolipid, α-galactosylceramide (α-GalCer). Indeed, treating mice with α-GalCer *in vivo* results in massive activation and cytokine responses by iNKTs, leading to fatal hepatitis (153). This further demonstrates that specific bacterial-derived products can have huge immune consequences in the liver. However, there is a caveat with this example in terms of human translatability. The human counterpart to iNKTs, which express Vα24-Jα18 as opposed to Vα14-Jα18 are a much smaller population in the human liver (151). Therefore, the magnitude of the effects seen in mice as a result of iNKTs may not parallel effects in humans.

NK cells make up about 5-10% of hepatic lymphocytes in mice and about 20-30% in humans (151). Liver NK cells differ from peripheral NK cells in their enhanced cytotoxic capabilities. There is evidence showing that liver NK cells exhibit higher amounts of TRAIL, IFNγ, perforin, and granzyme B (151). NK cells release these inflammatory mediators in response to bacterial products including LPS and TLR3 agonist Poly I:C (151, 154, 155). Bacterial translocation can also indirectly activate NK cells through Kupffer cells. Indeed, Kupffer cell depletion decreased the liver NK population, and stimulation of NK cells with Kupffer cell-conditioned media *in vitro* enhanced NK cell activation and toxicity (156).

Speaking more broadly than specific cell types, bacterial products can also activate cells via the inflammasome (157, 158), resulting in release of IL-1β and IL-18 (159). For example,

bacterial stimulation of KCs induced inflammasome activation, most notably though NLRP3 (143). Both IL-1β and IL-18 have a wide range of immunoregulatory effects. Due to its role in these gut-liver dissertation studies, the focus will be on IL-18. IL-18 is an IL-1 family member produced by macrophages, dendritic cells, and some epithelial cells (160). In the liver, KCs are a major source of IL-18. Of note, there is evidence showing that IL-22 can induce IL-18 expression by the intestinal epithelium (161). IL-18 binds to a dimeric receptor comprised of IL-18Rα, which is relatively ubiquitous, and IL-18Rβ, which is largely on T cells and DCs (160). IL-18 has numerous immunoregulatory functions and is therefore highly regulated though IL-18 binding protein (IL-18BP). Indeed, there are high amounts of serum IL-18BP to limit aberrant responses (160). Demonstrating the critical role of IL-18BP in health and disease, genetic IL-18BP deficiency in patients has been shown to increase susceptibility to viral-mediated fulminant hepatitis (162). While IL-18 was first described as an IFNγ inducing factor (163), numerous reports have detailed its effects on lymphocyte activation, chemokine release, and cell death, which is discussed in more detail below (163–173).

Death Receptors

A downstream consequence of bacterial translocation to the liver is activation of death receptors. Death receptors are members of the TNF superfamily of receptors that promote cell death upon binding of its cognate ligand (174). Notable examples include Fas, TNF receptors 1 (TNFR1) and 2 (TNFR2), and TNF-related apoptosis inducing ligand receptor (TRAILR) 1 through 4. The liver is rich in death receptors (174), and therefore very susceptible to death receptor-mediated cell death. Indeed, injection of anti-Fas antibody to crosslink and activate Fas caused hepatocyte cell death and lethal hepatitis in mice (175). Engagement of these death receptors promotes cell death through different signaling cascades. A key part of many of these

signaling cascades is the death domain, which is a 60-80 amino acid cytoplasmic domain that recruits the subsequent adaptor molecules required for the signaling cascade (174). Using Fas-FasL as an example, binding of cognate ligand FasL to Fas recruits the adaptor protein Fas-associated protein with death domain (FADD) to its death domain. Resulting signaling cascades then go through different caspases, ultimately converging at caspase 3 to induce cell death (174, 176). The many pathways by which this can occur further emphasizes the impact of these death receptors in liver health and disease.

The effects of bacterial translocation can, of course, be influenced by changes in the source of these products, including the intestinal microbiome. The next section will focus on how the microbiome and bacterial translocation have been implicated in liver disease.

2.1.3 The Intestinal Microbiome & Bacterial Translocation in Liver Disease

There is now a growing body of research linking alterations in the intestinal microbiome to liver pathologies. For example, patients with viral and autoimmune hepatitis (AIH) exhibit intestinal dysbiosis (103, 104). This included decreased *Bifidobacterium* in AIH and increased *Prevotella* in Hepatitis C (103, 104). Changes in the commensal microbiome were similarly seen in alcoholic liver disease (ALD) and non-alcoholic fatty liver disease (NAFDL). In both diseases, there were increased *Enterobacteriaceae* and decreased *Akkermansia muciniphila* (177). As these were descriptive studies, research in mouse models have been performed to evaluate a causal role of the microbiome in disease pathogenesis. In concanavalin A hepatitis, a T cell-dependent liver injury model often used to study AIH, germ free mice and mice treated with gentamicin exhibited decreased disease severity as measured by liver histology and serum markers of liver inflammation

(108, 178). In a mouse model using a genetic predisposition to autoimmune hepatitis, treatment with vancomycin or ampicillin ameliorated disease (179). This study by Kriegel and colleagues went further to identify *Enterococcus gallinarum* as an exacerbating factor in the mouse model. Moreover, they found DNA from *Enterococcus gallinarum* in biopsies of patients with AIH (179). In a mouse model of alcoholic liver disease, fecal transplant from patients with ALD into germ-free mice exacerbated disease with increased liver inflammation, lymphocyte infiltration, and cell death (180). Together, these examples demonstrate the potential role of the intestinal microbiome in liver disease pathogenesis.

Given the closely related vasculature of the liver and intestine, there is a normal physiological flux of bacterial products to the liver through the portal vein draining the intestine (88). This flux can become more pronounced in the diseased states. For example, in HIV-associated liver disease, increases in serum LPS have been documented and are thought to contribute to wasting and liver pathology (181). In patients with ALD and NAFLD, increased serum endotoxin as well as systemic and liver TLR ligands were described (177). Indeed, many liver diseases and their related models of liver inflammation have been associated with increased bacterial translocation (99, 103, 108, 182–184). Focusing on mouse studies, the work by Kriegel and colleagues mentioned above also described liver translocation of *E. gallinarum* (179). Furthermore, work by Henao-Mejia et al. showed that the inflammasome induced changes in the intestinal microbiota which led to increased bacterial translocation to the liver, exacerbating NAFLD (102).

Many of these diseases with changes in the microbiome and bacterial translocation have been associated with increased intestinal permeability as well (99, 103, 183). Increases in intestinal permeability allow greater access of the microbiome and bacterial products to the liver and

systemic circulation, magnifying their potential effects. Interestingly, Th17 cells, which play important roles in maintaining both the intestinal microbiome and permeability, have also been heavily implicated in liver disease.

2.1.4 Th17 Cells in Liver Disease

There is evidence in patients and mouse models linking Th17 cells to liver pathology. For example, both autoimmune and viral hepatitis patients displayed elevated serum IL-17 (105–107). In patients with alcoholic liver disease, there was increased Th17 cell infiltration that correlated with neutrophil recruitment, a known effect of Th17 cells (185). In non-alcoholic steatohepatitis (NASH), a subtype of NAFLD, increased circulating Th17 cells were described (100). Moreover, patients who progressed from non-alcoholic fatty liver (NAFL) to NASH exhibited more intrahepatic IL-17+ cells (101). In mouse models, the Kolls lab previously showed that global IL-17RA knockout mice (*Il17ra*$^{-/-}$) were protected from Con A hepatitis (186). In addition, numerous studies using high fat diet-induced models of NAFLD showed increased Th17 cells in the liver, visceral adipose tissue, and blood (100). The proposed mechanisms by which Th17 cells are thought to contribute to liver disease include neutrophil recruitment via Th17-mediated chemokine release, fibrogenic effects promoting collagen deposition by HSCs, alteration of lipid metabolism via PPARγ, and IL-17 and IL-21-mediated release of proinflammatory cytokines by nonparenchymal cells including KCs and HSCs (98, 100, 187, 188). Mechanistically, the following dissertation work proposes a novel role for intestinal Th17 cells in liver inflammation.

2.1.5 Study Overview

As previously discussed, Th17 cells play a critical role in regulating the intestinal microbiome and maintaining intestinal barrier integrity (35, 38, 40, 41, 48, 54, 189, 190). Given the importance of IL-17R in intestinal homeostasis and the reported links between liver disease and both intestinal dysbiosis and bacterial translocation, we hypothesized that intestinal IL-17R signaling plays a critical role in mitigating hepatic inflammation. To test this, we used intestinal epithelium-specific IL-17RA knockout mice (*Il17ra*$^{fl/fl}$ x *villin cre*$^{+}$ mice) in the concanavalin A (Con A) model of T-cell mediated hepatitis. Absence of enteric IL-17RA signaling induced commensal dysbiosis, expansion of intestinal Th17 cells, and intestinal *Il18* expression. After Con A administration, *Il17ra*$^{fl/fl}$ x *villin cre*$^{+}$ mice exhibited more severe hepatitis accompanied by increased hepatocyte cell death. Mechanistically, we found that disease exacerbation was microbiome dependent, specifically implicating a role of gram-negative bacteria. In addition, we found that intestinal specific knockout mice displayed increased translocation of unmethylated CpG DNA to the liver. Our data suggested that CpG DNA exacerbates liver inflammation by driving expression of hepatic IL-18 to promote lymphocyte activation and FasL production in hepatic T-cells. Thus, intestinal IL-17R regulates translocation of TLR9 ligands and constrains susceptibility to hepatic inflammation. Our studies elucidate the role of enteric Th17 signaling and the microbiome in hepatitis, with broader implications on the effects of impaired intestinal immunity and subsequent release of microbial products seen in other diseases.

2.2 Methods

2.2.1 Experimental Model and Subject Details

Mice

All mouse work was performed in accordance with the Institutional Animal Care and Use Committees (IACUC) and relevant guidelines at the University of Pittsburgh, School of Medicine (protocol #16109334). *C57BL/6* mice were obtained from Taconic Biosciences (Germantown, NY). *Nlrc4*^{mut}*Il18bp*$^{-/-}$ mice, which were bred and housed at the UPMC Children's Hospital of Pittsburgh, were kindly provided by Dr. Scott Canna. *Il17ra*$^{fl/fl}$ and *Il17ra*$^{fl/fl}$ *x villin cre*$^{+}$ mice were generated at the UPMC Children's Hospital of Pittsburgh by crossing *Il17ra*$^{fl/fl}$ mice to *Il17ra*$^{fl/fl}$ *x villin cre*$^{+}$ mice. Both male and female age-matched mice from 6-10 weeks of age were used for all experiments. The aforementioned breeding strategy allowed for controls and knockout mice within each experiment to be littermates. Littermate age-matched males and females were randomly assigned to experimental groups. Both males and females were used within each group in order to account for sex-differences while maintaining littermate controls and sufficient n for statistical power. All mice were housed in pathogen-free conditions at the UPMC Children's Hospital of Pittsburgh.

In vitro and ex vivo cultures

Mouse TLR9 and TLR4 reporter cells (HEK-blue mTLR9 and HEK-dual mTLR4 reporter cells) were obtained from Invivogen and maintained according to manufacturer's instructions.

Ex vivo stimulation of liver cells: Livers from 6-10-week-old naïve *Il17ra*$^{fl/fl}$ mice and *Il17ra*$^{fl/fl}$ *x villin cre*$^{+}$ mice were harvested and enriched for mononuclear cells by Percoll gradient. In addition to detailed experiment-specific stimuli, cells were maintained at 37°C in Iscove's Modified Dulbecco's Medium (IMDM) with GlutaMAX Supplement (Gibco), 10% heat-inactivated fetal bovine serum, 100 units/mL of penicillin and streptomycin, and 0.3mg/mL of L-glutamine.

Experimental Models

Concanavalin A (Con A) hepatitis was induced using concanavalin A from *Canavalia ensiformis* (jack bean) type IV (Sigma).

2.2.2 Method Details

Animal treatments

C57BL/6, *Il17ra*$^{fl/fl}$, and *Il17ra*$^{fl/fl}$ *x villin cre*$^{+}$ mice were injected with 10mg/kg or 25mg/kg Con A intravenously (IV) via tail vein. For antibiotic studies, mice were treated with either five days of 1g/L neomycin or 14 days of 0.5g/L vancomycin in the drinking water *ad libitum* prior to Con A injection and remained on antibiotics throughout the hepatitis model. For CpG DNA pre-treatments, Class C CpG (Invivogen) was injected 3x at 2.5mg/kg intraperitoneally (IP) prior to 10mg/kg IV Con A. For IFNγ inhibition, mice were injected with Anti-IFNγ (BioXCell, XMG1.2) at 500μg/mouse IP one hour prior to 25mg/kg Con A injection. For FasL inhibition, mice were injected with 250-500μg/mouse IV into the retro-orbital sinus one hour prior to 25mg/kg Con A injection. For IL-18 blockade, anti-IL-18 was injected IP at 0.5mg/mouse one day prior to 25mg/kg IV Con A injection.

Alanine aminotransferase quantification

Alanine aminotransferase (ALT) was measured in the serum of mice using the Vitros DT60 II chemistry system (Ortho-Clinical Diagnostics, Inc.) (191) or ALT Activity Assay (Sigma) per manufacturer's instructions. Method of ALT measurement was consistent within experiments.

TUNEL Staining

Liver tissues used for TUNEL staining were immediately fixed in 4% paraformaldehyde for 24-72 hours, washed 3x in PBS, and stored in 70% ethanol prior to paraffin embedding. Following paraffin embedding, slides were stained using the ApopTag® Peroxidase In Situ Apoptosis Detection Kit according to manufacturer's instructions.

Cohousing studies

Littermate *Il17ra*$^{fl/fl}$ and *Il17ra*$^{fl/fl}$ *x villin cre*$^{+}$ mice were either kept cohoused or separated for one week prior to Con A injection and remained in assigned housing conditions throughout hepatitis model.

qRT-PCR and RNA Sequencing

Livers and intestines from naïve 6-10-week-old littermate *Il17ra*$^{fl/fl}$ and *Il17ra*$^{fl/fl}$ *x villin cre*$^{+}$ mice were homogenized in Trizol buffer (Life Technologies). Total RNA extraction was performed according to Trizol manufacturer's instructions. RNA was transcribed into cDNA using iScript reagent (Bio-RAD) according to manufacturer's instructions.

For qRT-PCR, SYBR Green supermix (Bio-RAD) was used for analysis of small subunit ribosomal RNA gene (16S rRNA) expression. 16S primers included: forward: ACTCCTACGGGAGGCAGCAGT, reverse: ATTACCGCGGCTGCTGGC (47, 48, 192). SsoFast supermix (Bio-RAD) was used for qRT-PCR analysis with primers for mouse *Hprt* (Integrated DNA Technologies), *Ifng* (Applied Biosystems), and *Fasl* (Applied Biosystems). Expression of all genes was normalized relative to housekeeping gene mouse *Hprt*. Reaction: 95°C for 3 minutes, 49 cycles at 95°C for 10 seconds (s) and 60°C for 30s. SYBR Green reactions also had an additional melt curve at the end of the reaction above: 60°C for 5s with +0.5°C increment every cycle up to 95°C.

Terminal ileum bulk RNA sequencing data was sourced from dataset we previously published (48). See previous manuscript for detailed methods.

Single Cell RNA Sequencing

Livers from 6-week-old littermate *Il17ra*$^{fl/fl}$ and *Il17ra*$^{fl/fl}$ *x villin cre*$^{+}$ mice were harvested at the naïve state or ninety minutes post 25mg/kg IV Con A injection. Single cell suspensions were isolated and enriched for mononuclear cells via Percoll gradient. Briefly, livers were collected in IMDM with GlutaMax (Gibco) supplemented with 10% FBS, penicillin, streptomycin, and L-glutamine ("complete media"). Livers were minced into small pieces and digested in neat IMDM with 1mg/mL collagenase and 0.2mg/mL DNase at 37°C for 30 minutes with shaking. Cell suspension was further homogenized by flowing through an 18G needle in a 3mL syringe followed by filtering through a 70µm filter. Following a wash in complete media, mononuclear cells were enriched using a 70%/30% percoll gradient. Cells were washed 2x in complete media and resuspended for downstream applications.

For single cell RNA sequencing library preparation, liver cells were then separated into mini-reaction "partitions" or Gel bead in emulsion (GEM)s formed by oil micro-droplets, each containing a gel bead and a cell, by the Chromium instrument (10X Genomics). The reaction mixture/emulsion with captured and barcoded mRNAs were removed from the Chromium instrument followed by reverse transcription. The cDNA samples were fragmented and amplified per 10X protocol. The libraries were then purified, quantified, and sequenced on an Illumina NextSeq 550. Analysis was performed using the pipeline Cell Ranger developed by 10X Genomics as well as Seurat.

16S rRNA Gene Sequencing

Littermate *Il17ra*$^{fl/fl}$ and *Il17ra*$^{fl/fl}$ *x villin cre*$^{+}$ mice were sacrificed at the naïve state or 8 hours post Con A injection. Terminal ileum RNA was isolated using Trizol (Life Technologies) and transcribed to cDNA using the iScript Reverse Transcription Supermix (Bio-rad), both according to manufacturer's instructions. Extracted DNA was PCR amplified using the method/primers of Caporaso (193) and the Q5 HS High-Fidelity polymerase (NEB). Four microliters of each sample were amplified in a 25µl PCR reaction with barcoded V4 16S primers. Cycle conditions were 98°C for 30s, then 25 cycles of 98°C for 10s, 57°C for 30s, 72°C for 30s, with a final extension step of 72°C for 2 min. Reactions were purified with AMPure XP beads (Beckman) at a 0.8:1 ratio (beads:DNA) to remove primer-dimers. Eluted DNA was quantitated on a Qubit fluorimeter (Life Technologies). Sample pooling was performed on ice by combining 20ng of each purified band. For negative controls and poorly performing samples, 20µl of each sample was used. The sample pool was first purified/concentrated with the MinElute PCR purification kit. Next, two-sided AMPure XP bead purification was used at 0.8:1 (left-side) and

0.61:1 (right-side) ratios to remove small and large contaminants, respectively. A final cleanup in the Purelink PCR Purification Kit (Life Technologies) was performed to insure removal of all AMPure XP beads. The final, purified pool was quantitated in triplicate on the Qubit fluorimeter prior to sequencing.

Sequencing pool preparation was as per Illumina's recommendations, with an added incubation at 95°C for 2 minutes immediately following the initial dilution to 20 picomolar. The pool was then diluted to a final concentration of 6 pM + 15% PhiX control. Paired-end sequencing was done on an Illumina MiSeq platform using a MiSeq Reagent kit v2 (500 cycles).

Fecal Bacterial Flow Cytometry

Followed protocol as detailed in Gopalakrishna et al. (194). Briefly, fecal matter was collected and weighed. 1ml of sterile PBS was added to the fecal content and homogenized by vortex and pipetting. Stool suspension was then passed through a 40-micron strainer into a 50ml conical tube. 10µl of stool was added to a round-bottom 96-well plate for IgA staining. Plated stool was washed 2.5x in BAC-FACS buffer (filtered 1%BSA in PBS) at 4000rpm for 5 minutes at 4 degrees C. Stool was then stained in BAC-FACS buffer using Hoechst stain (1:1000dil), normal rat serum (1:5dil), and anti-mouse IgA PE or isotype control (1:500 dil). Samples were stained for one hour on ice in the dark and washed 2.5x with 100µl BAC-FACS buffer. Samples were reconstituted in BAC-FACS buffer, and 10µl of Accu-Check counting beads were added to each. Samples were analyzed by flow cytometry on the BD Fortessa cytometer. Bacterial calculations using Accu-Check beads were done using manufacturer's instructions.

mTLR reporter assays

For mTLR4 and mTLR9 reporter cell assays, cells were grown and maintained according to manufacturer's instructions (Invivogen). For the assay, cells were stimulated with serum or liver homogenate of naïve littermate *Il17ra*$^{fl/fl}$ and *Il17ra*$^{fl/fl}$ *x villin cre*$^{+}$ mice. For the liver homogenate, livers were homogenized in PBS plus protease inhibitor (Roche). BCA Protein Assay (Pierce) was performed according to manufacturer's instructions to measure total protein concentration. Dilutions were performed in PBS plus protease inhibitor to normalize concentrations between samples prior to reporter assay. SEAP levels were measured using QUANTI-Blue detection media (Invivogen). Assays were conducted according to the manufacturer's instructions.

For DNase treatment of liver homogenate, livers were harvested, homogenized in PBS plus protease inhibitors, and diluted to normalize total protein concentration as described above. An aliquot of liver homogenate was treated with DNase I from bovine pancreas (Sigma) reconstituted in PBS + MgCl to activate enzyme per manufacturer's instructions. Vehicle control treatment was PBS + MgCl without DNase. Liver homogenate plus DNase or vehicle control were incubated at 37 degrees C with shaking for 30 minutes. Digested samples were then plated on mTLR9 reporter cell line as described above. Positive control to ensure DNase treatment efficacy was *E. coli* dsDNA (Invivogen).

Flow cytometry

Liver single cell suspensions were isolated and enriched for mononuclear cells from *C57BL/6* mice or littermate *Il17ra*$^{fl/fl}$ and *Il17ra*$^{fl/fl}$ *x villin cre*$^{+}$ mice as described above in *Single Cell RNA Sequencing.* For staining, cells were washed in HBSS. Surface and live/dead stains were performed in 50µl-75µl in a 96 well round bottom plate in the dark on ice for 20 minutes. Cells

were washed 2.5x in cold FACS Buffer (0.5% FBS/0.01% NaN3/PBS). Cells were then fixed using BD Cyto-fix and incubated in the dark on ice for 20 minutes. If no further staining was required, cells were washed 2x in FACS buffer, resuspended in PBS or FACS buffer, and analyzed using the BD Fortessa flow cytometer. If additional intracellular stain analysis was required, cells were washed 1x in BD Perm/Wash. 50-75µl of intracellular stain cocktail made in BD Perm/Wash was then added to the cells and incubated in the dark on ice for 45 minutes. Cells were then washed 2x in BD Perm Wash, 1x in FACS buffer, and resuspended in PBS or FACS buffer for analysis on the BD Fortessa flow cytometer. Data analysis was performed on FlowJo. Cell number was quantified using the Nexcelom Cellometer Auto 2000. Flow cytometry antibodies used included: Live/Dead fixable aqua dead cell stain (Life Technologies) (1:500 dilution), BV786 Anti-mouse CD4 (BD Clone RM4-5) (1:200 dilution, APC Anti-mouse IFNγ (BD Clone XMG1.2) (1:200 dilution), APCe780 Anti-mouse TCRβ (BD Clone H57-597) dilution), BV421 Anti-mouse NK1.1 (BD clone PK136) (1:100 dilution), BV395 Anti-mouse CD3 (BD Clone 145-2C11) (1:200 dilution), PCP-Cy5 Rat-Anti-Mouse CD3 Molecular Complex (BD clone 17A2) (1:200 dilution), BV605 Anti-Mouse CD90.2 (BD clone 30-H12) (1:400 dilution), PE Anti-Mouse FasL (Biolegend Clone MFL3) (1:200 dilution), PE-Cy7 Anti-mouse CD8 (Invitrogen clone eBioH35-7.2) (1:400 dilution), Anti-Mouse CD16/CD32 (eBioscience Clone 93).

Ex vivo liver cell stimulations

Liver single cell suspensions were isolated and enriched for mononuclear cells from *C57BL/6* mice or littermate *Il17ra*$^{fl/fl}$ and *Il17ra*$^{fl/fl}$ *x villin cre*$^{+}$ mice as described above in *Single Cell RNA Sequencing.* Cells were then resuspended in IMDM with GlutaMax (Gibco) supplemented with 10% FBS, penicillin, streptomycin, and L-glutamine ("complete media") and

plated at a concentration of 5 x 10^5 or 1 x 10^6 cells per well in a 96-well round bottom plate. Cell number was kept consistent within experiments. Cells were then stimulated with various conditions at 37°C for the detailed incubation times. For TLR ligand stimulations: Lipoteichoic acid, flagellin, lipopolysaccharide, and CpG were all attained from Invivogen and used at 10ng/mL-1μg/mL or 1μM-5μM. Exact concentrations are detailed within each figure. During stimulations with TLR ligands ± Concanavalin A, 5ug/mL of Concanavalin A (Sigma) was used. Supernatants were harvested at 24 hours and analyzed for IFNγ and IL-18 levels by ELISA or Luminex. For downstream flow cytometry analysis, brefeldin A (BD) was added for 3 hours after 4 hours of 1μM CpG stimulation. Cells were then stained and fixed for flow cytometry analysis as described above in *Flow Cytometry.* For non-TLR ligand stimulations, cells were stimulated with Con A (5ug/mL) or anti-CD3/CD28 (Thermo Fisher, Dynabeads) stimulation for three days. Supernatants were harvested and cytokine levels were measured via Luminex.

FITC Dextran Assay for Intestinal Permeability

Four hours prior to FITC dextran gavage, water bottles were removed from the mouse cages. FITC-dextran (4kDa, Sigma) was dissolved in PBS at a concentration of 100 mg/ml and administered to each mouse at 44mg/100g body weight by oral gavage. Mice were euthanized after 4 hours, and blood was collected immediately after via cardiac puncture. Serum was isolated from blood samples.

For analysis, serum was diluted with an equal volume of PBS. 100μl of diluted serum was added to a 96-well microplate in duplicate. Concentration of FITC in serum was determined by florescence spectroscopy. The plate was read at an excitation of 485 nm (20 nm band width) and an emission wavelength of 528 nm (20 nm band width). Serially diluted FITC-dextran (0, 125,

250, 500, 1,000, 2,000, 4,000, 6,000, 8,000 ng/ml) was used as a reference standard to calculate serum concentrations. Serum from mice gavaged with PBS instead of FITC-dextran was used to determine background.

ELISA and Luminex Assays

Cytokines from serum, liver homogenate, and cell culture supernatants were measured using the following ELISA or Luminex kits according to the manufacturer's instructions: Mouse-IFNγ ELISA MAX Kit (BioLegend), MILLIPLEX Mouse Th17 Magnetic Bead Panel (Millipore Sigma), Cytokine & Chemokine 36-Plex Mouse Procarta Plex Panel 1A (Thermo Fisher Scientific-Affymetrix), and IL-18 Mouse ELISA Kit (Invitrogen).

2.2.3 Quantification and Statistical Analysis

TUNEL Image Quantification

To quantify TUNEL staining, five images spanning the width of the liver slice were taken at 10x magnification. Images were analyzed using Image J. Briefly, images were deconvoluted to isolate and analyze only the TUNEL diaminobenzidine (DAB) staining. A threshold of the TUNEL DAB stain was determined to minimize background staining (i.e. vascular endothelial cells, erythrocytes). Identical threshold was applied to all samples per experiment. Using the "measure" feature on Image J, TUNEL+ staining was then quantified as the percent of the total image area that was above the set color threshold. To ensure that focal batches of cell death throughout the liver were accounted for, the % area TUNEL+ of all five images were averaged to determine the % Area TUNEL+ per mouse.

Single Cell RNA Sequencing Analysis

Following sequencing described above, we used Cell Ranger version 2.1.1 (10x Genomics) to process raw sequencing data and Seurat suite version 2.2.1 for downstream analysis. Filtering was performed to remove multiplets and broken cells, and non-relevant sources of variation were regressed out. Variable genes were determined by iterative selection based on the dispersion vs. average expression of the gene. For clustering, principal component analysis was performed for dimension reduction. Top 10 principal components (PCs) were selected by using a permutation-based test implemented in Seurat and passed to t-SNE for visualization of clusters.

Bulk Intestinal RNA Sequencing Analysis

Data presented is sourced from the dataset we previously published (48). See previous manuscript for detailed statistical analysis.

16S rRNA Gene Sequencing Analysis

Sequence read quality control and classifications were completed using the Center for Medicine and the Microbiome in-house read processing and classification pipeline. The read processing pipeline applied low complexity filtering (NCBI dustmasker), QV trimming, sequence adapter trimming and primer trimming modules. Sequences with both forward and reverse read directions passing read processing metrics were assembled using the make.contig command from Mothur (195). Mated reads were further screened to limit overlap mismatch proportion (<0.2), limit N's allowed (4), and enforce a minimal overlap of 25bp. Merged sequences were classified with a Mothur-dependent in-house pipeline that combines OTU generation and taxonomic classifications using the RDP/Silva classifier and includes chimera screening, clustering and

taxonomic classification. The sample taxonomic profile was subsequently represented as a matrix with dimensions: number of samples x number of taxonomic units for compositional analysis with an in-house pipeline which incorporated statistical modules and graphics using the R package (196).

Statistical Tests

Statistical tests used are indicated in the figure legends. Data are presented as mean with individual samples visualized or mean + SEM. To compare differences between two groups, student-T test or non-parametric Mann-Whitney test was used depending on the distribution of the data. When comparing one variable in three or more groups, one-way ANOVA with multiple comparisons was used. When comparing multiple variables among two groups, two-way ANOVA with multiple comparisons or multiple T-tests per row was used. GraphPad Prism software was used to analyze experimental groups. For single cell RNA sequencing, statistical analysis was based on the non-parametric Wilcoxon rank sum test. For all data, statistically significant was defined as $p<0.05$. The degree of statistical significance was defined as: $p<0.05$*, <0.01**, <0.001***, <0.0001****.

Analysis Software

GraphPad Prism was used for statistical analysis described above. Image J was used for histology analysis. Seurat, Cell Ranger, and Loupe Browser were used for single cell RNA sequencing analysis.

2.2.4 Data and Software Availability

The raw terminal ileum RNA sequencing data have been deposited into the sequencing read archive under SRA accession number SRP069071. 16S rRNA sequencing data have been deposited in the SRA under SRA BioProject accession number PRJNA526489. The liver single cell RNA sequencing data discussed in this publication have been deposited in NCBI's Gene Expression Omnibus(197) and are accessible through GEO Series accession number GSE128284 (https://www.ncbi.nlm.nih.gov/geo/query/acc.cgi?acc=GSE128284).

Figure cartoons within this chapter were images adapted from Servier Medical Art by Servier. Original images are licensed under a Creative Commons Attribution 3.0 Unported License (https://creativecommons.org/licenses/by/3.0/legalcode).

2.3 Results

2.3.1 Deletion of IL-17RA in intestinal epithelium exacerbates Concanavalin A hepatitis.

To investigate how intestinal IL-17 signaling regulates liver inflammation, we generated intestinal epithelium-specific *Il17ra* knockout mice (*Il17ra*$^{fl/fl}$ *x villin cre*$^{+}$) (48). Mice were treated with intravenous concanavalin A (Con A), a plant lectin, to induce a T-cell dependent liver injury (198). We have previously shown that globally deleting *Il17ra* is protective in this model of hepatitis (186). Interestingly, deleting *Il17ra* signaling specifically in the intestinal epithelium exacerbated disease (Figure 2-2). As compared to littermate *Il17ra*$^{fl/fl}$ controls, *Il17ra*$^{fl/fl}$ *x villin cre*$^{+}$ mice exhibited elevated serum alanine aminotransferase (ALT), a marker of liver

inflammation, and increased mortality rates (Figure 2-2A-B). Liver pathology revealed substantially larger patches of cell death in the hepatic parenchyma (Figure 2-2C). Indeed, quantification of cell death by TUNEL staining showed approximately 50% more cell death on average in *Il17ra*$^{fl/fl}$ *x villin cre*$^{+}$ mice as compared to littermate floxed controls (Figure 2-2D).

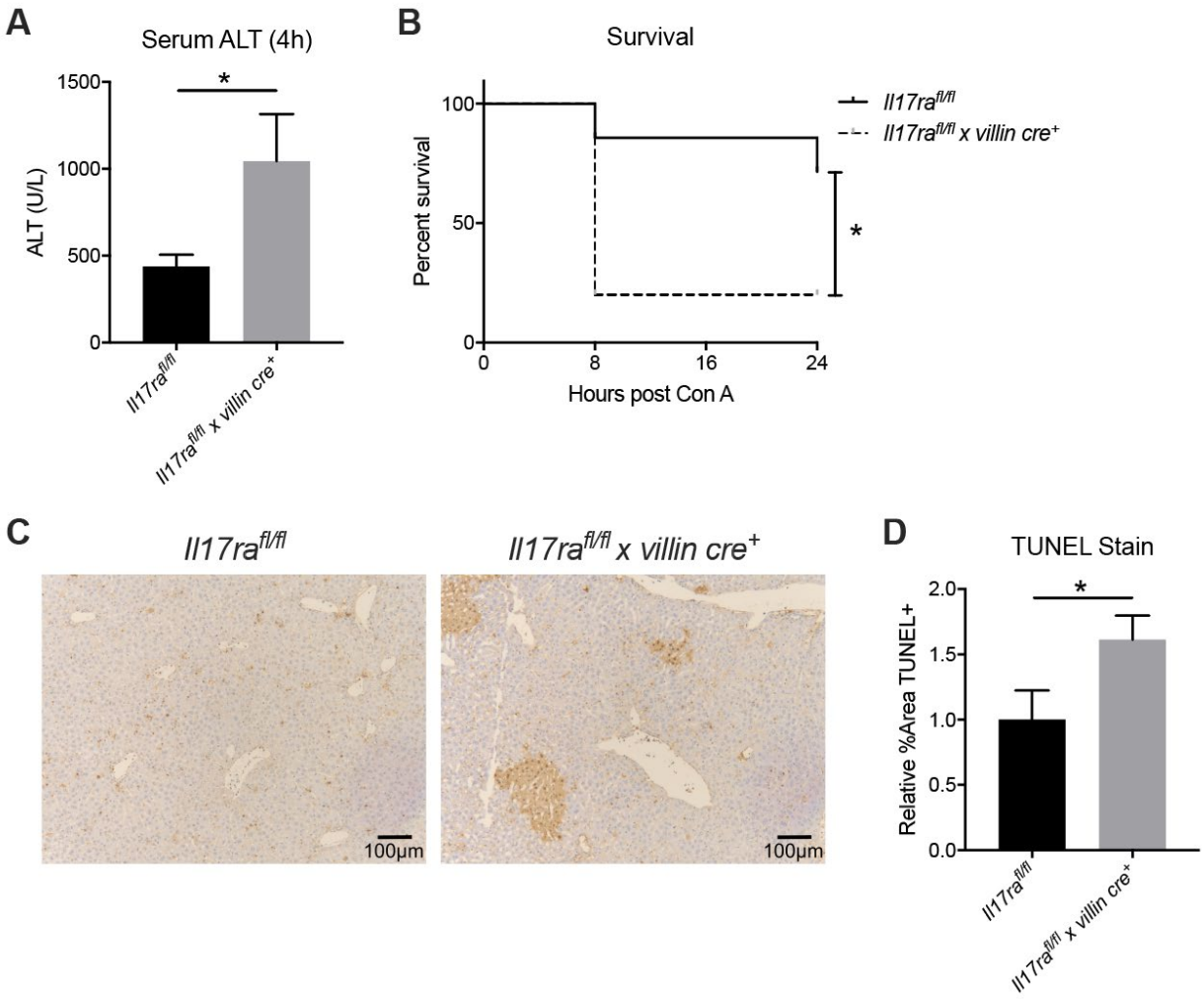

Figure 2-2. Deletion of IL-17RA in intestinal epithelium exacerbates Concanavalin A hepatitis.

Littermate *Il17ra*$^{fl/fl}$ and *Il17ra*$^{fl/fl}$ *x villin cre*$^{+}$ mice were injected IV with concanavalin A (Con A). (A) Serum alanine aminotransferase (ALT) at 4 hours post Con A (10mg/kg). (B) Survival curve after 24 hours post Con A (10mg/kg). (C) Quantification of TUNEL staining at 8 hours post Con A (25mg/kg). (D) Representative images of TUNEL-stained liver histology at 8 hours post Con A (25mg/kg). Data are represented as mean + SEM. (n=5-9 mice/group). p<0.05*, <0.01**, <0.001***, <0.0001**** (Mann-Whitney test, Gehan-Breslow-Wilcoxon test)

2.3.2 Exacerbated liver injury is dependent on the intestinal microbiota.

Given the role of Th17 cells in regulating the intestinal microbiota (48, 60, 199), we tested whether the exacerbated liver injury was microbiome dependent. To do this, we performed cohousing studies in which littermates were either cohoused or separated by genotype for one week prior to Con A injection. When separated, intestinal specific knockouts continued to demonstrate more severe disease as measured by ALT (Figure 2-3A). Cohousing the groups to share the intestinal microbiota between mice eliminated significant differences in post-Con A ALT levels (Figure 2-3B), suggesting that disease exacerbation is microbiome-dependent.

IL-17 has been strongly implicated in the regulation of bacteria in the small intestine, particularly those closely related to the intestinal epithelium such as segmented filamentous bacteria (Sfb) (48, 60). To that end, we performed 16S rRNA gene sequencing on the small intestine terminal ileum of littermate *Il17ra*$^{fl/fl}$ *x villin cre*$^{+}$ mice and floxed controls to examine changes in the microbiome due to IL-17R deficiency (Figure 2-3C). An outgrowth of Sfb in *Il17ra*$^{fl/fl}$ *x villin cre*$^{+}$ mice was seen in the naïve state and became more pronounced after Con A (Figure 2-3C). The only other difference observed at the family level was an outgrowth of *Enterobacteriaceae* seen in some *Il17ra*$^{fl/fl}$ *x villin cre*$^{+}$ mice after Con A administration (Figure 2-3C). To broadly assess which bacteria may be contributing to liver disease, we treated mice with 2 different antibiotic regimens prior to Con A. Mice either received neomycin to largely target gram-negative bacteria or vancomycin to target Sfb and other gram-positive bacteria. Based on ALT, neomycin protected mice while vancomycin had no effect, suggesting gram-negative bacteria may contribute to hepatitis in this model (Figure 2-3D-E).

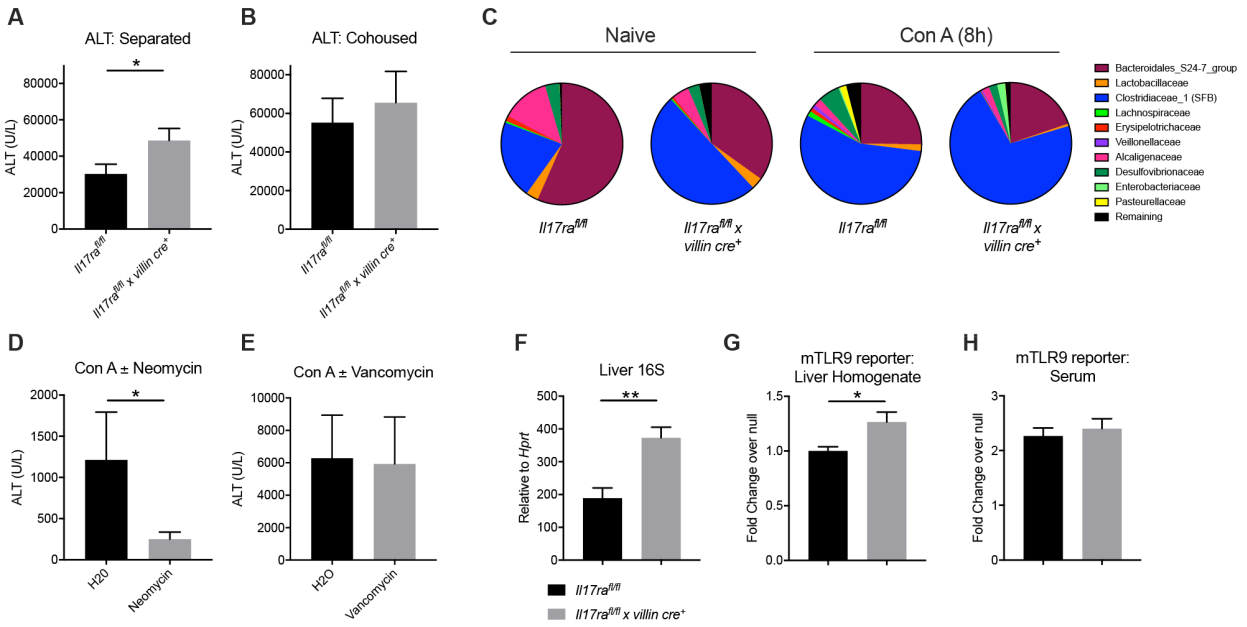

Figure 2-3. Exacerbated liver injury is dependent on the intestinal microbiota.

(A-B) Littermate *Il17ra*$^{fl/fl}$ and *Il17ra*$^{fl/fl}$ *x villin cre*$^{+}$ mice were either cohoused or separated for one week. Mice were then treated with IV concanavalin A (Con A) (25mg/kg), and serum alanine aminotransferase (ALT) was measured at 8 hours. (n=6-14 mice/group). (C) 16S sequencing on terminal ileum of littermate *Il17ra*$^{fl/fl}$ and *Il17ra*$^{fl/fl}$ *x villin cre*$^{+}$ mice at the naïve state and 8 hours post IV Con A (25mg/kg) (n=7-16 mice/group). (D-E) Mice were treated with either five days of 1g/L neomycin (D) or 14 days of 0.5g/L vancomycin (E) in the drinking water *ad libitum*. Mice were then injected with IV Con A and serum ALT was measured 8-9h post injection. (n=4-6 mice/group). (F) 16S rRNA transcript was measured by qRT-PCR in the liver of naïve littermate *Il17ra*$^{fl/fl}$ and *Il17ra*$^{fl/fl}$ *x villin cre*$^{+}$ mice (n=7-10 mice/group). (G-H) Serum and liver homogenate from naïve littermate *Il17ra*$^{fl/fl}$ and *Il17ra*$^{fl/fl}$ *x villin cre*$^{+}$ mice were plated on mTLR9 SEAP reporter cells. (n=4-8 mice/group). Absorbance of supernatants was measured and represented as ratio over null/unstimulated cells. (A-B, D-H) Data are represented as mean + SEM. p<0.05*, <0.01**, <0.001***, <0.0001**** (Unpaired T test; Multiple T tests per row; Mann-Whitney Test).

To characterize this further, we considered how the mechanisms by which Th17 cells regulate the microbiome are not necessarily specific to one bacterium. Rather, they affect the bacteria that generally reside close to the intestinal epithelium. Therefore, we hypothesized that there was a broad bacterial overgrowth in the gut specific knockout mice potentially contributing to disease. Utilizing flow cytometry partnered with counting beads (194), preliminary data showed increased fecal bacterial burden in *Il17ra*$^{fl/fl}$ *x villin cre*$^{+}$ mice as compared to littermate floxed controls (Figure 2-4A). Because intestinal secretory IgA is regulated by intestinal IL-17, IgA binding on bacteria was also analyzed. *Il17ra*$^{fl/fl}$ *x villin cre*$^{+}$ mice had an enrichment for IgA unbound (IgA-) bacteria, which were depleted with neomycin (Figure 2-4B-C). This suggested that the potentially detrimental bacterium or group of bacteria involved in exacerbating disease in gut specific knockout mice were IgA unbound bacteria overgrowing in the absence of intestinal IL-17 regulation through IgA.

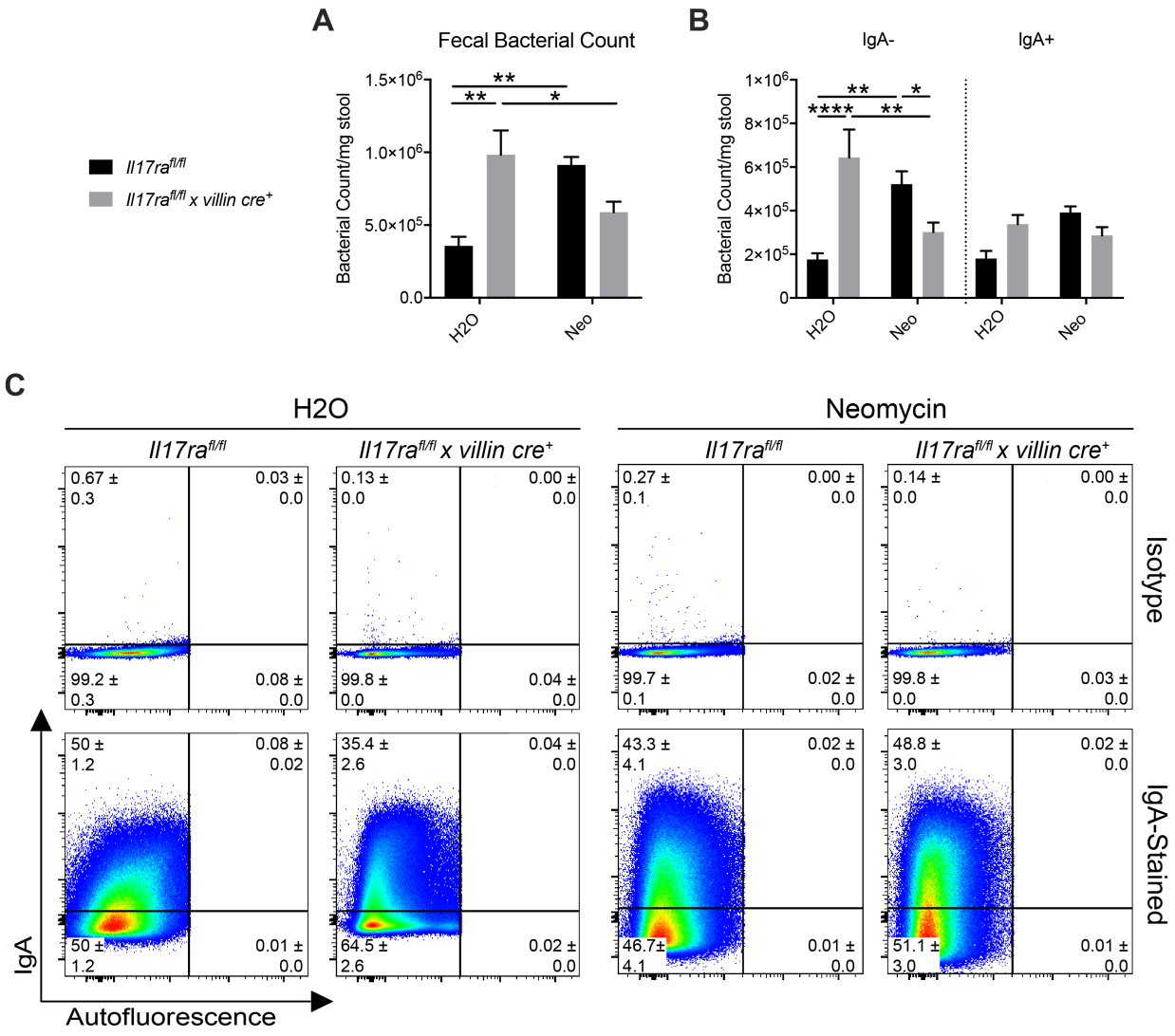

Figure 2-4. *Il17ra*$^{fl/fl}$ *x villin cre*$^{+}$ mice have an increased fecal bacterial burden, enriched with neomycin-sensitive, IgA-unbound bacteira.

(A) Fecal bacterial counts from naïve *Il17ra*$^{fl/fl}$ and *Il17ra*$^{fl/fl}$ *x villin cre*$^{+}$ mice treated with neomycin or H2O control as measured via flow cytometry. (B) Quantification of IgA unbound (IgA-) and IgA bound (IgA+) bacterial counts with and without neomycin treatment in *Il17ra*$^{fl/fl}$ and *Il17ra*$^{fl/fl}$ *x villin cre*$^{+}$ mice. (C) Representative FACS plots fecal bacteria stained with isotype or IgA (Gated by FSC, SSC, and Hoechst+). Data are representative of multiple experiments. (n = 4-5 mice/group). Data are represented as mean + SEM. p<0.05*, <0.01**, <0.001***, <0.0001**** (Two-way ANOVA with multiple comparisons).

Next, we sought to assess how the *Il17ra*$^{fl/fl}$ *x villin cre*$^{+}$ microbiota was influencing liver disease. Because Th17 signaling is critical for mucosal barrier integrity (40, 189, 199), and intestinal blood drains through the portal system to the liver, it is possible that bacteria were physically translocating to the livers of our intestinal-specific IL-17RA knockout mice. As an initial assessment, we performed 16S qRT-PCR on the livers of naïve *Il17ra*$^{fl/fl}$ *x villin cre*$^{+}$ mice and littermate controls. Results showed an increased 16S signal in gut-specific knockout mice (Figure 2-3F), suggesting more bacteria or bacterial products in the liver of these mice at baseline. We determined this signal was not from live bacteria as bacteria failed to grow from the liver in both aerobic and anaerobic conditions (data not shown). As such, mouse toll-like receptor (mTLR) reporter cell lines were subsequently utilized to assay for bacterial products. With a focus on gram-negative bacteria, serum and liver homogenate from naïve *Il17ra*$^{fl/fl}$ *x villin cre*$^{+}$ mice and littermate controls were plated on mTLR4 or mTLR9 reporter cells to measure lipopolysaccharide (LPS) and unmethylated CpG DNA levels, respectively. There were no differences in LPS levels in the serum or liver homogenate (Figure 2-5). However, there was elevated CpG DNA in the liver homogenate of *Il17ra*$^{fl/fl}$ *x villin cre*$^{+}$ mice as measured by the mTLR9 reporter line (Figure 2-3G). This was not seen in serum (Figure 2-3H), suggesting both that the liver is successfully filtering products from entering the circulation, and that CpG DNA may be signaling through TLR9 locally in the liver to influence disease. To model if elevated CpG DNA prior to disease induction exacerbates disease, wildtype *C57BL/6* mice were treated with 3 doses of CpG DNA through the week prior to Con A (Figure 2-6A). CpG DNA administration prior to Con A dramatically increased mortality rates as compared to Con A, CpG DNA, or vehicle control alone (Figure 2-6B), corroborating previous reports that CpG DNA exacerbates Con A hepatitis (147).

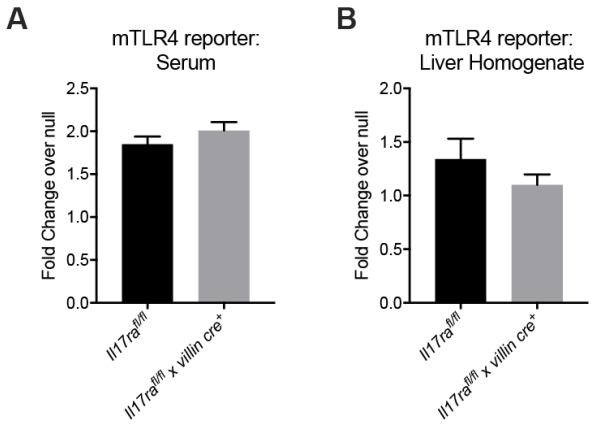

Figure 2-5. *Il17ra*$^{fl/fl}$ *x villin cre*$^{+}$ mice do not have elevated serum or liver LPS.

Serum (A) and liver homogenate (B) from naïve littermate *Il17ra*$^{fl/fl}$ and *Il17ra*$^{fl/fl}$ *x villin cre*$^{+}$ mice were plated on mTLR4 SEAP reporter cells. Absorbance of supernatants was measured and represented as ratio over null/unstimulated cells. Data are represented as mean + SEM. n =7-14 mice/group. Data are represented as mean + SEM. p<0.05*, <0.01**, <0.001***, <0.0001**** (Unpaired t- test)

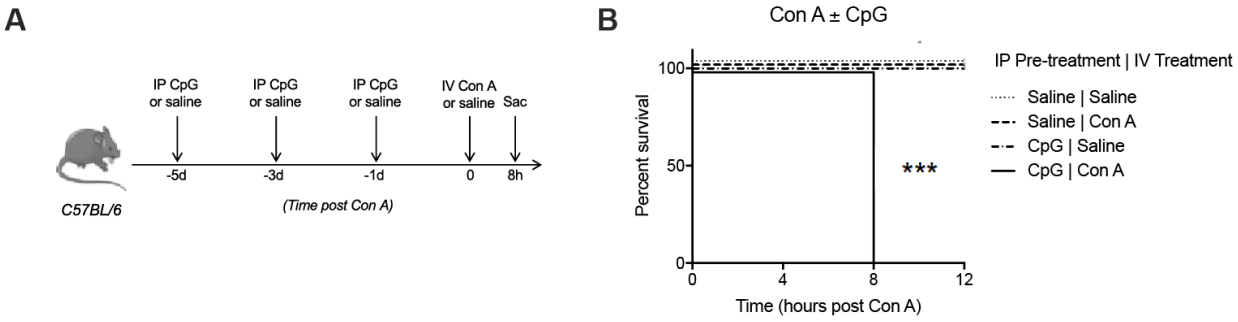

Figure 2-6. CpG DNA promotes fatal Con A hepatitis.

Wildtype *C57BL/6* mice were pretreated with IP 2.5mg/mL CpG 3x prior to IV Con A injection (10mg/mL). (A) Experimental schematic of treatment regimen. (B) Survival curve. (n=4-5 mice/group). (A-B) Data are represented as mean + SEM. p<0.05*, <0.01**, <0.001***, <0.0001**** (Log-rank (Mantel-Cox) test)

2.3.3 Intestinal IL-17RA constrains TLR9-induced Type I immune responses in the liver.

CpG DNA and subsequent TLR9 signaling are capable of eliciting a variety of inflammatory cytokines such as IL-12, IL-6, and interferons (200–202). To investigate which CpG-inducible cytokines may be contributing to worsened liver disease in gut-specific knockout mice, we first wanted to establish which cytokines were elevated in *Il17ra*$^{fl/fl}$ *x villin cre*$^{+}$ mice. To employ a broad, unbiased approach, we performed single cell RNA sequencing. Previous reports have detailed cytokine changes at the protein level within hours of Con A injection (203). Therefore, we chose a ninety-minute post-injection timepoint to investigate transcriptional changes induced early in the model. We compared the liver transcriptome of *Il17ra*$^{fl/fl}$ *x villin cre*$^{+}$ mice against littermate *Il17ra*$^{fl/fl}$ controls. Based on K-means clustering and upregulation of cell-specific genes (Table 2-1), we identified 12 distinct cell populations (Figure 2-7A). One of the significantly upregulated genes in *Il17ra*$^{fl/fl}$ *x villin cre*$^{+}$ mice was *Ifng* (Figure 2-7B-C). IFNγ is a known contributor to liver inflammation in Con A hepatitis and an indicator of lymphocyte activation (204–206). In the single cell RNA sequencing dataset, *Ifng* was expressed by T cells (CD4+ and CD8+ T cells), NK cells, and NKT cells (Figure 2-7C). There were also increases in downstream IFNγ targets such as *Cxcl9* and *Cxcl10* (Fig 3B), providing further evidence of *Ifng* upregulation.

Table 2-1. Single Cell RNAseq Cluster Gene Lists.

Cell-type specific gene lists (bold) and top 50 most significantly differentially expressed genes per cluster.

Cluster:	1	2	3	4	5	6	7	8	9	10	11	12
Cell Type:	Hepatic Stellate Cells	Kupffer Cells	Cholangio-cytes	Monos/ Macs	B Cells	Endothel-ial Cells	T Cells	NKT Cells	NK Cells	Neutro-phils	Hepato-cytes	RBCs
Genes:	**Col1a1**	**Clec4f**	**Krt7**	**Cd68**	**Cd79a**	**Ushbp1**	**Cd3e**	**Cd3e**	**Nkg7**	**S100a8**	**Alb**	**Hbb-bt**
	Col11a2	**Spic**	**Krt19**	**Ccr2**	**Cd38**	**Oit3**	**Cd4**	**Nkg7**	**Cd3e NEG**			**Hbb-bs**
	Acta1	**Marco**	**Tff2**	**Ly6c2**	**Igll1**	**F8**	**Cd8a**					**Hba-a2**
	Tagln	**Vsig4**	**Scgb3a1**	**Lyz1**	**Cd19**	**Bmp2**						**Hba-a1**
	Col13a1	**Cpvl**	**Fxyd2**	**Lyz2**	**Cd79b**	**Mmrn2**						**Bpgm**
	Rbp1	**Cd163**	**Defb1**									**Snca**
	Sparc	**Cd68**										
	Dpt	Clec4f	Krt19	Cd209a	Fcmr	Cldn5	Cd3d	Cd160	Gzma	S100a9	Hpd	Hbb-bt
	Ccl19	Cd5l	Fxyd3	Ms4a6c	Cd79a	Clec4g	Lat	Ccl1	Klrb1c	S100a8	Uox	Hba-a2
	Mfap4	C1qc	Spp1	Tnip3	Ms4a1	Gpihbp1	Cd3g	Il13	Ncr1	Retnlg	Gnmt	Hbb-bs
	Gsn	Folr2	Cldn7	Lgals3	Vpreb3	Cyp4b1	Cd2	Il4	Klre1	Il1f9	Cdo1	Hba-a1
	Mmp2	Vsig4	Upk3b	AA467197	Ebf1	Oit3	Nfkbid	Lat	Klra9	Ltf	Fabp1	Bpgm
	Htra3	C1qa	Msln	Ccl17	Cd79b	Fam167b	Lck	Ccl4	Ccl5	Mmp8	Arg1	Snca
	Lum	Fcna	Nkain4	Alox5ap	H2-DMb2	Gpr182	Ms4a4b	Furin	Klrd1	Pglyrp1	Fbp1	Alas2
	Sparcl1	Spic	Tm4sf4	H2-DMb1	Cd72	Lyve1	Satb1	Cd3d	Klra7	Mrgpra2b	Bhmt	Mkrn1
	Col1a2	Adgre1	Myl7	Plac8	Serpinb1a	Egfl7	Ifng	Ifng	Klrk1	Cd177	Sult2a8	Ube2l6
	Col1a1	C1qb	Clu	Spi1	Stap1	Ehd3	Cd160	Nfkbid	Nkg7	G0s2	Agxt	Cd24a
	Sfrp1	Wfdc17	Tstd1	Ifi205	Cd83	Apold1	Bcl2	Cd3g	Klrc1	Ly6g	Pck1	Car2
	Col3a1	Csf1r	Efemp1	Ly6c2	Ly6d	Dnase1l3	Gzmb	Hcst	Ctsw	Ngp	Aldob	Gpx1
	Clec3b	Cfp	Igfbp6	Lsp1	Pkib	Esam	Hcst	Xcl1	Txk	Ifitm6	Akr1c6	Creg1
	Crispld2	Aif1	Krt8	Osm	Il4i1	Bmp2	Il2rb	Il2	Cd7	Camp	Otc	Sec61g
	Cygb	Hmox1	Epcam	Mcemp1	Cd37	Stab2	Xcl1	Gzmb	AW112010	Mmp9	Ttc36	Rsad2
	Acta2	Marco	Krt18	Lyz2	Cd74	Ptprb	Vsir	Nr4a1	Il2rb	Hcar2	Angptl3	mt-Cytb
	Fbln1	Acp5	Bicc1	Tarm1	Samsn1	Eng	Ptprc	Id2	Serpinb9	Fpr1	Serpina1a	mt-Nd4
	Tagln	Cd68	Slpi	Ccl9	Cd69	Kdr	Srm	Dusp5	Rgs1	Clec4d	Tat	mt-Co3
	Gpx3	Oasl1	Alcam	Mpeg1	Ccr7	Rasip1	Il2	Nkg7	Gzmb	Fpr2	Adh1	mt-Atp6
	Myh11	Ctsc	Ankrd1	Clec4e	Ptprcap	Stab1	Nolc1	Il2rb	Ms4a4b	Chil1	Mat1a	mt-Nd1
	Col6a2	Lst1	Igfbp5	Bcl2a1a	H2-Aa	Ramp2	Vps37b	Lck	Selplg	Cd33	Serpina1b	mt-Co2
	Mustn1	Slc40a1	Gpm6a	H2-DMa	H2-Ab1	Plpp1	Nr4a1	Vsir	Xcl1	Chil3	Car3	mt-Co1
	Loxl1	Pilra	C3	Il1rn	Cd24a	Fabp4	Txk	Socs1	Car2	Irg1	Hgd	mt-Nd2
	Tnfaip6	Mpeg1	Cryab	Bcl2a1d	Mef2c	Nrp1	Cd53	Dusp2	Hcst	Lcn2	Apoc3	mt-Nd3
	Ccl11	C5ar1	Ces1d	Lilrb4a	H2-Eb1	Tspan7	Tagap	Ccnd2	Tyrobp	Mcemp1	Ass1	Hagh
	Tpm2	Ctss	Cystm1	Ccr1	Stk17b	Fcgr2b	Ctsw	Satb1	Serpinb6b	C5ar1	Ttpa	Blvrb
	Col6a1	Cxcl13	Sorbs2	Tyrobp	Camk2d	Adgrf5	Ccl4	Ccl3	Bcl2	Il1r2	Serpina1d	
	Cxcl12	Bcl2a1a	Rarres2	Cybb	H2-DMa	Akap12	Ccl1	Ddx21	Ifngr1	Clec4e	Rgn	
	Myl9	Ccl12	Has1	Ctss	Rac2	Mrc1	Nop56	Nfkb1	Ccl3	Cd300lf	Urah	
	Smoc2	Sdc3	Tnfrsf12a	Il1b	Coro1a	Icam2	Ddx21	Srgn	Ptprcap	Clec12a	Serpina1e	
	Thbs1	Mmp13	Aebp1	Fcgr3	Hmgb2	Sgk1	Il4	Bcl2	Vps37b	Wfdc21	Cth	
	Mylk	Il1b	Cp	H2-Eb1	Btg1	Flt1	Ccr7	Nolc1	Fcer1g	Slfn1	Hamp	
	Fstl1	Cybb	Bcam	Cd68	Satb1	Plpp3	Il13	Nop56	Cd52	Arg2	Tdo2	
	Serpinf1	Tnfaip2	Plscr1	H2-Ab1	Limd2	Gatm	Peli1	Serpinb6b	Id2	Asprv1	Orm1	
	Eln	Fcgr3	Timp2	Ccl6	Ppp1r16b	Gja1	Dusp5	Nhp2	Rac2	Slc7a11	Alb	
	Mgp	Fpr2	Nupr1	H2-Aa	Dusp2	Aqp1	Nkg7	Txk	Cd3g	Ccr1	Sds	
	Lhfp	Ccl24	Serping1	Cst3	Cd53	Tm4sf1	Socs1	Tomm20	Lck	Ptafr	Serpina3k	
	Dcn	Il1rn	Chka	Snx20	Foxp1	Tcn2	Furin	Ptpn18	Ptprc	Tarm1	Acaa1b	
	Igfbp3	Lyz2	Timp1	Clec4n	Ezr	Sdpr	Ncl	Ncl	Pglyrp1	Pilra	Gc	
	Tppp3	Bcl2a1b	F3	Ptafr	Rel	Pecam1	C1qbp	Cd82	Limd2	Glrx	Pecr	
	Ptx3	Spi1	Prss23	Cd44	Cd52	Cd55	Npm1	Srm	Laptm5	Anxa1	Gsta3	
	Col14a1	Arg2	Meg3	Lst1	Serp1	Cdh5	Rpl12	Ms4a4b	Ccl4	Fcgr3	Apoc4	
	Ogn	Kctd12	Ogn	Plek	Hmgn2	Cd36	Ptpn18	Gimap5	Cd82	Lilr4b	Azgp1	
	Il11ra1	Clec12a	Ambp	Clec12a	H3f3a	Sepp1	Cd82	Vps37b	Lcp1	Cd14	Hamp2	
	Meg3	Clec4n	Nbl1	Fam49b	Samhd1	Gng11	Eif5a	Ubald2	Cd2	Gm5483	Apoa2	
	Cd34	Fpr1	Bsg	Cd74	Laptm5	Rhoc	Mif	Rpl12	Fxyd5	Osm	Hmgcs2	
	Nbl1	Tyrobp	S100a6	Lilr4b	Lmnb1	Upp1	Fbl	Rpl7	Ptpn18	Il1b	Serpina1c	
	Adm	Ccl7	Rnase4	Syngr2	Ctsc	Serpina3f	Stk17b	Eif5b	Coro1a	Cxcl3	Ahsg	
	Ccl7	Lilrb4a	Gas6	Cd300lf	Anp32b	Klf7	Nhp2	Rpl31	Ubald2	Mxd1	Rbp4	
	Pcolce	Cd14	Crip1	Serpinb2	Stmn1	Fcgrt	Rplp0	Stk17b	Lgals1	Fbxl5	Fgg	

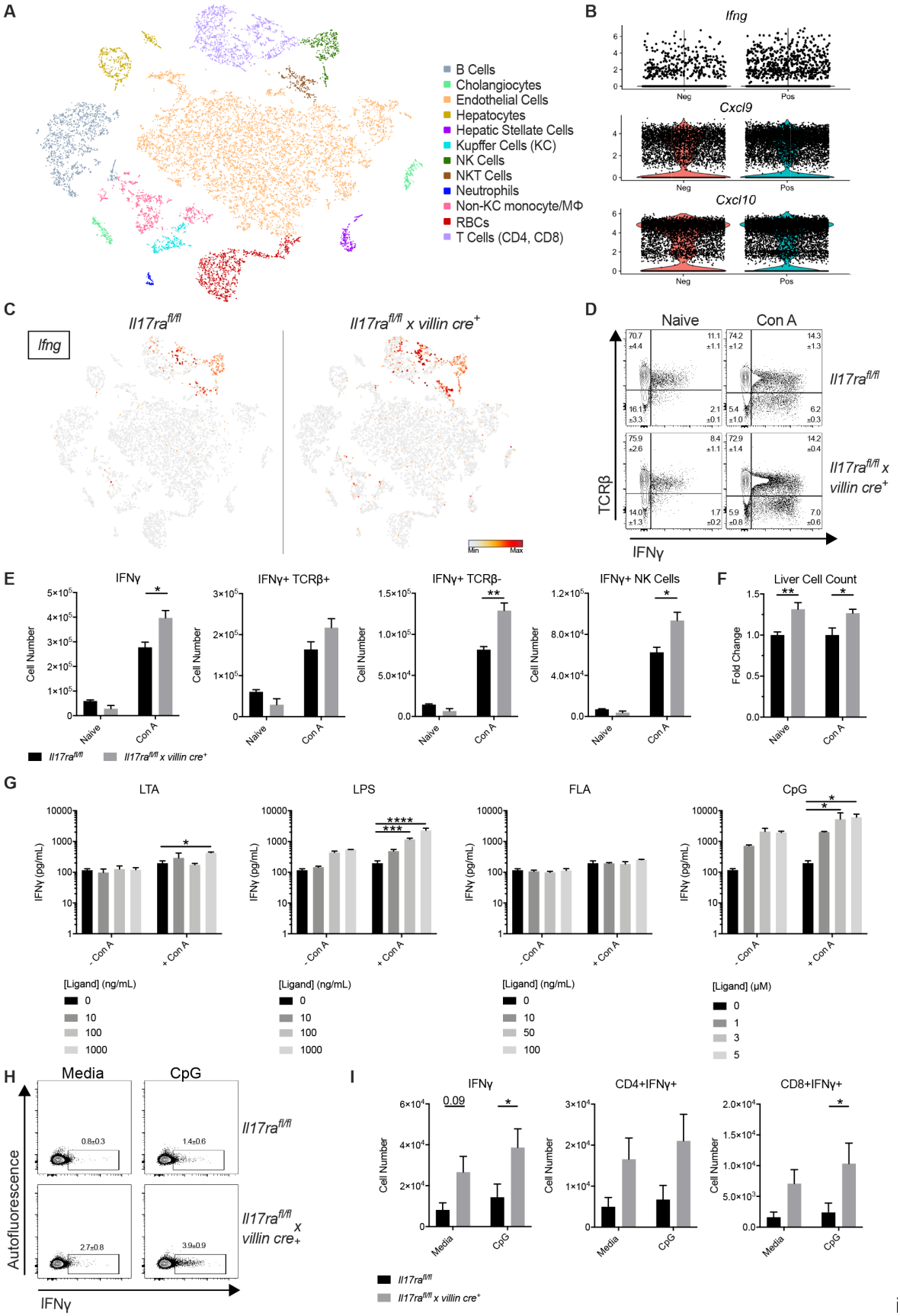
A
B Cells
Cholangiocytes
Endothelial Cells
Hepatocytes
Hepatic Stellate Cells
Kupffer Cells (KC)
NK Cells
NKT Cells
Neutrophils
Non-KC monocyte/MΦ
RBCs
T Cells (CD4, CD8)
B
Ifng
Cxcl9
Cxcl10
Neg
Pos
C
Ifng
Il17ra fl/fl
Il17ra fl/fl x villin cre+
Min
Max
D
Naive
Con A
Il17ra fl/fl
Il17ra fl/fl x villin cre+
TCRβ
IFNγ
E
IFNγ
IFNγ+ TCRβ+
IFNγ+ TCRβ-
IFNγ+ NK Cells
Cell Number
Naive
Con A
Il17ra fl/fl
Il17ra fl/fl x villin cre+
F
Liver Cell Count
Fold Change
G
LTA
LPS
FLA
CpG
IFNγ (pg/mL)
- Con A
+ Con A
[Ligand] (ng/mL)
0
10
100
1000
50
[Ligand] (μM)
1
3
5
H
Media
CpG
Il17ra fl/fl
Il17ra fl/fl x villin cre+
Autofluorescence
IFNγ
I
IFNγ
CD4+IFNγ+
CD8+IFNγ+
Cell Number
Media
CpG
Il17ra fl/fl
Il17ra fl/fl x villin cre+

Figure 2-7. Intestinal IL-17RA constrains TLR9-induced Type I immune responses in the liver.

(A-C) Ninety minutes after IV concanavalin A (25mg/kg), single cell RNA sequencing was performed on *Il17ra*$^{fl/fl}$ and *Il17ra*$^{fl/fl}$ *x villin cre*$^{+}$ liver cells enriched for mononuclear cells. (n=2 mice/group) (A)TSNE of cell type clustering based on K means clustering and cell-specific gene expression. There is minor overlap between NK and T cell populations. (B) Violin plots of *Ifng*, *Cxcl9*, and *Cxcl10* expression in *Il17ra*$^{fl/fl}$ ("Neg") and *Il17ra*$^{fl/fl}$ *x villin cre*$^{+}$ ("Pos") liver datasets. All violin plots displayed (B) show gene expression significantly increased in *Il17ra*$^{fl/fl}$ *x villin cre*$^{+}$ ("Pos") with a $p < 0.05$ by Wilcoxon rank sum test. (C) TSNE of *Ifng* expressing cells in *Il17ra*$^{fl/fl}$ and *Il17ra*$^{fl/fl}$ *x villin cre*$^{+}$ liver datasets colored according to relative expression level. (D-E) Flow cytometry analysis of liver cells of littermate *Il17ra*$^{fl/fl}$ and *Il17ra*$^{fl/fl}$ *x villin cre*$^{+}$ mice at the naïve state and 5 hours post IV Con A (25mg/kg) injection. (n=2-4 mice/group) (D) Representative flow cytometry plots. (E) Number of live IFNγ+ cells, live IFNγ+TCRβ+ cells, live IFNγ+TCRβ- cells, and live IFNγ+ NK Cells (gated on CD90+TCRβ-NK1.1+). (F) Total liver cell number plotted as fold change over *Il17ra*$^{fl/fl}$. (n= 3-16 mice/group). (G) Livers from wildtype *C57BL/6* mice were harvested and enriched for mononuclear cells. Cells were stimulated *ex vivo* with varying concentrations of TLR ligands (lipoteichoic acid (LTA), flagellin (FLA), lipopolysaccharide (LPS), or CpG) ± Con A (5μg/mL). IFNγ was measured in culture supernatants at 24 hours by Luminex. (n=2 replicates/condition). (H-I) Livers from naive littermate *Il17ra*$^{fl/fl}$ and *Il17ra*$^{fl/fl}$ *x villin cre*$^{+}$ mice were harvested and enriched for mononuclear cells. Cells were stimulated *ex vivo* with 1μM CpG for 4 hours plus an additional 3 hours with brefeldin A, and then analyzed by flow cytometry. (H) Representative FACS plots. (I) Number of live IFNγ+ cells, CD4+ IFNγ+ cells (gated on live CD90+TCRβ+), and CD8+ IFNγ+ cells (gated on live CD90+TCRβ+). (n=3-4 mice/group). (E-G, I) Data are represented as mean + SEM. $p<0.05$*, <0.01**, <0.001***, <0.0001**** (Unpaired T test, Two-Way ANOVA with multiple comparisons, Multiple T tests)

To confirm this at the protein level, we performed flow cytometry at the naïve state and 5 hours post-Con A injection (Figure 2-7D-E). There was a greater number of IFNγ+ cells in the liver of *Il17ra*$^{fl/fl}$ *x villin cre*$^{+}$ mice after Con A as compared to littermate controls (Figure 2-7D-E). This was due to significant increases in IFNγ-producing TCRβ- cells, namely NK cells, and trends toward increased IFNγ-producing TCRβ+ cells (Figure 2-7E). Though there were no differences in the percentage of IFNγ-producing cells, *Il17ra*$^{fl/fl}$ *x villin cre*$^{+}$ mice displayed an increase in actual IFNγ+ cell number due to a 25-30% increase in liver cellularity observed both at the naïve state and 5 hours after Con A (Figure 2-7F). These differences were eliminated upon cohousing, suggesting these IFNγ changes were microbiome-dependent (Figure 2-8).

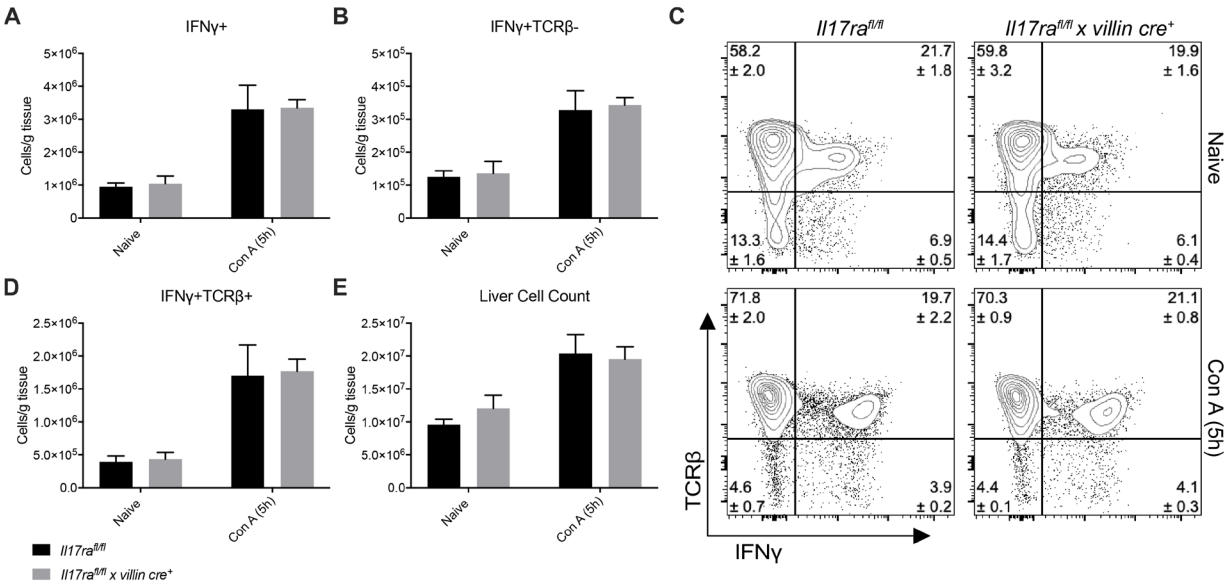

Figure 2-8. Cohousing eliminates differences in liver IFNγ between *Il17ra$^{fl/fl}$ x villin cre^{+}* mice and floxed controls.

Livers from *Il17ra$^{fl/fl}$* and *Il17ra$^{fl/fl}$ x villin cre^{+}* mice at the naïve state and 5h-post Con A were harvested, enriched for mononuclear cells, and analyzed via flow cytometry (n = 3-4 mice/group. (A) Number of IFNγ+ cells (gated on live cells). (B) Number of IFNγ+TCRβ- cells (gated on live CD90+). (C) Representative FACS plots. (D) Number of IFNγ+TCRβ+ cells (gated on live CD90+). (E) Total liver cell count per gram of tissue. Data are represented as mean + SEM. p<0.05*, <0.01**, <0.001***, <0.0001**** (Two-Way ANOVA with multiple comparisons).

To confirm that CpG DNA can induce IFNγ in the liver, we harvested livers from naïve wildtype *C57BL/6* mice, enriched for mononuclear cells, and stimulated with increasing concentrations of CpG DNA or other TLR ligands. Moreover, to assess whether these ligands can synergize with Con A, each TLR ligand was tested in the absence or presence of Con A. CpG DNA, LPS, and lipoteichoic acid (LTA), a TLR2 ligand, all induced IFNγ responses (Figure 2-7G). In contrast, flagellin (FLA), a TLR5 ligand, did not induce IFNγ responses (Figure 2-7G). Even at low concentrations, CpG DNA induced strong IFNγ responses, which added to IFNγ responses with Con A alone (Figure 2-7F). These data confirmed that CpG DNA is a potent inducer of liver IFNγ and suggested that CpG DNA may not only contribute to the elevated IFNγ observed in *Il17ra*$^{fl/fl}$ *x villin cre*$^{+}$ mice *in vivo* but synergize with Con A to enhance responses and worsen disease.

To assess differences in CpG-induced IFNγ responses and determine the cellular source of IFNγ, *Il17ra*$^{fl/fl}$ *x villin cre*$^{+}$ and littermate control livers were stimulated with CpG DNA *ex vivo* and analyzed by flow cytometry. Interestingly, there was already a slight increase in IFNγ+ cells in *Il17ra*$^{fl/fl}$ *x villin cre*$^{+}$ liver cells cultured in media alone (Figure 2-7H-I). This supported our hypothesis that the elevated CpG DNA at baseline may be inducing inflammatory cytokines locally. After CpG DNA treatment, the elevated IFNγ became more pronounced (Figure 2-7I), with much of the IFNγ proportionally coming from CD4+ and CD8+ T cells (Figure 2-7I, Figure 2-9). Of these cell populations, *Il17ra*$^{fl/fl}$ *x villin cre*$^{+}$ mice demonstrated significantly increased CD8+ IFNγ producers (Figure 2-7I).

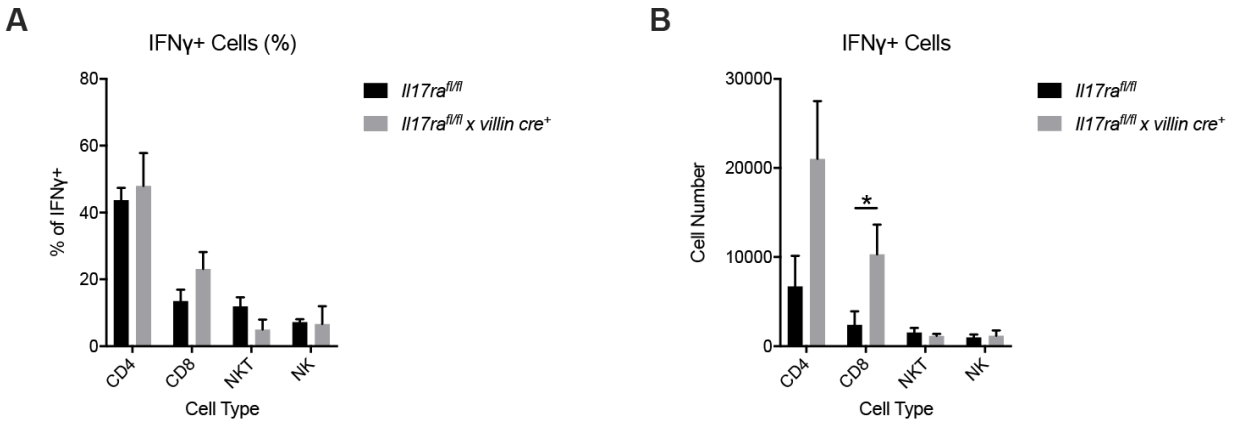

Figure 2-9. CD4 and CD8 T cells comprise the majority of IFNγ+ cells following CpG DNA stimulation.

Livers from naive littermate *Il17ra*$^{fl/fl}$ and *Il17ra*$^{fl/fl}$ *x villin cre*$^{+}$ mice were harvested and enriched for mononuclear cells. Cells were stimulated ex vivo with 1μM CpG for 4 hours plus an additional 3 hours with brefeldin A, and then analyzed by flow cytometry. Percent (A) and actual cell number (B) of IFNγ+ cells by cell type (gated on live IFNγ+ cells). Data are represented as mean + SEM. (n=3-4 mice/group). p<0.05*, <0.01**, <0.001***, <0.0001**** (Multiple T tests per row).

Taken together, these data suggest that in addition to having more CpG DNA in their livers at baseline, intestinal specific knockouts demonstrate a baseline low-level elevation in IFNγ and enhanced responses to CpG DNA. This then prompted the question of what factors were present in *Il17ra*$^{fl/fl}$ *x villin cre*$^{+}$ mice that were responsible for enhancing IFNγ responses. In addition, TLR9 is not highly expressed on T cells or NK cells, potentially implicating an intermediate factor to facilitate these IFNγ responses to CpG DNA.

2.3.4 Intestinal IL-17RA constrains hepatic and intestinal IL-18.

Single cell RNA sequencing also revealed increased *Il18* expression in *Il17ra*$^{fl/fl}$ *x villin cre*$^{+}$ livers (Figure 2-10A-B). IL-18 has been implicated in many inflammatory conditions such as macrophage activation syndrome, rheumatoid arthritis, and hepatitis (207–209). We chose to investigate IL-18 further due to its established ability to enhance IFNγ production (207, 210).

Within the liver, bacterial products like CpG DNA have been shown to activate cells close to the hepatic vasculature, such as Kupffer cells and hepatic stellate cells (159, 211–214). Indeed, analysis of the single cell sequencing data showed that *Il18* was expressed mainly in Kupffer cells, cholangiocytes, and to a lesser extent, a non-Kupffer cell monocyte/macrophage population (Figure 2-10A). Consistent with the single cell RNA sequencing data, we observed increased *Il18* transcript in the liver by qRT-PCR and IL-18 protein in liver homogenate and serum of naïve *Il17ra*$^{fl/fl}$ *x villin cre*$^{+}$ mice (Figure 2-10C-E).

Interestingly, we also observed elevated *Il18* transcript in the small intestine of *Il17ra*$^{fl/fl}$ *x villin cre*$^{+}$ mice (Figure 2-10F), suggesting that the elevated liver IL-18 may be coming from local hepatic IL-18 production as well as intestinal IL-18 through the portal circulation. Furthermore, neomycin treatment in the drinking water (which depletes gram-negative bacteria) decreased serum IL-18, providing additional support for not just intestinal involvement, but specifically microbiome involvement in IL-18 regulation (Figure 2-10G).

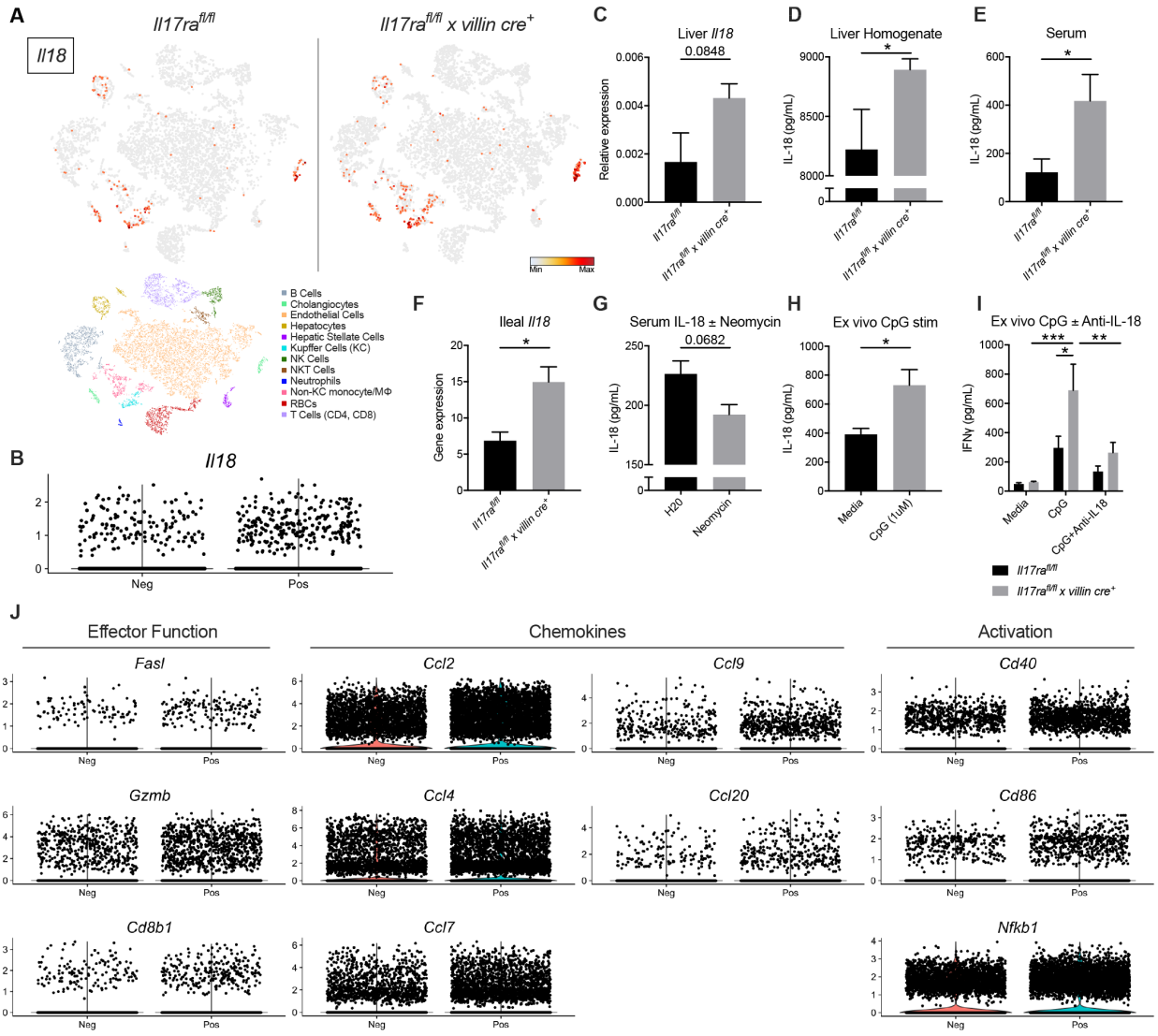

Figure 2-10. Intestinal IL-17RA constrains hepatic and intestinal IL-18.

(A-B, J) Ninety minutes after IV concanavalin A (25mg/kg), single cell RNA sequencing was performed on *Il17ra*$^{fl/fl}$ and *Il17ra*$^{fl/fl}$ *x villin cre*$^{+}$ liver cells enriched for mononuclear cells. (n=2 mice/group) (A) TSNE of *Il18* expressing cells in *Il17ra*$^{fl/fl}$ and *Il17ra*$^{fl/fl}$ *x villin cre*$^{+}$ liver datasets colored according to relative expression level. TSNE of cell type clustering for reference (Identical to Figure 3A). (B) Violin plot of *Il18* expression in *Il17ra*$^{fl/fl}$ ("Neg") and *Il17ra*$^{fl/fl}$ *x villin cre*$^{+}$ ("Pos") liver datasets. (C-F) In naïve littermate *Il17ra*$^{fl/fl}$ and *Il17ra*$^{fl/fl}$ *x villin cre*$^{+}$ mice, liver *Il18* transcript (C), liver IL-18 (D), serum IL-18 (E), and terminal ileum *Il18* (F) was measured. (G) Serum IL-18 was measured after mice were treated with 5 days of 1g/L neomycin in drinking water *ad libitum.* (H-I) Liver cells of naïve wildtype *C57BL/6* mice (H) or littermate *Il17ra*$^{fl/fl}$ and *Il17ra*$^{fl/fl}$ *x villin cre*$^{+}$ mice (I) were enriched for mononuclear

cells and stimulated with CpG (1μM) ± anti-IL-18 (5μg/mL) for 24 hours. IL-18 (H) and IFNγ (I) were measured in culture supernatants by ELISA. (J) Violin plots of various gene expression levels in *Il17ra*$^{fl/fl}$ ("Neg") and *Il17ra*$^{fl/fl}$ *x villin cre*$^{+}$ ("Pos") liver single cell RNA sequencing 90 minutes post IV Con A. All violin plots displayed (B, J) show gene expression significantly increased in *Il17ra*$^{fl/fl}$ *x villin cre*$^{+}$ ("Pos") with a $p < 0.05$ by Wilcoxon rank sum test. (C-I) Data are represented as mean + SEM. (n=3-8 mice/group). p<0.05*, <0.01**, <0.001***, <0.0001**** (Unpaired T Test, Two-Way ANOVA with Multiple Comparisons Test)

To assess whether CpG DNA plays a role in the elevated hepatic IL-18 levels, hepatic mononuclear cells were stimulated *ex vivo* with CpG DNA. Indeed, we observed IL-18 induction after CpG DNA stimulation (Figure 2-10H). Moreover, CpG-induced IFNγ was decreased *ex vivo* by treatment with anti-IL-18 antibody, suggesting that CpG DNA is inducing liver IFNγ in an IL-18 dependent manner (Figure 2-10I). To assess the contribution of IFNγ to exacerbated disease gut-specific knockout mice, *Il17ra*$^{fl/fl}$ *x villin cre*$^{+}$ mice were treated with anti-IFNγ prior to Con A injection. Interestingly, blockade of IFNγ did not ameliorate disease (Figure 2-11A) despite confirmation of IFNγ neutralization by serum ELISA (Figure 2-11B). Because of this, we examined other downstream IL-18 targets that may be contributing to disease.

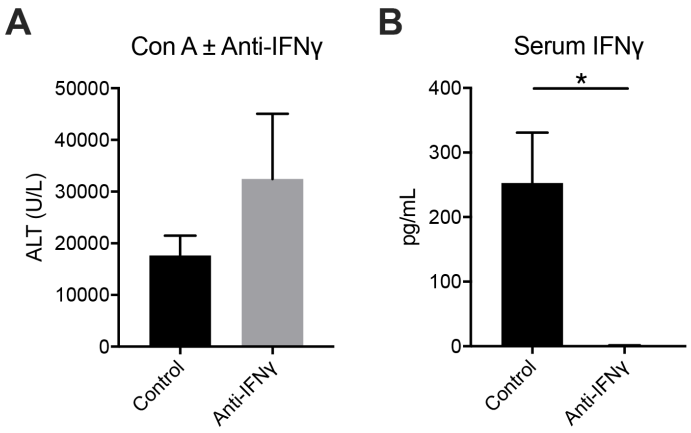

Figure 2-11. IFNγ blockade did not ameliorate hepatitis in *Il17ra*$^{fl/fl}$ *x villin cre*$^{+}$ mice.

(A) Con A (25mg/kg) was injected IV into *Il17ra*$^{fl/fl}$ *x villin cre*$^{+}$ mice treated with Anti-IFNγ or control two hours prior to Con A injection. (A) Serum ALT at 8h post injection (n = 9-13 mice/group). (B) Serum IFNγ at 8h post injection as measured by ELISA (n = 3-5 mice/group). Data are represented as mean + SEM. (n=3-8 mice/group). p<0.05*, <0.01**, <0.001***, <0.0001**** (Unpaired T Test)

2.3.5 IL-18-induced FasL exacerbates liver inflammation.

Fas ligand (FasL) has been strongly implicated in Con A hepatitis, as knockout of either *Fas* or *Fasl* is sufficient to ameliorate disease (215–217). Within the liver, *Fasl* was mainly expressed by T cells, NK cells, and NKT cells (Figure 2-12). In addition to increased *Fasl* in *Il17ra*$^{fl/fl}$ *x villin cre*$^{+}$ mice by scRNAseq (Figure 2-10J), we observed increased FasL+ cells in the liver of naïve *Il17ra*$^{fl/fl}$ *x villin cre*$^{+}$ mice by flow cytometry (Figure 2-13A). There was also more FasL produced per cell as measured by geometric mean fluorescence intensity (gMFI) (Figure 2-13B-C). These differences were eliminated upon cohousing, suggesting these FasL changes were microbiome-dependent (Figure 2-14).

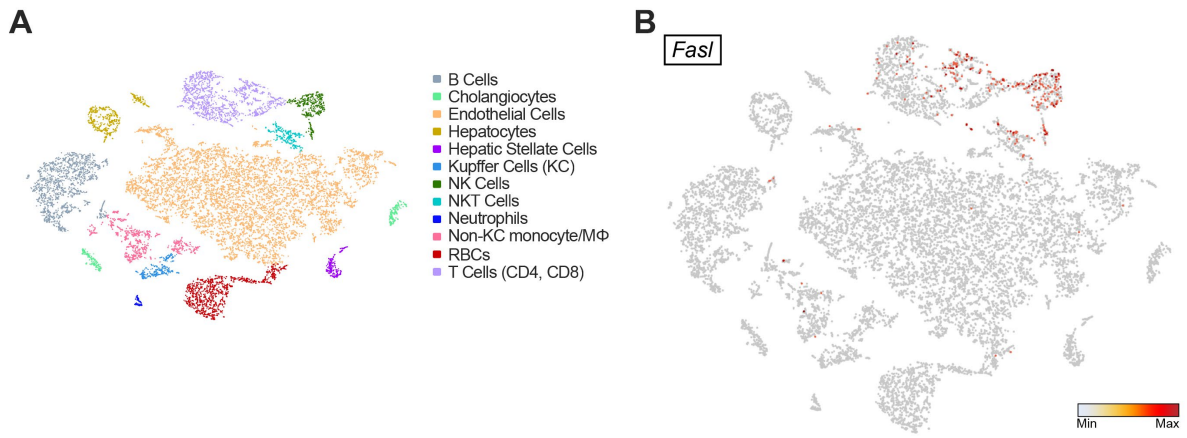

Figure 2-12. *Fasl* is expresed by liver T cells, NK cells, and NKT cells.

Single cell RNA sequencing was performed on *Il17ra*$^{fl/fl}$ and *Il17ra*$^{fl/fl}$ *x villin cre*$^{+}$ liver cells enriched for mononuclear cells 90min after IV Con A (25mg/kg). (n=4 mice). (A)TSNE of cell type clustering based on K means clustering and cell-specific gene expression. (B) TSNE of *Fasl* expressing cells colored according to relative expression level.

To test whether increases in FasL contributed to Con A hepatitis, we treated mice with anti-FasL one hour prior to Con A injection. Results suggested that anti-FasL treatment ameliorated disease in gut-specific knockout mice as measured by serum ALT and TUNEL staining (Figure 2-13D-F). To investigate whether IL-18 can induce liver FasL, livers of naïve littermate *Il17ra*$^{fl/fl}$ *x villin cre*$^{+}$ mice and floxed controls were enriched for mononuclear cells, stimulated *ex vivo* with IL-18 ± anti-IFNγ, and analyzed by flow cytometry (Figure 2-13G-H). While there were no significant differences between responses of *Il17ra*$^{fl/fl}$ *x villin cre*$^{+}$ mice and floxed controls, results showed that IL-18 stimulated FasL production in TCRβ+ cells in an IFNγ-independent manner (Figure 2-13G-H).

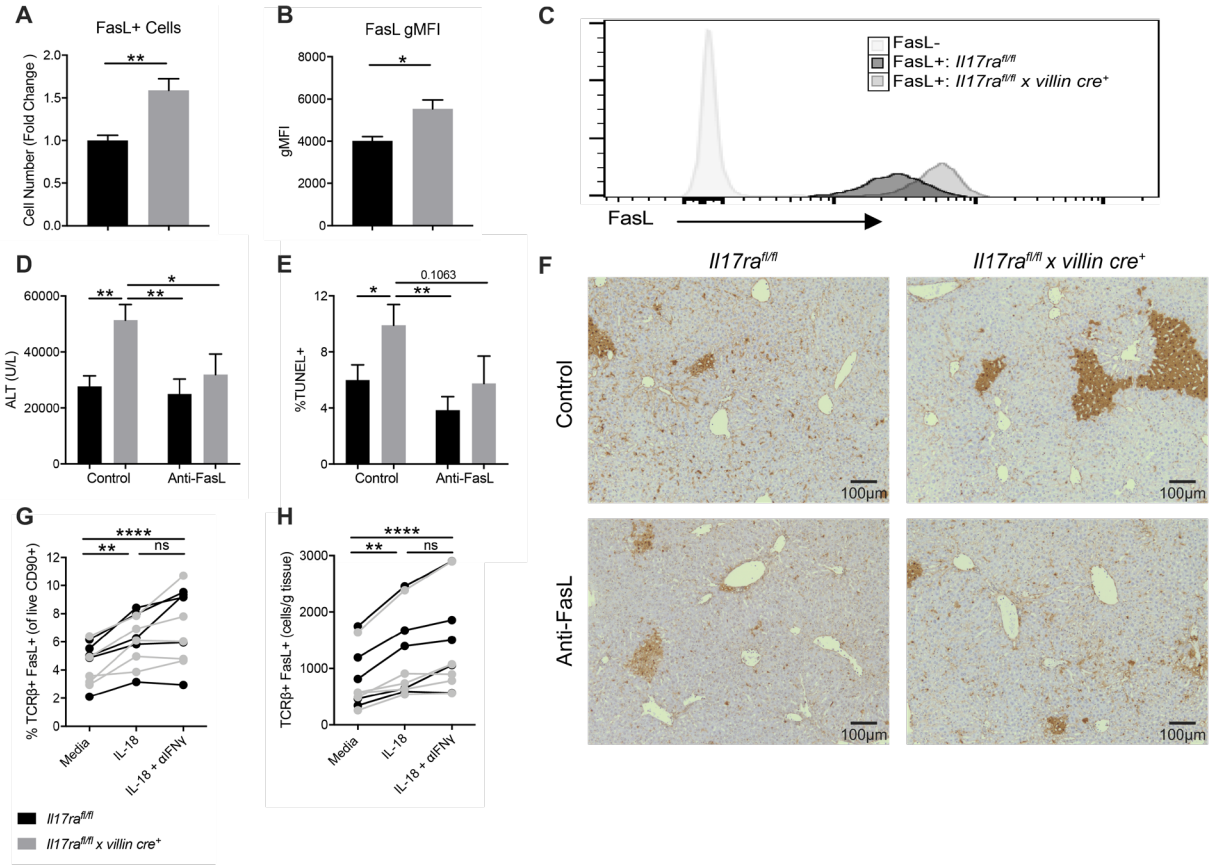

Figure 2-13. IL-18-induced Fasl exacerbates liver inflammation.

(A-C) Flow cytometry analysis of FasL in livers cells of naïve littermate *Il17ra*$^{fl/fl}$ and *Il17ra*$^{fl/fl}$ *x villin cre*$^{+}$ mice (n=7-11 mice/group). (A) Number of live FasL+ cells plotted as fold change over of *Il17ra*$^{fl/fl}$. (B) FasL geometric mean fluorescence intensity (gMFI) of live FasL+ cells. (C) Representative histogram of FasL+ cells. (D-F) Wildtype and *Il17ra*$^{fl/fl}$ *x villin cre*$^{+}$ mice were treated with IV anti-FasL (250-500µg/mouse) one hour prior to IV concanavalin A (25mg/kg). (D) Serum alanine aminotransferase (ALT) was measured 8 hours post IV Con A. (E) Quantification of TUNEL staining at 8 hours post Con A. (F) Representative images of TUNEL-stained liver histology at 8 hours post Con A. (G-H) Livers from naive littermate *Il17ra*$^{fl/fl}$ and *Il17ra*$^{fl/fl}$ *x villin cre*$^{+}$ mice were harvested and enriched for mononuclear cells. Cells were stimulated *ex vivo* with 50ng/mL IL-18 ± 5µg/mL anti-IFNγ (αIFNγ) and analyzed by flow cytometry. Percent (G) and actual number (H) of TCRβ+FasL+ cells (gated on live CD90+ cells). Lines connect paired samples. Each dot/line represents one mouse. (A-B, D-E) Data are represented as mean + SEM. $p<0.05$*, <0.01**, <0.001***, <0.0001**** (Unpaired T Test, Two-Way ANOVA with multiple comparisons test).

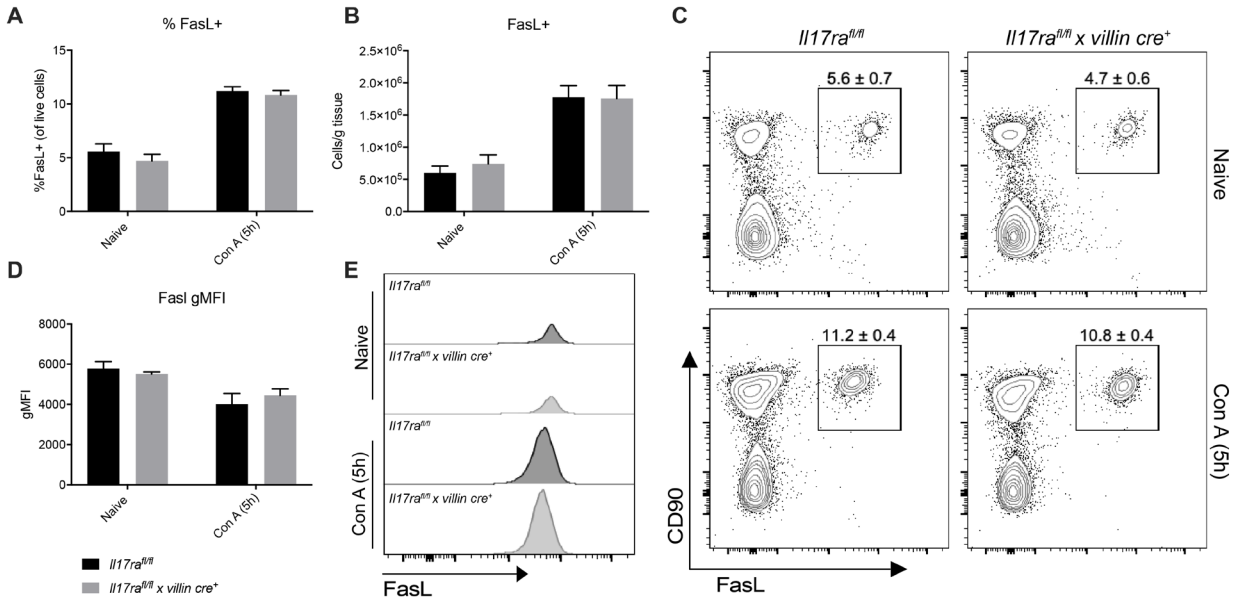

Figure 2-14. Cohousing eliminated liver FasL differences between *Il17ra$^{fl/fl}$ x villin cre^{+}* mice and floxed controls. Livers from *Il17ra$^{fl/fl}$* and *Il17ra$^{fl/fl}$ x villin cre^{+}* mice at the naïve state and 5h-post Con A were harvested, enriched for mononuclear cells, and analyzed via flow cytometry (n = 3-4 mice/group). Percent (A) and number (B) of FasL+ cells (gated on live cells). (C) Representative FACS plots. (D) FasL gMFI (gated on live FasL+ cells). (E) Representative histograms. Data are represented as mean + SEM. p<0.05*, <0.01**, <0.001***, <0.0001**** (Two-Way ANOVA with multiple comparisons).

2.3.6 Anti-IL18 mitigates liver injury in intestinal IL-17RA-deficient mice.

Finally, to assess whether the elevated IL-18 in *Il17ra$^{fl/fl}$ x villin cre^{+}* mice was contributing to worsened liver disease, we treated *Il17ra$^{fl/fl}$ x villin cre^{+}* mice and littermate controls with anti-IL-18 or isotype control one day prior to Con A injection. Anti-IL-18 treatment decreased liver inflammation in *Il17ra$^{fl/fl}$ x villin cre^{+}* mice to that of wildtype mice as measured by serum ALT (Figure 2-15A). Liver pathology correspondingly showed reduced areas of cell death in the liver parenchyma (Figure 2-15B-C). Quantification of TUNEL staining confirmed that cell death in *Il17ra$^{fl/fl}$ x villin cre^{+}* mice was substantially reduced to that of littermate floxed controls (Figure

2-15B). Furthermore, anti-IL-18 treatment reduced liver *Ifng* and *Fasl* transcript in *Il17ra*$^{fl/fl}$ *x villin cre*$^{+}$ mice 8 hours post-Con A as measured by qRT-PCR (Figure 2-15D-E).

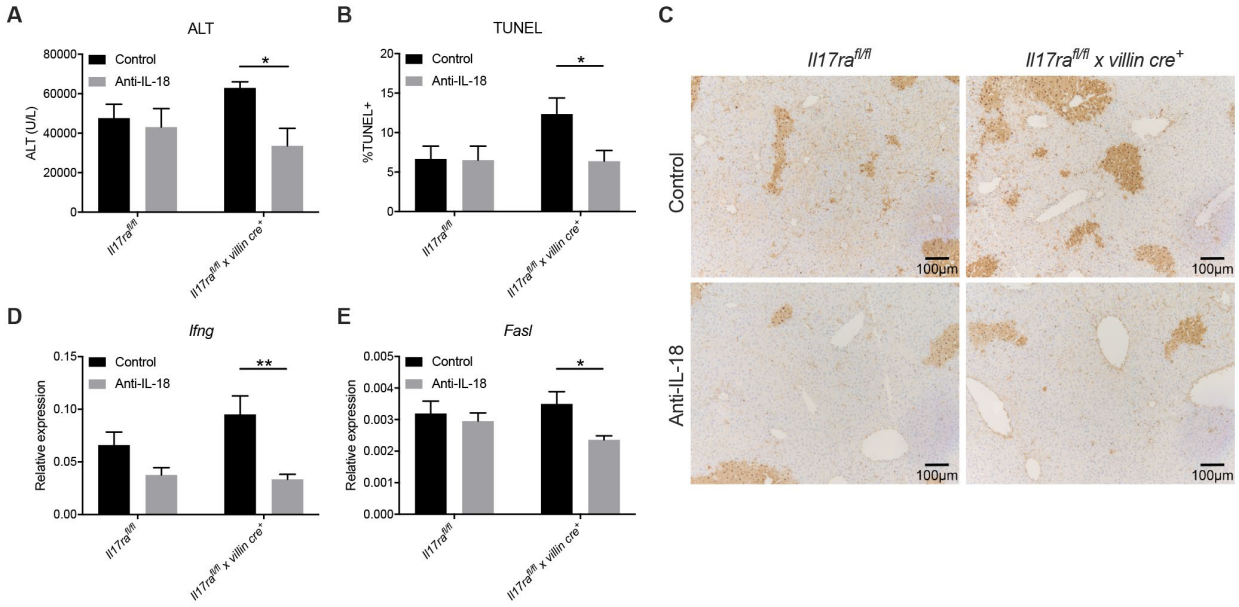

Figure 2-15. Anti-IL18 mitigates liver injury in intestinal Il17RA deficient mice.

Littermate *Il17ra*$^{fl/fl}$ and *Il17ra*$^{fl/fl}$ *x villin cre*$^{+}$ mice were pre-treated with anti-IL-18 (0.5mg/mouse) one day prior to IV concanavalin A (Con A) (25mg/kg) and sacrificed at 8 hours post Con A (n=7-9 mice/group). (A) Serum alanine aminotransferase (ALT). (B) Quantification of TUNEL staining. (C) Representative images of TUNEL-stained liver histology. Liver *Ifng* (D) and *Fasl* (E) gene expression as measured by qRT-PCR. Data are represented as mean + SEM. p<0.05*, <0.01**, <0.001***, <0.0001**** (Two-Way ANOVA with multiple comparisons test).

2.4 Discussion

Our results provide evidence that perturbation of intestinal IL-17 signaling is sufficient to exacerbate liver inflammation. Abrogation of intestinal IL-17RA disrupted the intestinal

microbiota and promoted translocation of bacterial products to the liver. Together, this induced IL-18 production and subsequent lymphocyte activation and cell death to worsen hepatitis.

Numerous studies have implicated Th17 cells in liver inflammation. For example, both autoimmune and viral hepatitis patients displayed elevated serum IL-17 (105–107). In Con A hepatitis, our lab previously showed that global IL-17RA knockout mice (*Il17ra*$^{-/-}$) were protected from disease (186). However, the role of Th17 cells in liver disease is complex. Here, by using intestinal epithelium-specific knockout mice, we uncouple intestinal IL-17 signaling from systemic signaling to reveal a novel protective role of intestinal IL-17RA in mitigating liver inflammation. Intestinal-specific IL-17RA knockout mice did have elevations in serum IL-17A (48) capable of signaling outside of the intestine to worsen disease. However, there were conflicting reports when IL-17A was reduced through genetic manipulation or antibody blockade during Con A hepatitis (186, 218–220). These discrepancies may be due to institutional differences in the microbiome. Alternatively, it may be due to the contribution of other IL-17RA cytokines. Our studies suggest this could also be a result of intestinal IL-17 signaling disruption with downstream consequences detrimental to liver inflammation. This unique contribution of intestinal IL-17 relative to systemic IL-17 paralleled findings in the experimental autoimmune encephalomyelitis (EAE) mouse model of multiple sclerosis described in Chapter 3 of this dissertation. In EAE, global IL-17RA knockout was protective (126), while intestinal specific IL-17RA knockout was detrimental (48), further validating the importance of intestinal IL-17 signaling in extra-intestinal diseases.

While reports have separately associated Th17 cells and the microbiome to liver inflammation, our study adds to the existing literature by linking these factors together in the

context of liver disease (98, 108, 221, 222). Our data showed that there were no differences in liver IL-17 in gut-specific knockout mice to exacerbate disease (Figure 2-16).

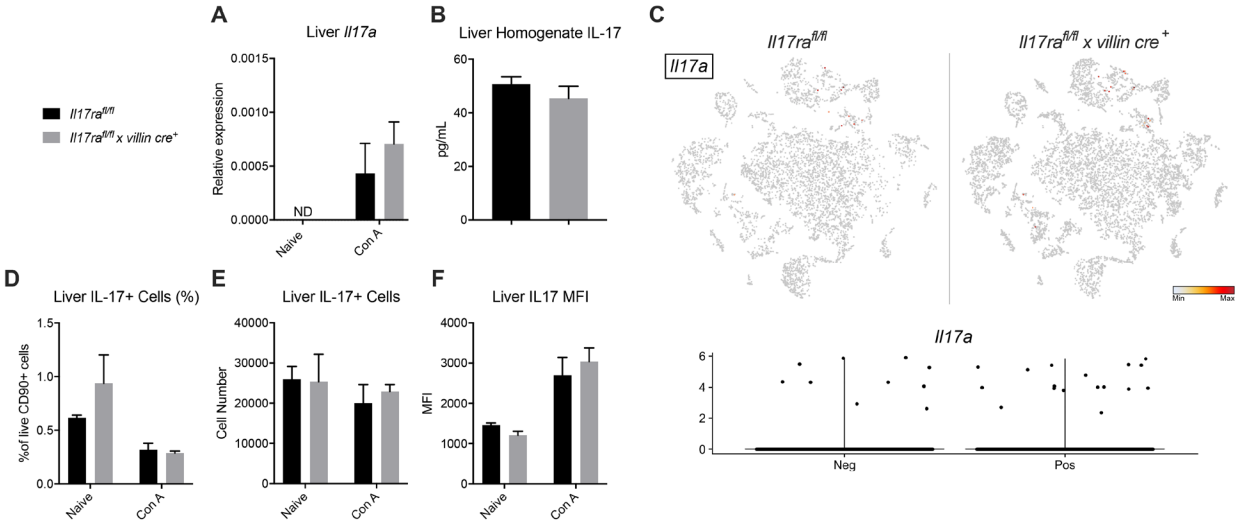

Figure 2-16. Liver IL-17 is not increased in *Il17ra$^{fl/fl}$ x villin cre^{+}* mice at the naïve state or 5h-post Con A.

(A) Liver Il17a expression in *Il17ra$^{fl/fl}$* and *Il17ra$^{fl/fl}$ x villin cre^{+}* mice at the naïve state and 5h-post Con A as measured by qRT-PCR (n = 3-4 mice/group). (B) IL-17 in liver homogenate of naïve *Il17ra$^{fl/fl}$* and *Il17ra$^{fl/fl}$ x villin cre^{+}* mice were measured by Luminex (n = 4-8 mice/group). (C) Ninety minutes after IV Con A (25mg/kg), single cell RNA sequencing was performed on *Il17ra$^{fl/fl}$* ("Neg") and *Il17ra$^{fl/fl}$ x villin cre^{+}* ("Pos") liver cells enriched for mononuclear cells. (n=2 mice/group). TSNE of Il17 expressing cells colored according to relative expression level and violin plot of Il17 expression. (D-F) Percent (D), number (E), and gMFI (F) of live IL-17+ cells in the livers *Il17ra$^{fl/fl}$ x villin cre^{+}* mice at the naïve state and 5h-post Con A (n = 2-4 mice/group). Data are represented as mean + SEM. p<0.05*, <0.01**, <0.001***, <0.0001**** (Two-Way ANOVA with multiple comparisons, Multiple T tests, Unpaired T test)

Rather, the data suggested that disruption of intestinal IL-17RA promoted the overgrowth of gram-negative, IgA unbound bacteria that exacerbated liver inflammation. This corroborates previous studies showing that germ free mice and mice treated with gentamicin are protected in Con A hepatitis (108, 178). *Ruminococcaceae,* a vancomycin sensitive gram-positive bacteria, was

previously associated with worsened liver inflammation (178), though we did not observe differences in this family within *Il17ra*$^{fl/fl}$ x *villin cre*$^{+}$ mice. Interestingly, at the naïve state, 16S data mainly showed differences in Sfb. However, we showed that vancomycin treatment, which eliminated Sfb and other gram-positive bacteria including *Ruminococcaeae*, had no effect on Con A hepatitis. Moreover, others showed that Sfb- wildtype mice sourced from Jackson Laboratories actually displayed worse Con A hepatitis than Sfb+ wildtype mice sourced from Taconic (178)**.** Taken together, these data suggested that Sfb overgrowth as a result of disrupted enteric IL-17RA signaling is not worsening disease in this model. Rather, disruption of intestinal IL-17 receptor signaling allowed for greater translocation of bacterial products to the liver, namely TLR9 agonists, to exacerbate disease. Because intestinal Th17 signaling plays a critical role in modulating bacteria close to the epithelium, it is also possible that a lack of intestinal IL-17R led to the general loss of host regulation of these bacteria as a whole, rather than specific bacteria. After Con A, *Il17ra*$^{fl/fl}$ x *villin cre*$^{+}$ mice did display a bloom of *Enterobacteriaceae,* which have particularly stimulatory CpG DNA (223). However, this overgrowth may simply be a consequence of inflammation as *Enterobacteriaceae* is known to outcompete other bacteria and bloom in inflammatory environments (224).

In addition to alterations in the intestinal microbiome, other groups have also observed increased bacterial translocation in both patients with and mouse models of liver inflammation (103, 108, 182). However, the downstream effects on local hepatic immune cell populations remain unclear. Here, we show that at the naïve state, disruption of intestinal IL-17R signaling was sufficient to increase flux of bacterial products, specifically CpG DNA, into the liver despite no functional manifestation of intestinal barrier defect (Figure 2-17).

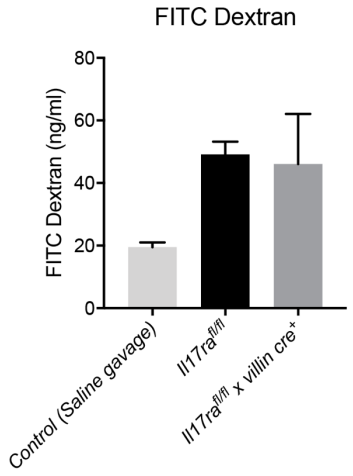

Figure 2-17. Naïve *Il17ra*$^{fl/fl}$ *x villin cre*$^{+}$ mice do not exhibit baseline intestinal barrier defects.

Serum FITC Dextran (4kDA) concentration in control saline-gavaged mice (n=2) and FITC dextran-gavaged *Il17ra*$^{fl/fl}$ and *Il17ra*$^{fl/fl}$ *x villin cre*$^{+}$ mice (n=3mice/group). Data are represented as mean + SEM. p<0.05*, <0.01**, <0.001***, <0.0001**** (One-Way ANOVA with multiple comparisons)

In addition, preliminary data showed that the CpG DNA signal in the liver homogenate was not sensitive to DNase treatment, raising the possibility of CpG DNA transport into the liver via bacterial outer membrane vesicle (OMV) release (Figure 2-18). This aligns with our data implicating gram-negative bacteria in our model, as gram-negative bacteria are producers of OMVs. Our data and a study by Jiang et al. both demonstrated that CpG DNA worsened Con A hepatitis (147). There was a conflicting report detailing hepatitis attenuation after CpG DNA stimulation (225), but we postulate this is due to differences in the CpG DNA and treatment regimen used in the experiments. In our study, we showed that CpG DNA induced IL-18-dependent liver IFNγ production from T cells, providing novel evidence that intestinal IL-17 signaling may play a role in constraining TLR9 induced-Type I responses in the liver.

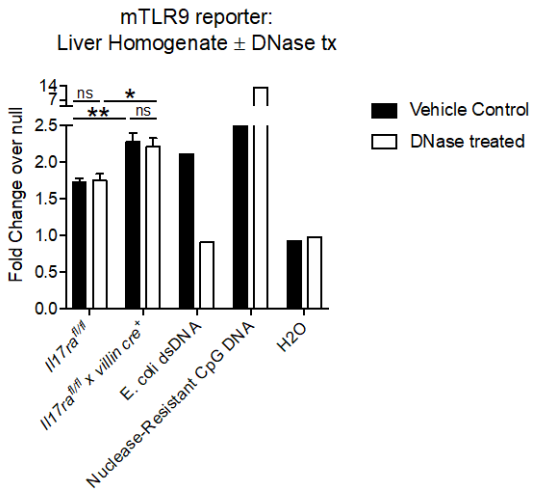

Figure 2-18. TLR9 ligands in *Il17ra*$^{fl/fl}$ and *Il17ra*$^{fl/fl}$ *x villin cre*$^{+}$ liver homogenate are DNase-resistant.

Liver homogenate from naïve littermate *Il17ra*$^{fl/fl}$ and *Il17ra*$^{fl/fl}$ *x villin cre*$^{+}$ mice were treated with DNase or vehicle control, then plated on mTLR9 SEAP reporter cells. (n=4-8 mice/group). Controls: DNase-sensitive *E. coli* dsDNA, Nuclease-resistant CpG DNA, nuclease free sterile H2O. Absorbance of supernatants was measured and represented as ratio over null/unstimulated cells. Data are represented as mean + SEM. p<0.05*, <0.01**, <0.001***, <0.0001**** (Two-Way ANOVA with multiple comparisons)

Il17ra$^{fl/fl}$ x *villin cre*$^{+}$ mice also exhibited increased IL-18 production in the intestine. This is consistent with previous reports that IL-18 is produced by intestinal epithelial cells in response to IL-22 (161). Indeed, we have previously shown that disrupted intestinal IL-17RA signaling increased IL-22+ cells in the small intestine lamina propria (48). Interestingly, serum IL-18 was partially decreased with neomycin treatment. Therefore, in addition to elevated IL-22, intestinal IL-17 signaling may regulate IL-18 through the microbiota. To further support the potential contribution of intestinal IL-18 in disease exacerbation, we have preliminary data with Con A in *Nlrc4*^{mut}*Il18bp*$^{-/-}$ mice. In these mice, IL-18 binding protein (IL-18BP), which is necessary for regulatory inhibition of IL-18, is knocked out, and the NLRC4 T337S mutation causes excess inflammasome-mediated IL-18 from the intestine (208). At the same concentration, these mice

exhibited lethal Con A hepatitis, while the *Nlrc4*^{mut} mice and *Il18bp*$^{-/-}$ mice survived (Figure 2-19). This suggested that excess IL-18 partnered with decreased systemic inhibition of IL-18 promotes hepatitis, and implies a pathogenic role for excess intestinal IL-18 in *Il17ra*$^{fl/fl}$ *x villin cre*$^{+}$ mice.

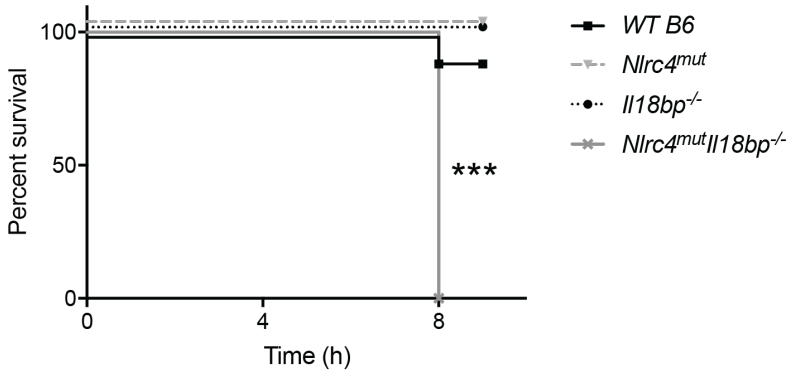

Figure 2-19. Excess intestinal IL-18 partnered with decreased systemic IL-18 control exacerbate hepatitis.

Con A (25mg/kg) was injected intravenously into wildtype (WT) B6 mice, NLRC4 mutants (Nlrc4^{mut}), IL-18 binding protein knockouts (*Il18bp*$^{-/-}$), and mice having both the NLRC4 mutation and IL-18BP deficiency (*Nlrc4*^{mut}*Il18bp*$^{-/-}$). Survival Curve (n = 3-10 mice/group). p<0.05*, <0.01**, <0.001***, <0.0001**** (Log-rank (Mantel-Cox) test)

The microbiome can influence immunity through direct mechanisms (i.e. activation of TLRs, NOD receptors) and indirect mechanisms (i.e. metabolites). Here, we provided evidence of CpG DNA inducing liver IL-18. Previous studies have described an indirect regulatory relationship between IL-18 and the intestinal microbiota in which unique metabolites derived from healthy and dysbiotic microbiota induced IL-18 production from the intestinal epithelium (226, 227). It is possible that disrupted intestinal IL-17 signaling and subsequent alterations in the microbiome may have induced IL-18 production through these mechanisms as well. Broadly, our data imply that perturbations in the microbiome and translocation of microbial products can enhance systemic IL-18 levels and affect extra-intestinal pathologies.

Excess IL-18 in *Il17ra*$^{fl/fl}$ x *villin cre*$^{+}$ mice also induced liver *Fasl* expression, increasing cell death and worsening hepatitis. This is consistent with reports implicating Fas-FasL in Con A hepatitis. Indeed, knockout of either Fas or FasL ameliorated disease within this model (215–217). In other model systems such as acetaminophen-induced liver injury, IL-18 has also been shown to induce *Fasl* expression (171, 172, 228). Here, we demonstrated that IL-18 induced FasL in an IFNγ-independent manner. Therefore, while IL-18 is able to independently induce FasL and IFNγ, our data suggest that the elevated IFNγ in *Il17ra*$^{fl/fl}$ x *villin cre*$^{+}$ mice was more a reflection of increased lymphocyte activation, and FasL was the major IL-18-downstream contributor to disease exacerbation. Beyond our model, we established a novel connection between intestinal IL-17 signaling and hepatic FasL, potentially implicating intestinal IL-17 in the many liver diseases linked to Fas-FasL associated cell death including fulminant, alcoholic, and viral hepatitis as well as liver carcinoma and fibrosis (229–232).

There are various unanswered questions remaining. It is unclear if the microbiome is influencing IL-18 levels indirectly through bacterial metabolites, cytokines (161), or the inflammasome (233). Particularly given the lack of changes observed by 16S sequencing, metabolomics to assess bacterial metabolites and metatranscriptomics to investigate changes in bacterial behavior would be important to further characterize how the microbiome is influencing disease within our model. There is also a regulatory relationship between the liver and intestinal microbiome through the modulation of bile acid metabolism (88). Changes in bile acid composition within the liver alter the intestinal microbiome, while bacterial metabolites influence bile acid production (88, 99, 234). Alternations in intestinal IL-17RA signaling may potentially disrupt this relationship to worsen disease as well. Lastly, it appears that the local hepatic immune cell populations *Il17ra*$^{fl/fl}$ x *villin cre*$^{+}$ mice were poised to secrete more inflammatory cytokines

upon stimulation, whether by CpG DNA, Con A, or anti-CD3/CD28 (Figure 2-10I, Figure 2-20). Further examination of the epigenetic landscape of these cells may provide insight into how alterations in the intestinal microbiome and subsequent bacterial products influence immunity through modulation of the epigenome.

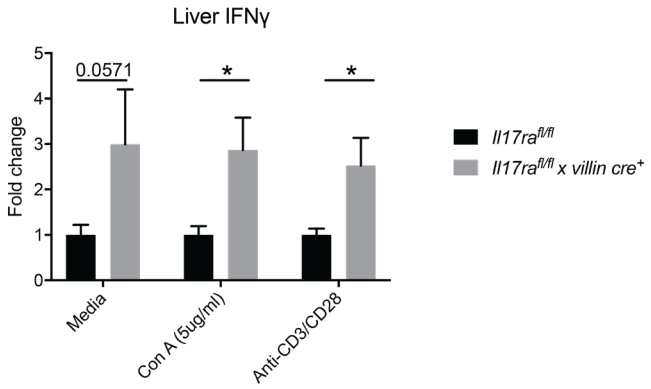

Figure 2-20. Liver mononuclear cells from naïve *Il17ra$^{fl/fl}$ x villin cre^{+}* exhibit increased IFNγ upon *ex vivo* stimulation.

Liver cells of naïve littermate *Il17ra$^{fl/fl}$* and *Il17ra$^{fl/fl}$ x villin cre^{+}* mice were enriched for mononuclear cells and stimulated with media (unstimulated control), Con A (5μg/mL), or anti-CD3/CD28 beads for 72 hours. IFNγ was measured in culture supernatants by luminex. (n = 3-9mice/group).

While the Concanavalin A model certainly has its limitations as with other animal models of disease, the data within the literature suggest our work is consistent with observations in human disease. There are multiple reports showing the Con A model parallels aspects of autoimmune, viral, and fulminant hepatitis. Specific to our data, there is evidence showing that IFNγ and Fas were increased in bone marrow mononuclear cells of patients with autoimmune hepatitis (AIH) (235). Analysis of liver tissue and peripheral blood lymphocytes of AIH patients further confirmed elevated Fas/FasL compared to healthy controls (236, 237). Furthermore, IFNγ in liver biopsies (238) and serum IL-18 (239) were both elevated and correlated with disease severity. In chronic

hepatitis C, Zeremski et al. showed that intrahepatic levels of IFNγ-inducible chemokines including CXCL9 and CXCL10 were increased as compared to controls and associated with disease severity (240). Similar to AIH, serum IL-18 levels were also elevated and correlated with severity of liver damage (241). In fulminant hepatitis, there were increases in circulating IFNγ+ CD8 T cells (242) and serum IL-18 (243). In addition, a recently published report showed that excessive IL-18 due to genetic IL-18BP deficiency in human patients can promote fulminant viral hepatitis (162). As such, we believe the mechanisms described in our work are potentially translatable to clinical hepatitis in patients.

Our data also have implications on hepatic diseases and illnesses beyond the gut-liver axis in conditions with "leaky gut" and increased bacterial translocation. This study reveals potential immune consequences of the subclinical bacteremia observed in many patients. For example, in HIV/AIDS, much emphasis has been placed on leakage of LPS across the gut barrier causing wasting and chronic inflammation (181). Our data suggests extra-intestinal TLR9 ligand dissemination is regulated by intestinal IL-17R signaling and may therefore be another underlying mechanism in HIV/AIDS liver dysfunction (244). Taken together, the connection our data established between intestinal Th17 cells, the microbiome, and hepatic immune signaling elucidate new therapeutic avenues to explore and target to treat hepatitis and other extra-intestinal diseases.

2.5 Working Model

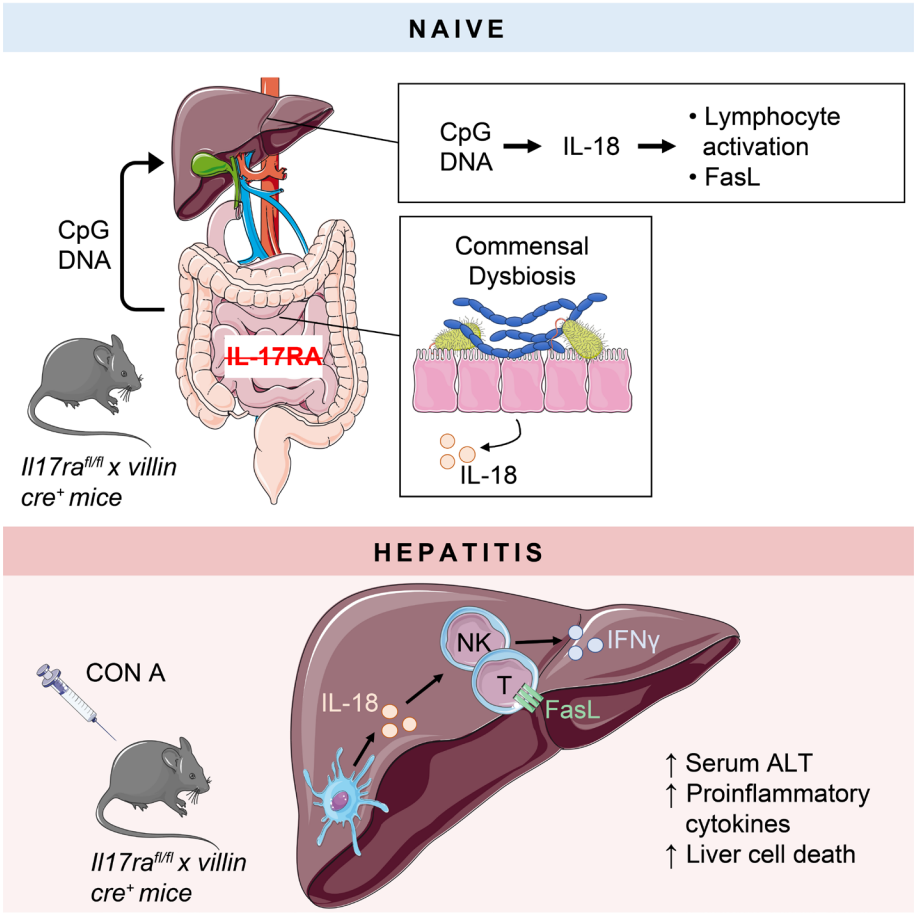

Figure 2-21. Working Model

At the naïve state, intestinal epithelial-specific IL-17RA-deficient mice (*Il17ra*$^{fl/fl}$ x *villin cre*$^{+}$ mice) exhibited microbiome dysbiosis and increased translocation of bacterial products (CpG DNA) from the gut to the liver to drive intestinal and hepatic IL-18 production, respectively. Upon induction of Concanavalin A (Con A)-mediated hepatitis, absence of enteric IL-17RA signaling exacerbated hepatitis and hepatocyte cell death. IL-18 was necessary for disease exacerbation and associated with increased activated hepatic lymphocytes based on *Ifng* and *Fasl* expression. Thus, intestinal IL-17R regulates translocation of TLR9 ligands and constrains susceptibility to hepatitis in a microbiome-dependent manner.

3.0 Gut-Central Nervous System Axis: Disruption of Intestinal Th17 Signaling and the Microbiome Exacerbate Autoimmune Neuroinflammation

Parts of this chapter have been published in the following article:

Kumar, P., L. Monin, P. Castillo, W. Elsegeiny, W. Horne, T. Eddens, A. Vikram, M. Good, A. A. Schoenborn, K. Bibby, R. C. Montelaro, D. W. Metzger, A. S. Gulati, and J. K. Kolls. 2016. Intestinal Interleukin-17 Receptor Signaling Mediates Reciprocal Control of the Gut Microbiota and Autoimmune Inflammation. Immunity 44: 659–671.

3.1 Introduction

Connections between the brain and intestine have been historically described. In early experiments, Ivan Pavlov showed that visual and auditory stimuli could elicit intestinal secretions in dogs (245). In psychiatric disease, patients with major depression were more likely to develop intestinal symptoms such as functional gastrointestinal diseases (FGID), while patients with FGID were more likely to develop depressive symptoms (246). This interaction of the gut-brain axis is also observed in neurologic disease. For example, the intestinal microbiome altered IL-17 production in γδ T cells to affect neurologic outcomes in a mouse model of ischemic stroke (247). This chapter will focus on the gut-central nervous system (CNS) axis in the context of Multiple Sclerosis (MS).

3.1.1 Overview of Multiple Sclerosis

MS is a chronic autoimmune demyelinating disease of the central nervous system. Signals are communicated within the CNS and to the peripheral nervous system (PNS) through action potentials transmitted along axons. Oligodendrocytes, specialized glial cells in the CNS, extend processes to support and insulate axons, forming the myelin sheath. Myelin dramatically increases the signal transduction through an axon to facilitate effective communication within the brain and spinal cord and to the rest of the body. In MS, the myelin sheath around the nerves is damaged resulting in motor, sensory, and sometimes cognitive dysfunction. In addition to demyelination, there is often inflammation and axonal loss due to the lack of protection and support offered by the myelin sheath (248, 249). The etiology of the disease remains unknown, though it is generally accepted that it is immune-mediated involving autoreactive lymphocyte activation, microglial activation, and chronic degeneration (249).

3.1.1.1 Epidemiology

MS is the most prevalent disabling neurologic disease in young adults, affecting nearly 1 million people in the United States and about 2.5 million people worldwide (250–253). Like other autoimmune diseases, MS is more common in women with an estimated female to male ratio of about 3-4:1 (254). Disease onset is 28-31 years old on average but varies with the type of MS (255). There are a number genetic polymorphisms associated with disease, most notably HLA-DRB1 (256). Interestingly, there is only a 25.3% concordance rate among monozygotic twins (257), suggesting the role of TCR/BCR sequence variation or environmental factors in disease risk and development. Indeed, this is one reason why we are investigating the microbiome in the context of MS pathogenesis.

3.1.1.2 Disease Manifestations

MS can be broken down into four subtypes: clinically isolated syndrome, relapsing-remitting MS, primary progressive MS, and secondary progressive MS (249). The clinically isolated syndrome represents the first episode of MS symptoms. Recurrence and progression of these symptoms categorizes the disease into one of the other three subtypes which differ on the basis of disease activity and rate disease of progression. Relapsing-remitting MS (RRMS) is episodic with recovery between each episode. There is often little to no disease progression between exacerbations. However, recovery from each attack can vary, establishing a new baseline of neurological disability. Disease symptoms in primary progressive MS (PPMS) advance continually from the clinically isolated syndrome, often causing more substantial deterioration due to the continuous progression. Secondary progressive MS (SPMS) begins in a pattern resembling RRMS but then shifts to a continual progressive decline as seen in PPMS. (249, 258)

MS typically presents to the clinic between age 15-50 with acute or subacute development of symptoms of sensory dysfunction in the limbs, visual loss or disturbances such as diplopia, or impaired motor function in the absence of fever or other illness (258). Clinical signs more suggestive of MS include the Lhermitte sign (electric shock sensations going down the back or limbs when neck is flexed) and the Uhthoff phenomenon (symptom exacerbation as body temperature rises with normal activity) (249). While other symptoms may have occurred at initial presentation (i.e. bowel dysfunction, gait disturbance), concrete diagnosis of MS is determined per the criteria in the following section.

3.1.1.3 Diagnosis

In addition to the clinical symptoms, MS is diagnosed via MRI confirmation. MS typically shows focal enhancing lesions in the white matter of brain and/or spinal cord during MRI. Diagnosis of MS depends on the fulfillment of the McDonald Criteria shown below (258).

Table 3-1. 2017 McDonald Criteria

	# of lesions with objective clinical evidence	Additional data needed for MS diagnosis
≥2 clinical attacks	≥2	None
	1 (as well as clear-cut historical evidence of a previous attack involving a lesion in a distinct anatomical location)	None
	1	Dissemination in space demonstrated by an additional clinical attack implicating a different CNS site or by MRI
1 clinical attack	≥2	Dissemination in time demonstrated by an additional clinical attack or by MRI OR demonstration of CSF-specific oligoclonal bands
	1	Dissemination in space demonstrated by an additional clinical attack implicating a different CNS site or by MRI AND Dissemination in time demonstrated by an additional clinical attack or by MRI OR demonstration of CSF-specific oligoclonal bands

Table sourced from *Thompson AJ, Banwell BL, Barkhof F, et al. Diagnosis of multiple sclerosis: 2017 revisions of the McDonald criteria. Lancet Neurol 2018; 17:162.* (258)

3.1.1.4 Prognosis

Multiple factors are thought to contribute to patient prognosis. Disease type is one factor with RRMS having a better prognosis compared to the progressive types. In patients with RRMS, early intestinal or bladder-related symptoms, shorter time between the initial and subsequent episode, and early disability are indicative of poor prognosis (259). Increased CNS lesion burden and CNS atrophy are also associated with worse disease outcomes (260). In terms of demographics, race has been investigated as a potential prognostic factor, but conclusions from

these studies remain controversial. Though women are more likely to develop MS, men who develop MS are more likely to undergo a more severe disease course (261). In addition, pregnancy is associated with an overall decrease in MS relapse during pregnancy with increased risk postpartum (262). Interestingly, there are T cell changes during pregnancy (263, 264) as well as significant differences in the microbiome that were associated with changes in host inflammation and metabolism (265).

While assessment of these factors are helpful, it is important to note that their prognostic reliability remains limited (260). Ongoing research is required to better identify and describe these factors to improve disease management. Beyond this, further studies to investigate the etiology of disease are critical to develop novel therapeutics strategies.

3.1.1.5 Treatment

Acute exacerbations are treated with glucocorticoids with the purpose of shortening the episode rather than addressing long term disease course (266). There is also evidence suggesting a benefit of plasmapheresis in RRMS acute episodes (249) but not for treatment in the progressive MS subtypes. Symptom-specific treatments are prescribed as well to assist with isolated problems such as bladder control (266). While both acute management and targeted symptomatic interventions are very important for disease management, disease modifying drugs and immunotherapies appear to provide more sustained responses.

Disease-modifying therapies (DMTs) do not constitute as cures, but they can potentially affect disease progression and maintenance. A recent 2019 observational study of over 1500 patients investigated the role of DMTs on prevention of RRMS conversion to SPMS (267). The study found that initial treatment with fingolimod, alemtuzumab, or natalizumab lowered the risk of RRMS conversion to SPMS as compared to glatiramer acetate and interferon beta. In

progressive MS, the suggested DMTs include ocrelizumab, cladribine, and siponimod. A brief description of each of the aforementioned therapies are listed below.

Table 3-2. Disease-Modifying Therapies Approved for MS

Drug	Alternative Names	Description	Function
Fingolimod	FYT720, Gilenya	Structural analog of natural sphingosine	Prevents lymphocyte egress from lymphoid tissue into circulation by activating and subsequently downregulating sphingosine-1-phosphate receptor (268, 269)
Alemtuzumab	Lemtrada	Monoclonal Human anti-CD52	Depletes circulating T and B cells (270–272)
Natalizumab	Tysabri	Humanized anti-α4β1integrin monoclonal	Prevent leukocyte trafficking into the CNS (273–275)
Glatiramer Acetate	Copaxone, Glatopa	Mixture of synthetic peptides similar to myelin basic protein	Competitive inhibitor of MHC to prevent presentation of myelin antigens; promotes immunosuppressive responses in CNS (276–278)
Interferon beta	Avonex, Rebif	Type 1 interferon, Formulations: IFNβ-1a and IFNβ-1b	Broad range of anti-inflammatory effects including decreasing pro-inflammatory cytokines while increasing anti-inflammatory cytokines, decreasing cell migration into the CNS, promoting nerve growth factor for CNS repair, and other effects on T cells, B cells, and DCs (279–281)
Ocrelizumab	Ocrevus	Recombinant anti-human CD20 monoclonal antibody	B cell depletion (282)
Cladribine	Mavenclad	Purine nucleoside analogue	Lymphocyte depletion due to cytotoxic effects on cell metabolism and DNA synthesis & repair (283)
Siponimod	BAF312, Mayzent	sphingosine 1-phosphate receptor modulator	Prevents lymphocyte egress from lymphoid tissue into circulation by activating and subsequently downregulating sphingosine-1-phosphate receptors 1 and 5 specifically (284)

These therapies demonstrate the critical role of the immune system in MS pathogenesis. In addition, the above therapies target different aspects of the immune system, emphasizing the complexity of disease pathogenesis and the potential benefit of targeting multiple aspects of the immune system for effective treatment. To that end, the dissertation studies in this chapter

investigate the role of intestinal Th17 cells and the intestinal microbiome in MS pathogenesis with the ultimate goal of identifying novel therapeutic strategies.

3.1.2 Th17 Cells and the Microbiome in Multiple Sclerosis

Th17 cells and the intestinal microbiome have both been implicated in MS. When considering the mechanisms by which these factors can affect disease, it is important to understand the barriers limiting contact with CNS as an immunoprivileged site.

3.1.2.1 Barriers of the CNS

The CNS is separated from the rest of the body through its three membranes (the dura mater, pia mater, and arachnoid membrane) and specialized barriers (Figure 3-1). The blood brain barrier (BBB), which includes the blood-leptomeningeal barrier for the purposes of this discussion, separates the CNS parenchyma from the CNS vasculature (Figure 3-1A). In this way, the body can tightly regulate vascular entry into the CNS by cells and other potentially inflammatory mediators. Indeed, the BBB is able to prevent entrance to greater than 98% of antibodies and small molecules while maintaining its ability to transport materials out (285). It is comprised of specialized endothelial cells and the combination of the parenchymal basement membrane and astrocyte foot processes together termed the glia limitans (286). Therefore, should external components breach the specialized tight junction network of the BBB vascular endothelial cells, there exists an additional barrier unique to the CNS in the form of the glia limitans. Another interface between the CNS and periphery is the blood-cerebrospinal fluid barrier (BCSFB) (Figure 3-1B). This is located at the choroid plexus within the ventricles of the brain. The choroid plexus is a structure derived form of ependymal cells lining the ventricle and includes the epithelial cells that secrete

CSF (286). The endothelial cells lining the choroid plexus do not have specialized tight junctions, offering a more accessible entry point for lymphocytes into the subarachnoid space containing the CSF. It is thought that this degree of accessibility is actually critical for immune surveillance. Indeed, this region is rich in antigen presenting cells, and the CSF actually contains a proportionately large amount of memory CD4+ T cells relative to the systemic circulation (286, 287). Especially interesting in the context of these dissertation studies, research from patients with non-inflammatory neurological disease showed the presence of skin and gut homing memory T cells in the CSF (287). This emphasizes the potential for crosstalk between the gut and the brain and suggests direct communication between the two systems via lymphocyte migration.

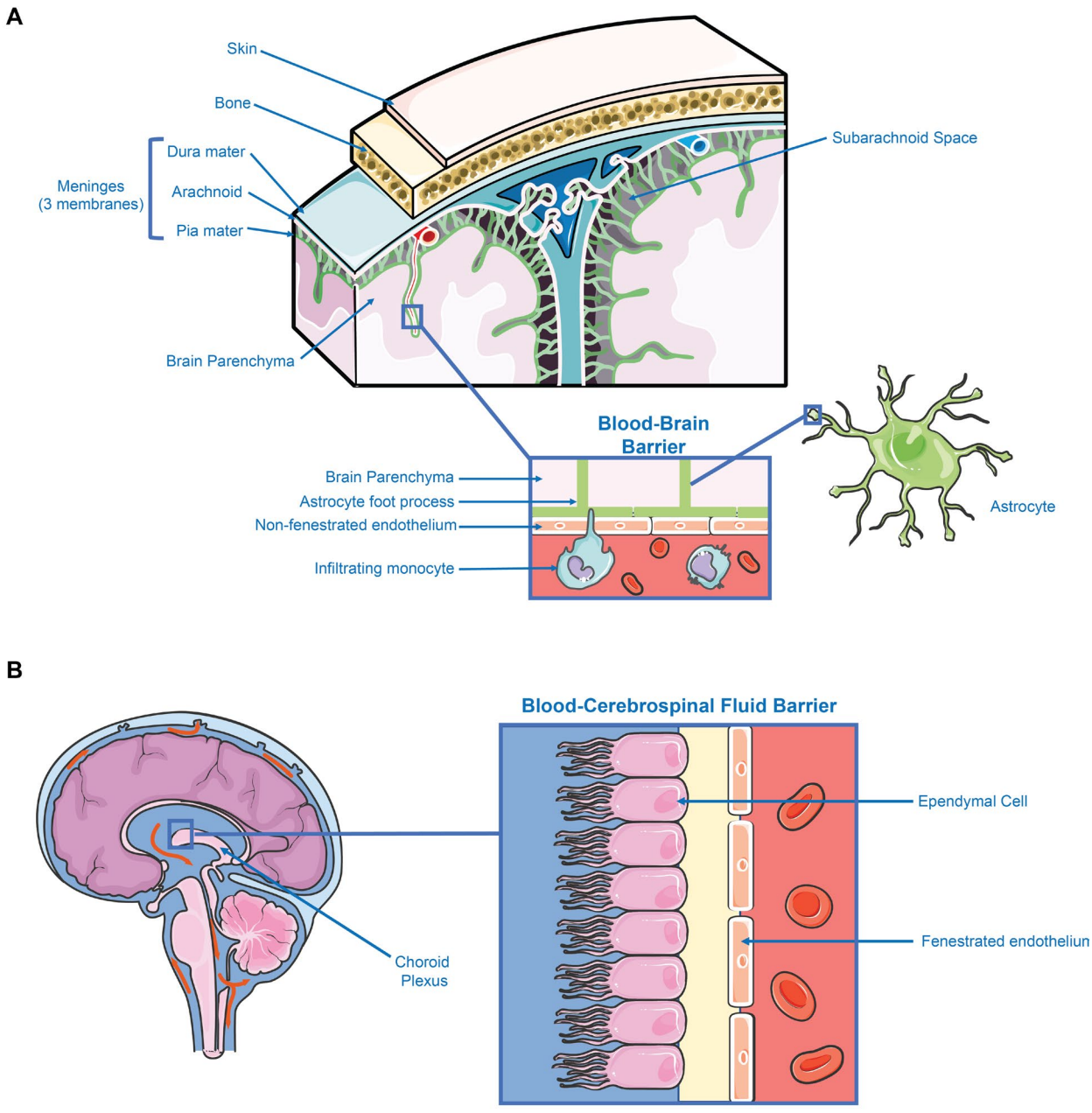

Figure 3-1. CNS Barriers

(A) The CNS is separated from the rest of the body through its meninges (3 membranes: the dura mater, pia mater, and arachnoid membrane) and specialized barriers. The blood-brain barrier separates the CNS parenchyma from the CNS vasculature. It is comprised of specialized non-fenestrated endothelial cells and the combination of the parenchymal basement membrane and astrocyte foot processes together termed the glia limitans. (B) Another interface between the CNS and periphery is the blood-cerebrospinal fluid barrier (BCSFB). This is located at the choroid plexus within the ventricles of the brain. The choroid plexus is a structure derived form of ependymal cells lining the ventricle

and includes the epithelial cells that secrete CSF. The fenestrated endothelial cells lining the choroid plexus do not have specialized tight junctions, offering a more accessible entry point for lymphocytes into the subarachnoid space containing the CSF.

There are physiological mechanisms to enter the CNS. Trafficking of small molecules, antigens, and other potentially immunomodulatory components can occur through passive diffusion, transcytosis, or specific transporters located at the BBB/BCSFB (288). Proper trafficking of immune cells into the CNS requires expression of specific signaling and adhesion molecules on both the part of the entering cell as well as the cells comprising the CNS barriers. For example, expression of α4 and β2 integrin expression on the immune cells are required for interaction with intercellular and vascular adhesion molecules (i.e. ICAM1-2, VCAM-1) on the BBB endothelial cells in order to adhere and commence rolling on the endothelium (286). In EAE, integrin β3 is important for CNS migration (289). Studies have also shown that endothelial P-selectin is required to cross the brain-leptomeningeal barrier (290). Though brain-specific chemokine/receptors have not been identified, there are certain chemokines commonly expressed in the brain. For example, CCL19 is constitutively expressed by CNS endothelial cells (286), and CCL20 is expressed by the choroid plexus, promoting migration of CCR6+ CD4+ T cells (285). Beyond these interactions, studies tracing radioactively labeled resting and active T cells showed that lymphocyte activation is necessary to cross the BBB in the spinal cord (291). These physiological mechanisms can be manipulated to recruit immune assistance during infection and inflammation. Conversely, they can be compromised during disease, allowing aberrant breach the brain barriers.

In MS and the EAE mouse model, the BBB becomes compromised, permitting increased lymphocytic infiltration. The mechanisms through which this disruption occurs is a topic of continued investigation. However, there is evidence that matrix metalloproteinases (MMPs) play a role. Specifically, MMP2 and MMP9 were shown to disrupt the astrocyte-parenchymal basement membrane interaction to decrease the integrity of the glia limitans (292). Lymphocytic breach of the BBB is accompanied by proinflammatory changes that induce additional infiltration. When autoreactive T cells enter the CNS and encounter their cognate antigen, they set off a positive feedback loop in which chemokine and adhesion signaling changes in the CNS barriers promote immune cell recruitment to further exacerbate inflammation and subsequent damage (286). While different cells may promote BBB compromise and MS immunopathology, many reports have described Th17 cells as a major contributor.

3.1.2.2 Th17 Cells in Multiple Sclerosis

Numerous studies have linked Th17 cells to MS pathogenesis. As previously mentioned, patients with MS have increased serum IL-17 and increased IL-17 in MS lesions (123, 124). In RRMS, there was also a correlation with serum IL-17F levels and 2 year relapse rate (293). In terms of the BBB, hallmark Th17 cytokines have been implicated in disruption and infiltration. Specifically, in a human brain-derived microvascular endothelial cell model of the BBB, there was greater migration of Th17-polarized human CD4+ T cells as compared to Th1- polarized CD4+ T cells (294). This study showed that IL-17 and IL-22 stained positively in highly infiltrated MS lesions, and that there was an upregulation of IL-17 and IL-22 receptors on the brain endothelial cells within these lesions (294). *Ex vivo*, both cytokines were able to promote migration of lymphocytes through the human BBB model, accompanied with increases in CCL2 and CXCL8

(294). Together, these human and patient data support a role for Th17 in MS with specific involvement in immune infiltration.

In the EAE model of MS, mice were protected by deficiency of IL-17RA (126), IL-17RC (295), and transcription factors required for Th17 differentiation including RORγt, BATF, and JUNB (14, 296, 297). However, there are conflicting reports regarding relative contributions of IL-17A and IL-17F to EAE (125, 298, 299), raising the possibility of institutional microbiome differences contributing to these mixed reports as well as the potential role of other Th17 related cytokines in disease pathogenesis.

Pathogenic Th17 cells that double produce IL-17 and IFNγ or IL-17 and GM-CSF have been identified. Mice deficient in IFNγ and knockout of the IFNγ receptor actually developed worse EAE, suggesting a protective role of IFNγ in disease pathogenesis (300–302). Conversely, GM-CSF has been shown to be detrimental, as GM-CSF deficient mice were resistant to EAE (303, 304). Two cytokines known to favor the differentiation of pathogenic Th17 cells are IL-23 and IL-1β (30). Both cytokines are thought to contribute to EAE pathology. Knockout of IL-1R1 or IL-1β was protective (305, 306) along with knockout of IL-23RA or IL-23p19 (29, 307). Studies have now shown that IL-23 is necessary for *in vivo* terminal differentiation and maintenance of Th17 cells (26, 29). Moreover, Codarri et al. and El-Behi et al. showed that IL-23 (27, 308), master Th17 transcription factor Rorγt (308), and IL-1β (27) was required for T cell GM-CSF production in EAE. In both reports, GM-CSF from Th17 cells contributed to EAE pathology (27, 308).

Interestingly, recent work suggested a role for intestinal Th17 cell signaling in MS. The study evaluated intestinal biopsies from RRMS patients and healthy controls via flow cytometry and found that increased intestinal Th17 cells correlated with MS disease activity based on MRI and disability score (309). In addition to this, 16S sequencing of microbial DNA isolated from

tissue biopsies showed specific differences in RRMS patients as compared to controls (309), providing human data implicating not only intestinal Th17 signaling in MS but the intestinal microbiome as well.

3.1.2.3 Intestinal Microbiome in Multiple Sclerosis

A number of studies have examined the microbiome in the context of multiple sclerosis. Patients with MS exhibit an altered microbiome compared to healthy controls. A metanalysis of these works have described an increase in *Methanobrevibacter* and *Enterobacteriaceae* in MS patients with enrichment of *Fecalibacterium prausnitzii* and SCFA-producing bacteria such as *Prevotella* and *Lachnospiraceae* in controls (310). Additional studies have been done in EAE that further support the role of the microbiome in MS. Germ-free mice and mice treated with broad spectrum antibiotics were protected in EAE (311–313). This included combinations of metronidazole, ampicillin, neomycin, and vancomycin as well as kanamycin, colistin, and vancomycin. To show that the differences observed in patients may point to the microbiota as a cause rather than an association, a fecal microbiota transplant (FMT) was performed from MS patients into germ free mice prior to EAE induction. Results showed that mice receiving stool from MS patients as compared to healthy controls exhibited worsened EAE clinical scores (129). These data are highly suggestive of the microbiota as a contributing factor in MS, but also prompt the question of mechanism.

The ways the microbiota is able to affect health and disease detailed in the initial introduction of this dissertation also apply here. There is evidence that the microbiome is influencing T cell immunology in EAE. The protection from EAE in germ-free mice and mice treated with broad spectrum antibiotics were all associated with a decrease in Th1 and Th17 cells partnered with an increase in Tregs (311–313). This suggests that the microbiota plays a role in

balancing the Treg population and the Th1/Th17 effector population. Though contradictory to the previous data showing increased Tregs in germ free mice, there is also evidence showing that SCFAs from the microbiota can promote Treg cell expansion and activation (62). SCFAs have been shown to signal through G protein-coupled receptors on Tregs, macrophages, dendritic, and intestinal epithelial cells (314, 315). For example, binding of butyrate on GPR109A on macrophages and dendritic cells promoted intestinal differentiation of Tregs (315). Moreover propionate binding to GPR43 on Tregs enhances intestinal Treg proliferation (314). In EAE, oral supplementation with the SCFA propionic acid increased T regulatory cells and ameliorated EAE (316). In contrast, long chain fatty acid (LCFA) lauric acid had the opposite effect (316). As a proof of concept study, propionic acid supplementation was implemented in a small cohort of MS patients. The treatment regimen called for 1g of oral propionic acid supplementation daily. Results showed that as compared to controls, supplementation with oral propionic acid increased Treg- and decreased Th17-cell frequencies (317). Aside from SCFAs, bacterial products that can activate toll like receptors (TLRs) also influence EAE. While there are conflicting reports regarding the relative contribution of specific TLRs in EAE, there is evidence showing that knockout of TLR4 in CD4+ T cells was protective (318). In addition, global knockout of TLR2, TLR9, and MyD88 also ameliorated disease (319). Taken together, these data and those previously discussed point to a role of the microbiome in EAE pathogenesis and supports the investigation of the microbiome as a potential therapeutic target in MS.

3.1.3 Study Overview

Given the relationship between the intestinal microbiome and Th17 cells and the role of each of these factors in MS/EAE, we investigated the significance of enteric IL-17R signaling in

EAE using intestinal specific IL-17 receptor knockouts (*Il17ra*$^{fl/fl}$ *x villin cre*$^{+}$ mice). We hypothesized that disruption of the reciprocal regulatory relationship between enteric IL-17 signaling and the gut microbiota leads to dysbiosis, expansion of Th17 cells, and increased predisposition to autoimmune neuroinflammation. Our data suggested that *Il17ra*$^{fl/fl}$ *x villin cre*$^{+}$ mice, which have higher Sfb levels, exhibited earlier EAE onset and increased EAE incidence and severity as compared to littermate *Il17ra*$^{fl/fl}$ controls. Treatment with vancomycin ameliorated disease, further supporting our hypothesis. Disease exacerbation was accompanied by systemic increases in IL-17 and GM-CSF responses. In addition, preliminary data indicated that *Il17ra*$^{fl/fl}$ *x villin cre*$^{+}$ mice have increased intestinal expression of *Csf2, Ccr2,* and *Ccr6* and increased spinal cord expression of *Nos2* immediately prior to disease onset. Together, this suggested that there could be increased migration into the CNS of *Il17ra*$^{fl/fl}$ *x villin cre*$^{+}$ mice, contributing to exacerbated disease. These studies elucidate how dysregulation of enteric IL-17R signaling and the commensal microbiota can contribute to the pathogenesis of MS and other autoimmune conditions. Moreover, it can provide insight into novel therapeutic strategies targeting the gut-brain axis.

3.2 Methods

3.2.1 Experimental Model and Subject Details

Mice

All mouse work was performed in accordance with the Institutional Animal Care and Use Committees (IACUC) and relevant guidelines at the University of Pittsburgh, School of Medicine

(protocol #16109334). *Il22ra2*$^{-/-}$ mice were bred and housed at the UPMC Children's Hospital of Pittsburgh. *Il17ra*$^{fl/fl}$ and *Il17ra*$^{fl/fl}$ *x villin cre*$^{+}$ mice were generated at the UPMC Children's Hospital of Pittsburgh by crossing *Il17ra*$^{fl/fl}$ mice to *Il17ra*$^{fl/fl}$ *x villin cre*$^{+}$ mice. Both male and female age-matched mice from 6-10 weeks of age were used for all experiments. The aforementioned breeding strategy allowed for controls and knockout mice within each experiment to be littermates. Littermate age-matched males and females were randomly assigned to experimental groups. Both males and females were used within each group in order to account for sex-differences while maintaining littermate controls and sufficient n for statistical power. All mice were housed in pathogen-free conditions at the UPMC Children's Hospital of Pittsburgh.

Ex vivo cultures

Ex vivo stimulation of splenocytes and lamina propria lymphocytes. Cells from 6-10-week-old naïve *Il17ra*$^{fl/fl}$ mice and *Il17ra*$^{fl/fl}$ *x villin cre*$^{+}$ mice were harvested and processed into single cell suspensions (protocol described below). In addition to detailed experiment-specific stimuli, cells were maintained at 37°C in Iscove's Modified Dulbecco's Medium (IMDM) with GlutaMAX Supplement (Gibco), 10% heat-inactivated fetal bovine serum, 100 units/mL of penicillin and streptomycin, and 0.3mg/mL of L-glutamine.

Experimental Models

Experimental autoimmune encephalomyelitis (EAE) was induced using myelin oligodendrocytes glycoprotein (MOG_{35-55}) (Bio-Synthesis, Inc.) in complete Freund's adjuvant (CFA) containing 100 μg M. tuberculosis strain H37Ra (Difco) as well as pertussis toxin (Sigma-Aldrich) (29).

3.2.2 Method Details

Animal treatments

ll17ra$^{fl/fl}$ x villin cre^{+} and littermate control *Il17ra$^{fl/fl}$* mice were used for EAE experiments. Co-housed cre^{+} and cre^{-} mice were separated and kept in separate cage 1 week before EAE induction. These mice were immunized at both sites on the hind flank with 100 μg peptide corresponding to the immunodominant epitope of myelin oligodendrocytes glycoprotein (MOG_{35-55}) (Bio-Synthesis, Inc.) in 200 μl CFA containing 100 μg M. tuberculosis strain H37Ra (Difco) as described previously (29). All immunized mice also received 200 ng of pertussis toxin (Sigma-Aldrich) intraperitoneally on days 0 and 2. Mice severity scores for EAE were evaluated blindly according to the following scale: 1: flaccid tail; 2: impaired righting reflex and hind limb weakness; 3: partial hind limb paralysis; 4: complete hind limb paralysis; 5: hind limb paralysis with partial fore limb paralysis; 6: moribund.

EAE was also induced after 2 weeks of vancomycin (0.5 g/L) in the drinking water *ad libitum* or control water treatment. Vancomycin or control water-treated *ll17ra$^{fl/fl}$ x villin cre^{+}* mice were immunized as above. Mice were maintained on antibiotic water throughout EAE time course.

Mice were also treated with 0.5mg/mouse Anakinra (Kineret) twice daily for 21 days beginning at day 0 of EAE and maintained throughout the disease course.

qRT-PCR

Spinal cords and intestines were harvested from 6-10-week-old littermate *Il17ra$^{fl/fl}$* and *Il17ra$^{fl/fl}$ x villin cre^{+}* mice at the naïve state and day 9 post EAE induction. Tissues were homogenized in Trizol buffer (Life Technologies). Total RNA extraction was performed according

to Trizol manufacturer's instructions. RNA was transcribed into cDNA using iScript reagent (Bio-RAD) according to manufacturer's instructions.

For qRT-PCR, SYBR Green supermix (Bio-RAD) was used for analysis of small subunit ribosomal RNA gene (16S rRNA) expression. 16S primers included: forward: ACTCCTACGGGAGGCAGCAGT, reverse: ATTACCGCGGCTGCTGGC (47, 48, 192). SsoFast supermix (Bio-RAD) was used for qRT-PCR analysis with primers (Applied Biosystems) for mouse *Hprt, Il17a, Csf2, Ccr2, Ccr6, Nox2, Il1b,* and *Il1rn.* Expression of all genes was normalized relative to housekeeping gene mouse *Hprt*. Reaction: 95°C for 3 minutes, 49 cycles at 95°C for 10 seconds (s) and 60°C for 30s. SYBR Green reactions also had an additional melt curve at the end of the reaction above: 60°C for 5s with +0.5°C increment every cycle up to 95°C.

RNA sequencing

Total RNA from terminal ileum (1-4 μg) of 6-week-old *Il17ra*$^{fl/fl}$ *x villin cre*$^{+}$ and littermate *Il17ra*$^{fl/fl}$ control mice were used as starting material for deep sequencing using the in-house Illumina TrueSeq RNA Sample Preparation v2 Guide. Briefly, mRNA was purified with oligo-dT beads, fragmented with magnesium and heat-catalyzed hydrolysis, and used as a template for first- and second-strand cDNA synthesis with random primers. The cDNA 3' ends were adenylated, followed by adaptor ligation and a 15-cycle PCR to enrich DNA fragments. Quantification of cDNA libraries were performed by using Kapa Biosystems primer premix kit with Illumina-compatible DNA primers. The cDNA libraries were pooled at a final concentration 1.8 pM. Single-read sequencing was performed on Illumina Genome Analyzer IIx and NextSeq 500.

Lamina propria lymphocyte isolation

Briefly, 10 cm pieces of terminal small intestine were separated from mesentery and Peyer's patches were carefully excised. Tissues were opened longitudinally and washed with HBSS. Epithelial cells were separated from lamina propria by incubating 1 cm pieces of small intestine in 5 mM EDTA on a shaker (100 rpm) for 10 minutes. Tissue were washed with HBSS without EDTA until supernatant was not cloudy. Tissues were cut into small pieces and incubated for 10 minutes at 37^0C in HBSS containing 0.3 mg/ml collagenase, 0.1 mg/ml DNase, 1 mM $CaCl_2$ and 1 mM $MgCl_2$. 10% FBS was added and digested tissue suspension was filtered using 70-micron cell strainer. After centrifugation, digested tissue pellet was re-suspended with 44% percoll and layered over 67% percoll. Mononuclear cells were isolated from an interphase of percoll gradients, washed, and resuspended for downstream applications.

Splenocyte Isolation

Spleens were harvested from mice into Iscove's Modified Dulbecco's Medium (IMDM) with GlutaMAX Supplement (Gibco), 10% heat-inactivated fetal bovine serum, 100 units/mL of penicillin and streptomycin, and 0.3mg/mL of L-glutamine ("Complete Media"). Spleens were then crushed and passed through a 70µm filter into a 50ml conical tube. Cells were washed with serum-free media. RBC lysis was performed. Cells were then washed 2x in complete media described above and resuspended for downstream applications.

Flow cytometry

Small intestine lamina propria lymphocytes were isolated from littermate *Il17ra*$^{fl/fl}$ and *Il17ra*$^{fl/fl}$ *x villin cre*$^{+}$ mice as described above. Single cell suspensions were stained with

eBiosciences antibodies against CD3 (17A2) and CD4 (RMA4-5) in a 96 well round bottom plate in the dark on ice for 20 minutes. Cells were washed 2.5x in cold FACS Buffer (0.5% FBS/0.01% NaN3/PBS), then fixed using BD Cyto-fix and incubated in the dark on ice for 20 minutes. Cells were washed and resuspended in PBS or FACS buffer and analyzed using the BD LSR II flow cytometer and FlowJo Software.

ELISPOT

MOG-specific IL-17A-producing T cells from the spleen of day 9 EAE induced mice were enumerated using peptide-driven ELIS POT. Briefly, 96-wells ELISPOT plates were coated with monoclonal anti-mouse IL-17, blocked with media containing 10% FBS. Cells from spleen were seeded at an initial concentration of 5×10^5 cells/well and subsequently diluted two-fold. Irradiated B6 splenocytes were used as APCs at a concentration of 1×10^6 cells/well in the presence of MOG (10 μg/ml) peptide. After 24 hours, plates were washed and probed with biotinylated anti-mouse IL-17. Spots were visualized and enumerated using a CTL-Immunospot S5 MicroAnalyzer and corrected with CD4 T cells number. Absolute $CD4^+$ T cells percentage and number were determined by using flow cytometry and cells count. No spots were detected in cultures lacking antigen or when using cells from uninfected mice.

Ex vivo cell stimulations

Splenic and small intestine lamina propria lymphocytes were isolated as described above. Cells were plated at a concentration of 5×10^5 or 1×10^6 cells per well in a 96-well round bottom plate. Cells were then stimulated with various conditions at 37°C for the detailed incubation times.

Lamina propria lymphocytes were isolated from day 9 MOG immunized ll17ra$^{fl/fl}$ x villin cre^{+} and littermate control ll17ra$^{fl/fl}$ control mice, and re-stimulated with MOG peptide (200 μg/ml) for 24 hours. Cell culture supernatants were analyzed for GM-CSF using BioLegend mouse GM-CSF ELISA kit as per manufacturer's instruction (BioLegend).

Splenocytes were isolated at the naïve state and day 9 post immunization of MOG-CFA or OVA-CFA. Cells were stimulated with MOG peptide (200ug/mL), OVA protein (200ug/mL), or anti-CD3/CD28 for three days. Supernatants were harvested and cytokine levels were measured via ELISA or Luminex.

ELISA and Luminex Assays

Cytokines from serum and cell culture supernatants were measured using the following ELISA or Luminex kits according to the manufacturer's instructions: Mouse-IL-17 ELISA MAX Kit (BioLegend), Mouse GM-CSF ELISA MAX Kit (BioLegend), MILLIPLEX Mouse Th17 Magnetic Bead Panel (Millipore Sigma), and Cytokine & Chemokine 36-Plex Mouse Procarta Plex Panel 1A (Thermo Fisher Scientific-Affymetrix), Human IL-1RA ELISA (Ebioscience).

3.2.3 Quantification and Statistical Analysis

Intestinal RNA sequencing

Raw reads from Illumina NextSeq500's in fastq format were trimmed to remove adaptor/primer sequences. Trimmed reads were then aligned using BWA (version 0.5.9, settings aln -o 1 -e 10 -i 5 - k 2 -t 8) against the mouse genome build 37.2 in geneSifter Analysis Edition for Next Generation Sequencing (Geospiza, Seattle, WA). Additional alignment and post-processing were done with Picard tools (version 1.58) including local realignment and score

recalibration to generate a finale genomic aligned set of reads. Reads mapping to the genome were characterized as exon, intron, or intergenic using the matched annotation for the genomic reference sequence. The remaining unmapped reads from the genomic alignment were then aligned to a splice reference created using all possible combinations of known exons and then categorizing these as known or novel splice events. This aligned data was then used to calculate gene expression by taking the total of exon and known splice reads for each annotated gene to generate a count value per gene. For each gene there was also a normalized expression value generated in two ways: 1) Reads per Mapped Million (RPM), which was calculated by taking the count value and dividing it by the number of million mapped reads, 2) Reads per Mapped Million per Kilobase (RPKM), which was calculated by taking the RPM vale and dividing it by the kilobase length of the longest transcript for each gene. The RPM values were subsequently used for comparing gene expression across samples to remove the bias of different numbers of reads mapped per sample. RPKM values were subsequently used for comparing relative expression of genes to one another to remove the bias of different numbers of mapped reads and different transcript lengths.

Statistical Tests

Statistical tests used are indicated in the figure legends. Data are presented as mean with individual samples visualized or mean + SEM. To compare differences between two groups, student-T test or non-parametric Mann-Whitney test was used depending on the distribution of the data. When comparing one variable in three or more groups, one-way ANOVA with multiple comparisons was used. When comparing multiple variables among two groups, two-way ANOVA with multiple comparisons or multiple T-tests per row was used. GraphPad Prism software was

used to analyze experimental groups. For all data, statistically significant was defined as $p<0.05$. The degree of statistical significance was defined as: $p<0.05$*, <0.01**, <0.001***, <0.0001****.

Analysis Software

GraphPad Prism was used for statistical analysis described above. Image J was used for histology analysis. BWA (version 0.5.9) in geneSifter Analysis Edition for Next Generation Sequencing (Geospiza, Seattle, WA) and Picard tools (version 1.58) were used for RNA sequencing analysis.

3.2.4 Data and Software Availability

The raw RNA sequencing data have been deposited into the sequencing read archive under SRA accession number SRP069071.

Figure cartoons within this chapter were images adapted from Servier Medical Art by Servier. Original images are licensed under a Creative Commons Attribution 3.0 Unported License (https://creativecommons.org/licenses/by/3.0/legalcode).

3.3 Results

3.3.1 Disruption of enteric IL-17RA signaling exacerbates neuroinflammation.

To investigate how intestinal IL-17 signaling regulates neuroinflammation, we induced experimental autoimmune encephalomyelitis (EAE) in intestinal epithelium-specific *Il17ra*

knockout mice (*Il17ra*$^{fl/fl}$ *x villin cre*$^{+}$) (48). Knockout mice and littermate *l17ra*$^{fl/fl}$ controls were treated with subcutaneous injections of myelin oligodendrocyte glycoprotein (MOG) in complete Freund's adjuvant along with intraperitoneal injections of pertussis toxin (PTx) given at day 0 and 2 post immunization as described in Figure 3-2A.

It has been previously shown that globally deleting *Il17ra* is protective in this model of EAE (126). Interestingly, deleting *Il17ra* signaling specifically in the intestinal epithelium exacerbated disease (Figure 3-2B). As compared to littermate *Il17ra*$^{fl/fl}$ controls, *Il17ra*$^{fl/fl}$ *x villin cre*$^{+}$ mice exhibited earlier onset and increased clinical severity (Figure 3-2B). This correlated with an increase in proinflammatory cytokine production in the terminal ileum and serum as measured at the transcript and protein level prior to disease onset (day 9 post immunization) (Figure 3-2C-F). More specifically, there were increases in terminal ileum (TI) *Il17a* and *Csf2* (encodes GM-CSF) transcript (Figure 3-2E-F), but only significant differences in serum GM-CSF (Figure3-2D). Together, these data showed that disruption of intestinal IL-17RA signaling exacerbated disease potentially due to aberrant systemic cytokine responses reflective of cytokine changes observed in the intestine.

Multiple IL-17 family cytokines signal through IL-17RA. IL-17A and IL-17F bind to IL-17RA only through a multimeric receptor with IL-17RC (15). In order to test whether exacerbated disease is specifically due to IL-17A and F signaling, we induced EAE in *Il17rc*$^{fl/fl}$ *x villin cre*$^{+}$ mice. Compared to littermate floxed controls, gut specific IL-17RC knockout mice appeared to have worse, but not significantly exacerbated disease (Figure 3-3A). In addition, disease onset was identical for both knockouts and controls (Figure 3-3A). This suggested that IL-17A and IL-17F may affect disease severity but not onset. Because knockout of intestinal IL-17RC did not

exacerbate disease to the same severity as IL-17RA, it also implicates other IL-17 family members such as IL-25 (320)in disease progression.

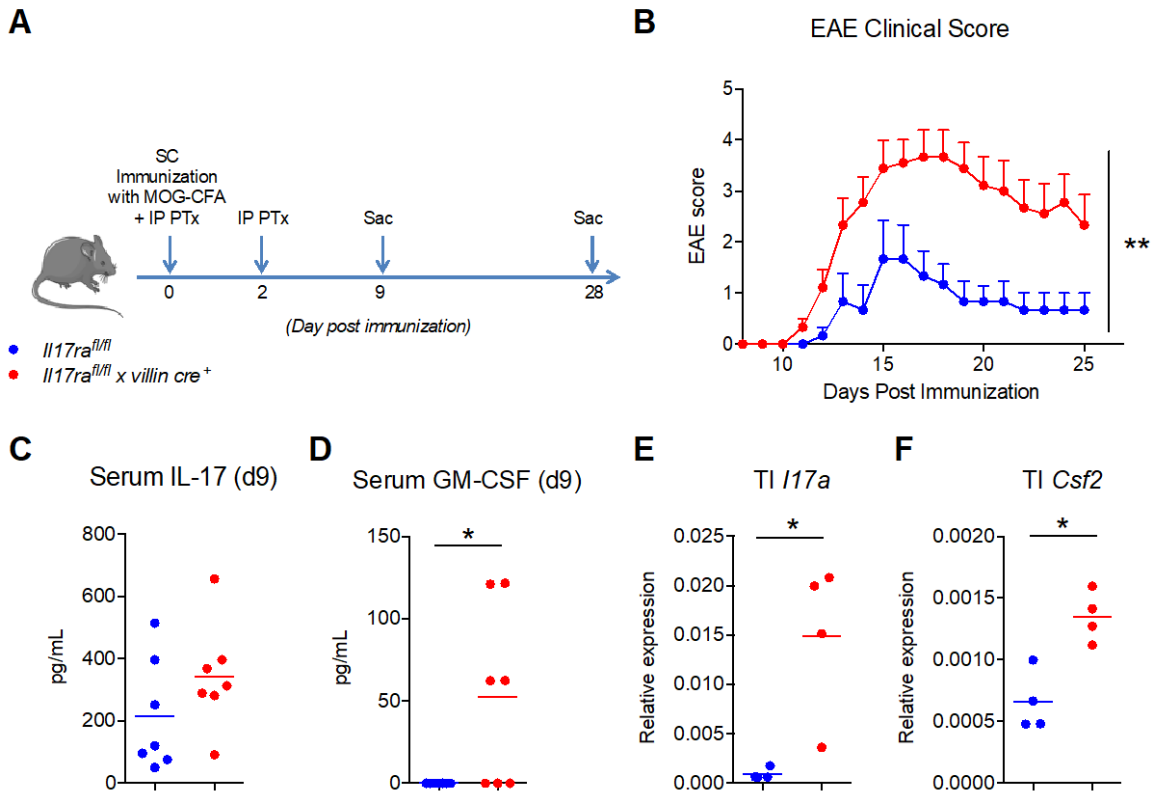

Figure 3-2 Disruption of enteric IL-17RA signaling exacerbates neuroinflammation.

(A) Schematic of experimental autoimmune encephalomyelitis (EAE) model. (B) Data shown are EAE severity score in *Il17ra*$^{fl/fl}$ *x villin cre+* (n = 8) mice and littermate *Il17ra*$^{fl/fl}$ controls (n = 6). (C-D) *Il17ra*$^{fl/fl}$ *x villin cre+* and littermate *Il17ra*$^{fl/fl}$ control mice serum were harvested on day 9 after MOG immunization. Serum IL-17A and GM-CSF concentrations were determined in the serum by Luminex assay. (E-F) Terminal ileum of *Il17ra*$^{fl/fl}$ *x villin cre+* and littermate *Il17ra*$^{fl/fl}$ mice were harvested on day 9 post EAE induction and analyzed for *Il17a* and *Csf2* expression by qRT-PCR. p<0.05*, <0.01**, <0.001***, <0.0001**** (Mann-Whitney Test, Unpaired T Test for Area Under the Curve)

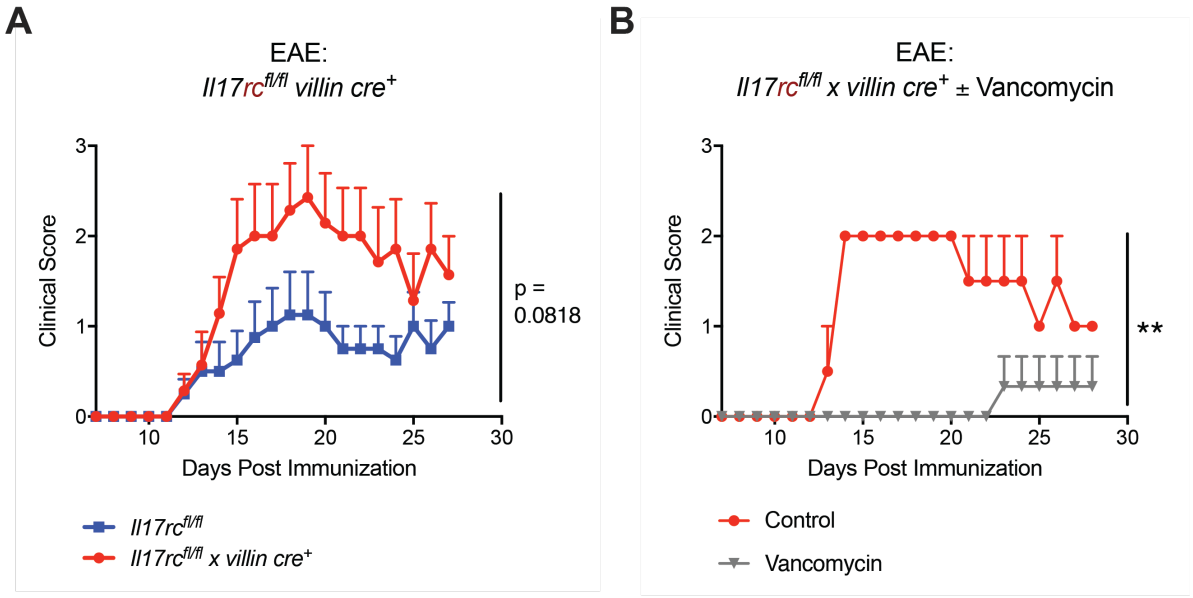

Figure 3-3. Moderately exacerbated EAE in *Il17rc$^{fl/fl}$ x villin cre^{+}* mice is microbiome-dependent.

(A) EAE severity score in *Il17rc$^{fl/fl}$ x villin cre^{+}* (n = 8) mice and littermate *Il17rc$^{fl/fl}$* controls (n = 7). (B) *Il17rc$^{fl/fl}$ x villin cre^{+}* mice were treated with and without vancomycin (0.5g/L) in the drinking water *ad libitum* for two weeks followed by EAE induction. EAE severity scores in water control (n = 2) or vancomycin-treated (n = 3) *Il17rc$^{fl/fl}$ x villin cre^{+}* mice. p<0.05*, <0.01**, <0.001***, <0.0001**** (Unpaired T Test for Area Under the Curve)

3.3.2 Disease in *Il17ra*$^{fl/fl}$ *x villin cre*$^{+}$ mice is microbiome-dependent.

We next tested whether disease in *Il17ra*$^{fl/fl}$ *x villin cre*$^{+}$ mice was dependent on the microbiome. Literature showed that segmented filamentous bacteria (Sfb) induced intestinal Th17 responses (60). In *Il17ra*$^{fl/fl}$ *x villin cre*$^{+}$ mice, we found an overgrowth of Sfb and discovered that IL-17 worked to constrain the Sfb population in a reciprocal regulatory relationship (48). Because Sfb is a gram-positive bacteria, we focused our investigation of the microbiome on this group of bacteria. For two weeks prior to EAE induction, mice were given vancomycin (0.5g/L) in the drinking water *ad libitum* to target gram-positive bacteria. Antibiotic treatment abrogated disease (Figure 3-4A, Figure 3-3B) along with intestinal levels of *Sfb, Il17a,* and *Csf2* (Figure 3-4B-D). This suggested that disease in *Il17ra*$^{fl/fl}$ *x villin cre*$^{+}$ mice was microbiome-dependent potentially due to microbiome regulation of *Il17a* and *Csf2.*

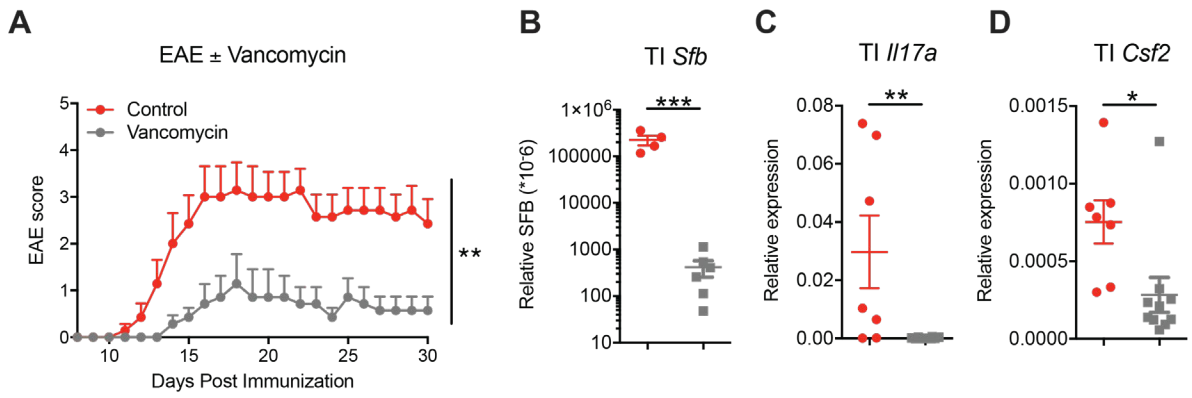

Figure 3-4. Disease in *Il17ra*$^{fl/fl}$ *x villin cre*$^{+}$ mice is microbiome-dependent.

Il17ra$^{fl/fl}$ *x villin cre*$^{+}$ mice were treated with and without vancomycin (0.5g/L) in the drinking water *ad libitum* for two weeks followed by EAE induction. (A) EAE severity scores in water control (n = 7) or vancomycin-treated (n = 7) *Il17ra*$^{fl/fl}$ *x villin cre*$^{+}$ mice. (B-D) Terminal ilea of water control or vancomycin treated *Il17ra*$^{fl/fl}$ *x villin cre*$^{+}$ mice were harvested on day 9 after MOG-CFA immunization. Terminal ileum *Sfb* (B), *Il17a* (C), and *Csf2* (D) gene expression were analyzed by qRT-PCR. p<0.05*, <0.01**, <0.001***, <0.0001**** (Mann-Whitney Test, Unpaired T Test, Area Under the Curve)

3.3.3 *Il17ra*$^{fl/fl}$ *x villin cre*$^{+}$ mice exhibit increased splenic IL-17 responses and increased antigen-specific GM-CSF responses.

Because the differences in disease severity occurred very early in the disease course, we hypothesized that there may be an increase in circulating effectors by disease onset. To test if there were increased antigen-specific effector responses prior to disease onset, we sacrificed the mice at day 9 post immunization when clinical disease scores were still zero. ELISPOT analysis of splenic CD4+ T cells showed there was not a significant increase in the number of splenic MOG-specific IL-17A+ cells (Figure 3-5A). In addition, we assessed the amount of cytokine produced by ELISA. *Ex vivo* stimulation of bulk splenocytes with MOG and negative control ovalbumin (OVA) showed no difference in the amount of antigen-specific IL-17 in culture supernatants (Figure 3-5B). To

validate this with another antigen, mice were immunized with CFA-OVA instead of CFA-MOG as detailed Figure 3-2A. *Ex vivo* OVA restimulation of splenocytes taken at day 9 post immunization replicated these findings (Figure 3-5C), confirming that *Il17ra*$^{fl/fl}$ *x villin cre*$^{+}$ mice did not exhibit increased splenic IL-17 responses specific to the antigen used in immunization. However, when splenic T cells taken from naïve mice were non-specifically stimulated with anti-CD3/CD28, there was a significant increase in the amount of IL-17 produced (Figure 3-5D). Together, this suggested that while there was not an increase in MOG-specific IL-17 responses, there was an increase in general splenic IL-17A production. Because there was also an increase in serum GM-CSF at day 9 post immunization (Figure 3-2D), similar assays were performed to assess antigen specific GM-CSF production. Interestingly, increased antigen-specific GM-CSF was observed in both the intestinal lamina propria and in the spleen at day 9 post immunization (Figure 3-5E-F).

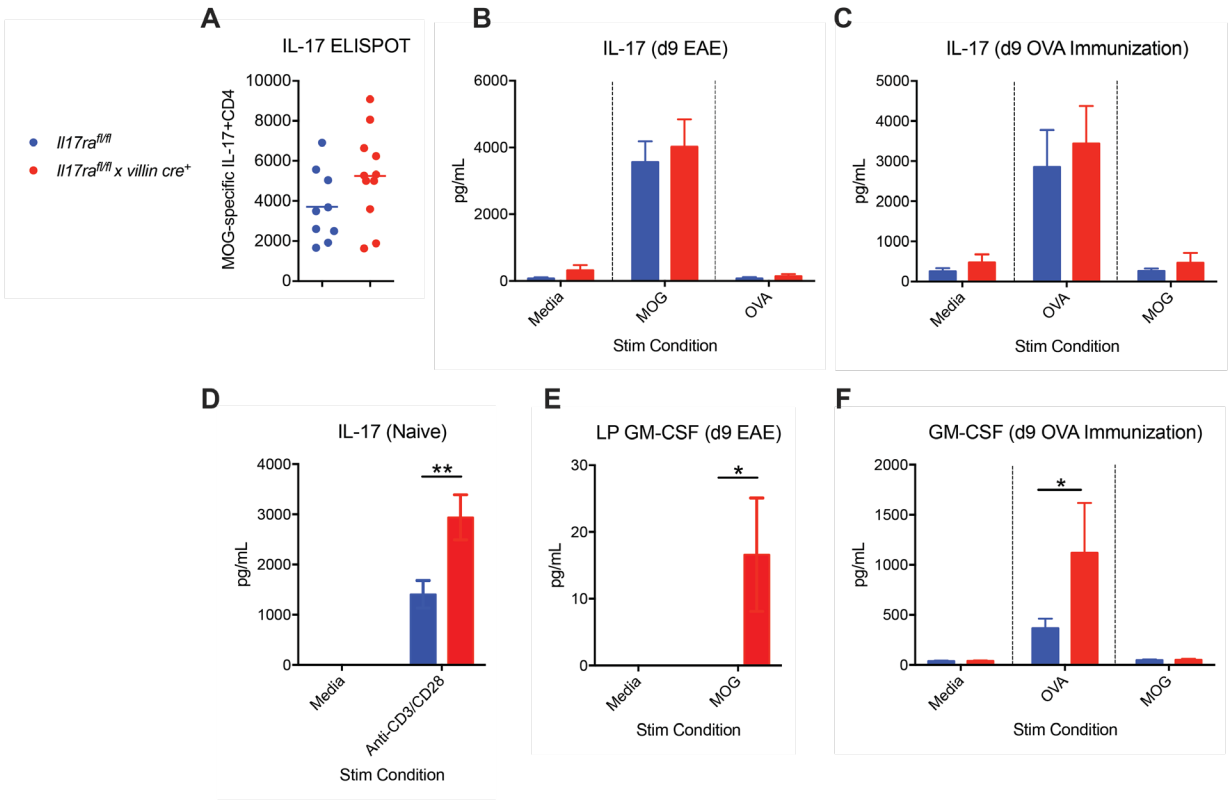

Figure 3-5 *Il17ra*$^{fl/fl}$ *x villin cre*$^{+}$ mice exhibit increased splenic IL-17 responses and increased antigen-specific GM-CSF responses.

(A-B) Splenocytes from *Il17ra*$^{fl/fl}$ and *Il17ra*$^{fl/fl}$ *x villin cre*$^{+}$ mice were isolated 9 days post myelin oligodendrocyte glycoprotein (MOG)-CFA immunization. (A) MOG specific IL-17 producing CD4+ T cells were measured by ELISPOT. (B) Bulk splenocytes were stimulated for *ex vivo* with media (unstimulated control), MOG, or ovalbumin (OVA) as a negative control. IL-17A was measured in culture supernatants by ELISA. (C, F) Splenocytes from *Il17ra*$^{fl/fl}$ and *Il17ra*$^{fl/fl}$ *x villin cre*$^{+}$ mice were isolated 9 days post-OVA-CFA immunization and stimulated *ex vivo* with media (unstimulated control), OVA, or MOG as a negative control. (C) IL-17A was measured in culture supernatants by ELISA. (D) Splenocytes from naïve *Il17ra*$^{fl/fl}$ and *Il17ra*$^{fl/fl}$ *x villin cre*$^{+}$ mice were isolated and stimulated *ex vivo* with media (unstimulated control) or anti-CD3/CD28. IL-17A was measured in culture supernatants by ELISA. (E) Small intestine lamina propria lymphocytes from *Il17ra*$^{fl/fl}$ and *Il17ra*$^{fl/fl}$ *x villin cre*$^{+}$ mice were isolated 9 days post myelin MOG-CFA immunization and stimulated *ex vivo* with media (unstimulated) or MOG. GM-CSF was measured in culture supernatants by ELISA. (F) GM-CSF in culture supernatants following stimulation described in (C). $p<0.05$*, <0.01** (Unpaired T Test, Two-way ANOVA with multiple comparisons)

3.3.4 *Il17ra*$^{fl/fl}$ *x villin cre*$^{+}$ disease exacerbation is IL-1β-independent.

Pathogenic Th17 cells implicated in EAE characteristically double produce IL-17 and GM-CSF (28, 30). Specific inflammatory signals favor the differentiation of these pathogenic Th17 cells (Table 1-2). One of those factors is IL-1β (28). Previous data suggested that IL-1β was detrimental in EAE (305, 306). In *Il17ra*$^{fl/fl}$ *x villin cre*$^{+}$ mice, *Il1b* expression was increased by RNA sequencing in the terminal ileum at the naïve state and by qRT-PCR at day 9 post immunization (Figure 3-6A-B). In addition, transcript of *Il1rn,* which encodes for IL-1R antagonist (IL-1RA), was decreased at day 9 post immunization (Figure 3-6C). IL-1RA competitively inhibits binding of IL-1β to the IL-1 receptor (321). Because *Il1b* was increased and regulation of IL-1 was decreased based on *Il1rn* expression, we hypothesized that disease exacerbation was dependent on IL-1 promotion of pathogenic Th17 differentiation. To test this hypothesis, anakinra, the pharmaceutical name for IL-1RA, was injected into *Il17ra*$^{fl/fl}$ *x villin cre*$^{+}$ mice twice daily for 21 days starting at immunization (Figure 3-6D). Contrary to our hypothesis, disease severity with treatment was unaltered compared to control treatment (Figure 3-6E). Due to previously documented concerns about drug half-life, a serum IL-1RA ELISA was performed to assess levels of IL-1RA prior to each of the two doses given per day. This confirmed that anakinra was indeed present systemically prior to each dose in the treated mice as compared to PBS-injected controls (Figure 3-6F). As expected, there was a higher level of drug on board prior to the PM dose as compared to the AM dose due to the smaller break between doses (Figure 3-6F). These data confirm that disease exacerbation in *Il17ra*$^{fl/fl}$ *x villin cre*$^{+}$ mice was not dependent on IL-1β signaling.

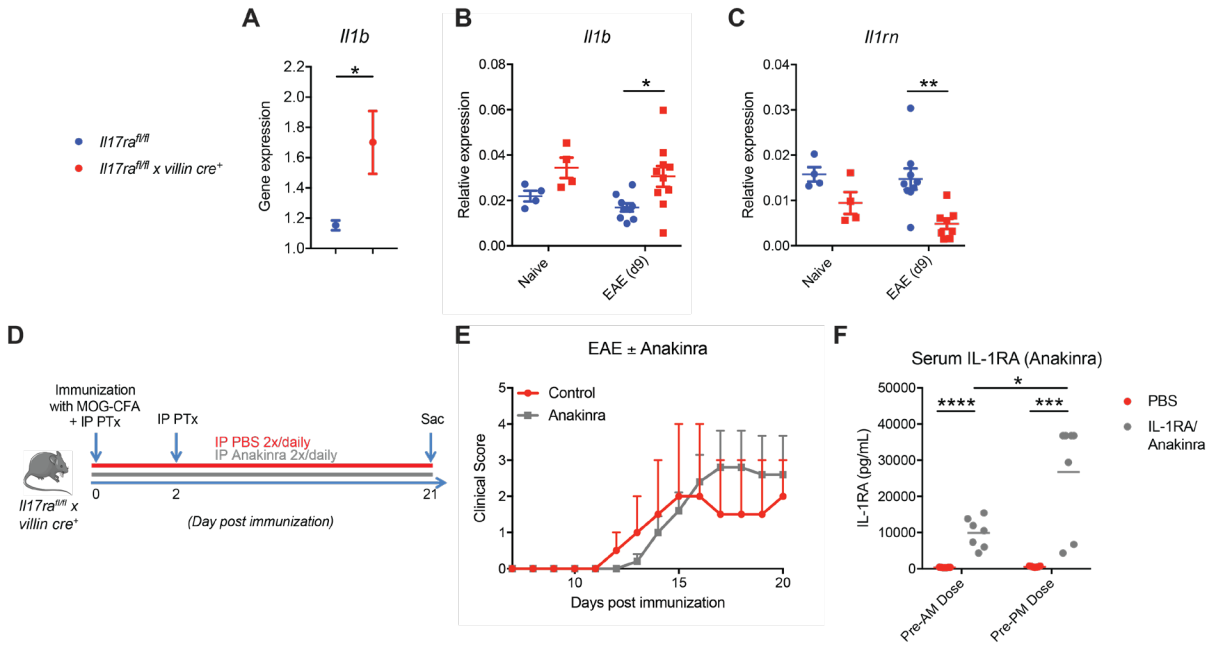

Figure 3-6 *Il17ra$^{fl/fl}$ x villin cre^{+}* disease exacerbation is IL-1β-independent.

(A) RNA sequencing was performed on the terminal ileum of naïve *Il17ra$^{fl/fl}$* and *Il17ra$^{fl/fl}$ x villin cre^{+}* mice. Data shows *Il1b* expression. (B-C) Terminal ileum *Il1b* and *Il1rn* expression was measured by qRT-PCR in *Il17ra$^{fl/fl}$* and *Il17ra$^{fl/fl}$ x villin cre^{+}* mice at the naïve state and 9 days post EAE immunization. (D-F) *Il17ra$^{fl/fl}$ x villin cre^{+}* mice were treated with intraperitoneal (IP) Anakinra (IL-1RA) or PBS control injection twice daily for 21 days beginning on day 0 of EAE induction. (D) Experiment schematic. (E) EAE disease severity scores. (F) IL-1RA was measured by ELISA on serum harvested prior to the AM and PM dose of anakinra. p<0.05*, <0.01**, <0.001***, <0.0001**** (Unpaired T Test, Area Under the Curve, Two-Way ANOVA with multiple comparisons)

3.3.5 *Il17ra*$^{fl/fl}$ *x villin cre*$^{+}$ mice have increased intestinal *Ccr2* and *Ccr6* and spinal cord *Nos2* prior to EAE onset.

In addition to its function as a granulocyte and macrophage growth factor, GM-CSF has been shown to promote activation and infiltration of immune cells into the CNS during EAE. Indeed, GM-CSF deficient mice exhibited less severe EAE with less CNS myeloid cell infiltration (304, 308). In addition, GM-CSF can promote IL-23 production by dendritic cells to perpetuate a cycle of Th17 effector generation and activation (27). In *Il17ra*$^{fl/fl}$ *x villin cre*$^{+}$ mice, there is evidence of increased intestinal GM-CSF (Figure 3-2, 3-5). To explore these potential effects of GM-CSF within the gut specific knockout mice during EAE, intestinal *Ccr2* expression, an inflammatory macrophage marker, was measured via qPCR at day 9 post immunization. There were significantly increased expression levels in *Il17ra*$^{fl/fl}$ *x villin cre*$^{+}$ mice as compared to littermate floxed controls (Figure 3-7A). Knockout mice also exhibited increased intestinal *Ccr6* (Figure 3-7B), a marker highly expressed by Th17 cells, though this may simply be due to the Sfb overgrowth previously mentioned. Expression of these genes were also measured in the spinal cord 9 days after immunization. *Ccr6* expression was undetectable (Figure 3-7C), but there were trends toward increased *Ccr2* (Figure 3-7D) and significantly increased *Nos2* (Figure 3-7E). *Nos2* is expressed on proinflammatory M1 macrophages, suggesting there may be increased proinflammatory macrophages in the spinal cord already at day 9 post immunization.

To assess what may be occurring during vancomycin-mediated protection, *Il17ra*$^{fl/fl}$ *x villin cre*$^{+}$ terminal ileum and spinal cord gene expression were measured by qRT-PCR at day 9 post immunization under vancomycin treatment. *Ccr2, Ccr6,* and *Cd4* were all decreased in the terminal ileum (Figure 3-7F-H). In the spinal cord, there were trends toward decreased *Cd4* expression (Figure 3-7I). At the cellular level, the increase in small intestine lamina propria CD4+

T cells during EAE was reduced by vancomycin treatment to levels similar to naïve mice (Figure 3-7J-K). While additional experiments are certainly necessary to validate these findings and demonstrate causation, these preliminary data suggest that there may be increased spinal cord immune infiltration potentially due to a microbiome-dependent increase of intestinal immune cells.

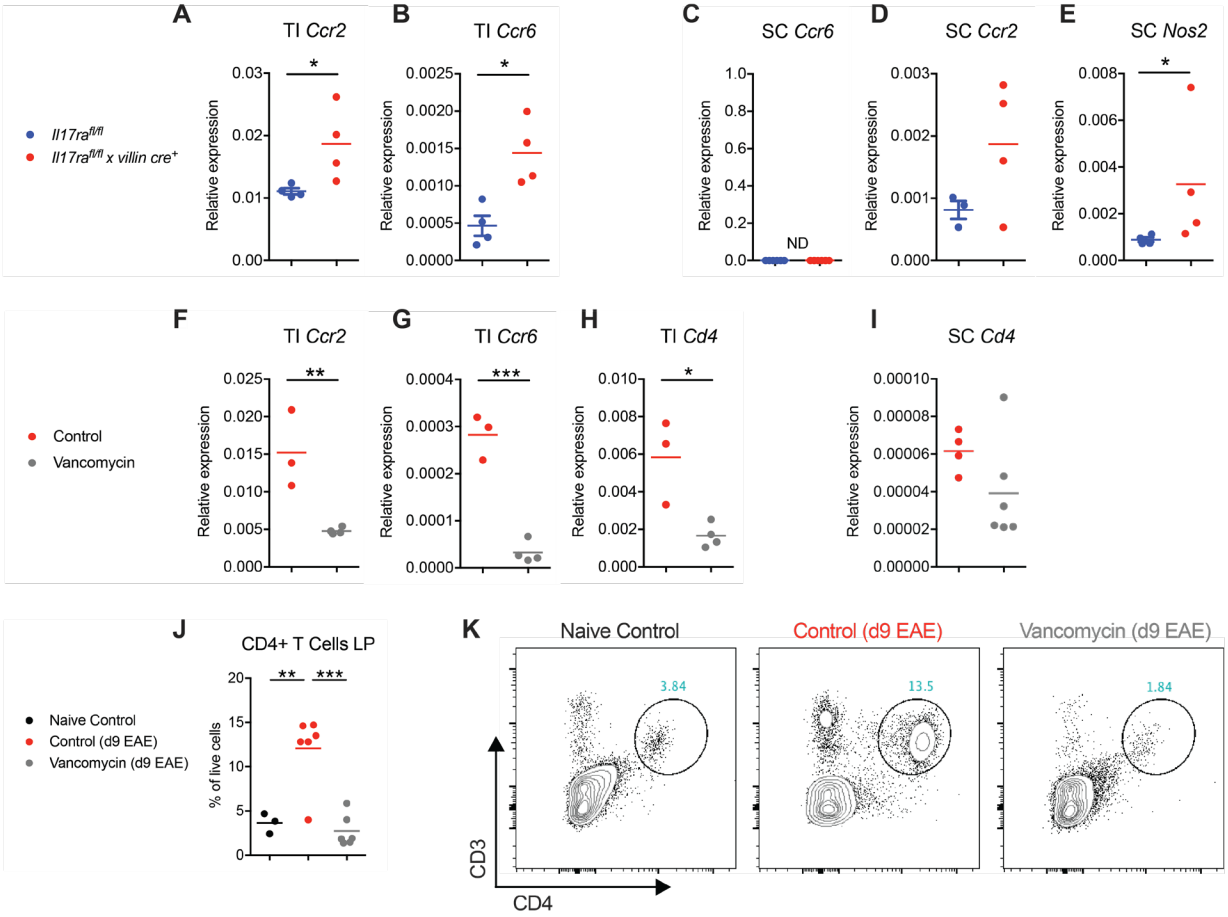

Figure 3-7 *Il17ra*$^{fl/fl}$ *x villin cre*$^{+}$ mice have increased intestinal *Ccr2* and *Ccr6* and spinal cord *Nos2* prior to EAE onset.

(A-E) Terminal ilea and spinal cords were harvested from *Il17ra*$^{fl/fl}$ and *Il17ra*$^{fl/fl}$ *x villin cre*$^{+}$ mice 9 days post-MOG-CFA immunization. Terminal ileum (TI) *Ccr2* (A) and *Ccr6* (B) were measured by qRT-PCR. Spinal cord *Ccr6* (C), *Ccr2* (D), and *Nos2* (E) were measured by qRT-PCR. (F-K) *Il17ra*$^{fl/fl}$ *x villin cre*$^{+}$ mice were treated 2 weeks with vancomycin in the drinking water *ad libitum* followed by MOG-CFA immunization. Mice were sacrificed at 9 days post immunization. (F-H) Terminal ileum *Ccr2* (F), *Ccr6* (G), and *Cd4* (H) was measured by qRT-PCR. (I) Spinal cord (SC) *Cd4* was measured by qRT-PCR. (J) Quantification of lamina propria (LP) CD4+ T cells as measured by flow cytometry. (K) Representative FACS plots. p<0.05*, <0.01**, <0.001***, <0.0001**** (Mann-Whitney Test, Unpaired T Test, One-way ANOVA with multiple comparisons)

3.4 Discussion

Our results provide evidence that perturbation of intestinal IL-17 signaling is sufficient to exacerbate neuroinflammation. Abrogation of intestinal IL-17RA disrupted the intestinal microbiota and increased intestinal *Il17* and *Csf2* and systemic responses in both cytokines. Preliminary data also suggested a potential increase of inflammatory monocyte infiltration into the CNS, together exacerbating disease.

As previously mentioned, Th17 cells have been previously implicated in EAE and MS as a detrimental factor. In mice, global knockout of IL-17RA was protective (126). However, the role of Th17 cells in autoimmune neuroinflammation is complex. By using *Il17ra*$^{fl/fl}$ *x villin cre*$^{+}$ mice, we again uncoupled intestinal IL-17RA signaling from systemic signaling to reveal a novel protective role of IL-17RA in neuroinflammation. This protection was accompanied by an increase in terminal ileum *Csf2.* This aligned with other reports on the pathogenicity of GM-CSF within this model (303, 304). It also raises the possibility of the intestine as a source of pathogenic GM-CSF within EAE and MS. The intestine does play a large role in the regulation of Th17 cells (322). Moreover, a recent study showed an upregulation of Th17 cells with intestines of MS patients (309). As such, it is possible that pathogenic Th17 cells that are detrimental in EAE can also arise from the intestine. These data may also help explain why there is only partial protection conferred by IL-17A deficiency or anti-IL-17A neutralization (298, 299). This partial protection may suggest a role for other Th17 related cytokines, or that IL-17 expression is associated with a gene module that allows traffic into the brain but is not critical for direct CNS damage. Our data suggest that the protective effects of blockade may also be diminished as a result of intestinal IL-17 signaling disruption with downstream consequences detrimental to neuroinflammation. Alternatively,

differences in results could be due to institutional differences in the intestinal microbiome of the respective mice.

Our data showed that vancomycin treatment conferred protection in *Il17ra*$^{fl/fl}$ *x villin cre*$^{+}$ mice, implying a role of gram-positive bacteria in EAE. A gram-positive targeted antibiotic approach was employed to eliminate the bacteria we believed the most likely contributor in our model—Sfb. We previously showed that Sfb was overgrown in *Il17ra*$^{fl/fl}$ *x villin cre*$^{+}$ mice (48) and as expected, vancomycin treatment decreased the intestinal Sfb burden. These data corroborate with another report that monocolonization with Sfb in germ-free mice is sufficient to exacerbate EAE compared to germ-free mice (313). However, monocolonization with Sfb did not restore full susceptibility to EAE as compared to conventional SPF mice (313), implying a role of other bacteria in disease pathogenesis or that Sfb requires cooperation with other bacteria to exert its effects. This may explain why a report by Stockinger and colleagues showed that mice reconstituted with feces with high Sfb levels had no effect on EAE as compared to disease in mice reconstituted with low-Sfb feces (323). It is possible the "Sfb+" feces lacked the bacterial strains with which Sfb coordinates. Alternatively, it may have additional strains protective in EAE. With that said, it cannot be ruled out that there are other microbiota differences in *Il17ra*$^{fl/fl}$ *x villin cre*$^{+}$ mice that may exacerbate disease. Indeed, intestinal Th17 signaling is especially important for controlling microbes close to the intestinal epithelium. Similarly, it also cannot be ruled out that there are other bacteria that can induce pathogenic Th17 responses. In humans, Honda and colleagues identified a consortium of 20 bacterial strains capable of adhering to the mouse intestinal epithelium to induce a robust Th17 response (36). Vancomycin-mediated protection from EAE was accompanied by a decrease in intestinal *Il17a* and *Csf2*, suggesting that the microbiome may worsen disease through the intestinal regulation of these two cytokines.

When investigating the systemic responses of these cytokines, *Il17ra*$^{fl/fl}$ *x villin cre*$^{+}$ mice exhibited increased non-specific IL-17 responses. These responses may contribute disease through the bystander effect. The bystander effect refers to the non-antigen-specific activation of cells through other stimuli in the environment, which can in turn affect health and disease (324). Indeed, it has been shown that non-myelin specific bystander T cells can exacerbate EAE pathology (324, 325). Lee et al. showed that adoptive transfer of activated memory OTII CD4+ T cells with myelin-specific 2d2 cells into RAG knockout mice induced more severe EAE as compared to transfer of 2d2 cells alone (324). In *Il17ra*$^{fl/fl}$ *x villin cre*$^{+}$ mice, it is possible that the disruption of intestinal Th17 signaling and subsequent changes in the microbiome caused increased activation of Th17 cells potentially from an altered intestinal cytokine milieu and microbiome-induced activation. Studies showed that non-specific activation with anti-CD3/CD28 induced a greater IL-17 response in memory cells as compared to naïve cells (324). This paralleled results in *Il17ra*$^{fl/fl}$ *x villin cre*$^{+}$ mice in which non-specific anti-CD3/CD28 stimulation of splenocytes from naïve *Il17ra*$^{fl/fl}$ *x villin cre*$^{+}$ mice produced more IL-17 compared to *Il17ra*$^{fl/fl}$ controls. This may suggest that there are increased memory-like cells in *Il17ra*$^{fl/fl}$ *x villin cre*$^{+}$ mice.

These activated Th17 cells can then act systemically to influence disease. Though discussed in more detail later, one possibility is that these cells may be migrating into the CNS to influence disease directly, especially since T cell activation is required to cross the BBB (291). A more likely possibility is that the inflammatory mediators produced/induced by the cells as opposed to the cells themselves can act on the blood brain barrier and promote immune cell infiltration. Indeed IL-17RA, IL-17RC, and IL-22R are expressed on the BBB cells. Both IL-17 and IL-22, which is also increased in *Il17ra*$^{fl/fl}$ *x villin cre*$^{+}$ mice (48), promoted migration of CD4+ T cells across human BBB endothelial cells with specific enrichment of migrating CD45RO+

memory cells and increases in CCL2 and CXCL8 (294). Furthermore, immunostaining of autopsied patient brain specimens revealed numerous CD45RO+ cells co-staining with IL-17 or IL-22 in infiltrated MS lesions (294). In EAE, preliminary experiments with IL-22 binding protein knockout mice (*Il22ra2*$^{-/-}$), which have increased IL-22 signaling, are protected from disease (Figure 3-8), supporting a protective role of IL-22. Therefore, Th17-induced cytokines and chemokines may contribute to EAE exacerbation through these mechanisms.

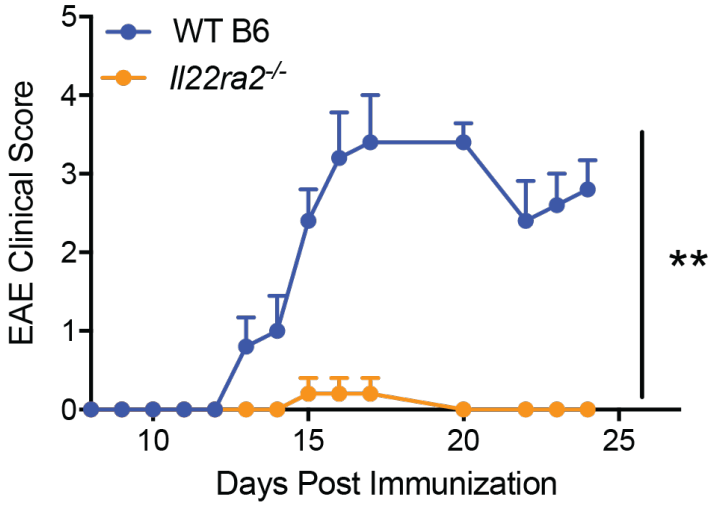

Figure 3-8. *Il22ra2*$^{-/-}$ mice are protected from EAE.

EAE severity scores in wildtype (WT) B6 mice (n = 5) and *Il22ra2*$^{-/-}$ mice (n = 5). p<0.05*, <0.01**, <0.001***, <0.0001**** (Unpaired T Test for Area Under the Curve)

While the presence of bystander cells can worsen EAE, they can only do so in the presence of MOG-specific cells (324). In our study, *Il17ra*$^{fl/fl}$ *x villin cre*$^{+}$ mice exhibited increased antigen-specific GM-CSF responses. The increase in MOG-specific GM-CSF response was perhaps indicative of the increase in pathogenic Th17 cells detrimental in EAE. The increase of this response in the intestine suggests that the systemic elevations in GM-CSF may also originate from

the intestine. Elevation in MOG-specific splenic responses at day 9 post immunization aligns with other reports describing increased MOG-specific effector responses in the spleen during the priming phase of EAE (326). Interestingly, this antigen-specific response was not limited to MOG. Rather, OVA-CFA immunization prompted the same elevated splenic GM-CSF response. Therefore, while the specific antigen dictates the site of tissue damage (i.e. MOG and the CNS), in this case it appears to play less of a role in the type of cytokine response. This emphasizes that the type of response to a given antigen is largely dependent on the host environment, whether that be the state of the immune system, the microbiome, genetic susceptibility, or even the epigenetic landscape. Disruption of intestinal Th17 signaling appears to be fostering a host environment that promotes increased antigen-specific GM-CSF responses characteristic of pathogenic Th17 cells.

Because IL-1β has been shown to promote pathogenic Th17 differentiation (30, 327) and was increased by gene expression in the intestine of *Il17ra*$^{fl/fl}$ *x villin cre*$^{+}$ mice, we hypothesized that it was a contributing factor to disease exacerbation. Contrary to some reports showing that IL-1R1 and IL-1β were detrimental in EAE (305, 306), treatment with anakinra, IL-1R antagonist (IL-1RA) did not ameliorate disease in gut-specific knockouts. However, there are other cytokines that promote pathogenic Th17 differentiation—namely IL-23. Multiple reports have shown that IL-23 is critical for T cell-GM-CSF production in EAE (27, 308). While IL-23 is not increased in *Il17ra*$^{fl/fl}$ *x villin cre*$^{+}$ mice at baseline, it is possible that IL-23 is increased during the disease course, which may be more important in the context of EAE. Indeed, IL-23 was found to be critical during the effector phase of EAE and not the initiation (27). This is consistent with previous reports showing high tissue expression of IL-23, which can enhance local CNS effector function to drive neuroinflammation (29). In addition, IL-23 can act on APCs to stimulate a positive feedback loop in which IL-23 promotes GM-CSF production in Th17 cells, and GM-CSF then promotes IL-23

production in APCs (27). As such, further characterization of IL-23 in *Il17ra*$^{fl/fl}$ *x villin cre*$^{+}$ mice during EAE and its relation to IL-17 and GM-CSF production is warranted.

The increase in GM-CSF found in *Il17ra*$^{fl/fl}$ *x villin cre*$^{+}$ mice during EAE could contribute to immune activation and infiltration in to the CNS. More specifically, GM-CSF can activate microglia within the CNS and promote recruitment of circulating monocytes (303, 328, 329). In GM-CSF deficient mice, myeloid cells, which express the GM-CSF receptor, do not accumulate in the CNS (303, 304). Our preliminary data show that there is a vancomycin-sensitive increase in terminal ileum *Ccr2* and *Ccr6* with a corresponding increases in spinal cord *Ccr2* and *Nos2*, a gene upregulated in proinflammatory M1 macrophages. While these changes may be association, the fact that gene expression in the spinal cord reflects the changes in intestine also poses the hypothesis that there could be immune cell trafficking from the intestine into the circulation and CNS.

This preliminary data must be confirmed at the cellular level and additional studies must be done, but there is evidence in the literature that supports the possibility of intestinal migration to distant immunoprivileged sites. Though not in EAE, Caspi and colleagues showed that autoreactive T cells in experimental autoimmune uveitis were primed in the intestine, migrated to the eye, and were activated via molecular mimicry to contribute to ocular pathology (121). In addition, Benakis et al. showed that intestinal cells migrated to the meninges after a mouse model of ischemic stroke (247). Benakis et al. utilized KikGR33 mice that ubiquitously expressed a fluorescent protein whose emission changed from green to red after violet light exposure. These mice underwent a laparotomy and exposure to violet light only on the intestine, distinguishing cells of intestinal origin. Analysis following ischemic stroke showed intestinal red-emitting T cells in the meninges (247). However, a caveat to this study is exposing cells within the gastrointestinal

vasculature already in circulation. In addition to these studies, there are data showing that during EAE, encephalitogenic Th17 cells that produce GM-CSF switch from CCR6+CCR2- to CCR6-CCR2+ (330). These cells were found in the CNS of mice already at day 5 post EAE immunization with increasing percentages observed at days 10 and 15 post immunization (330). Therefore, while the increase in spinal cord *Ccr2* and *Nox2* at day 9 post immunization in *Il17ra*$^{fl/fl}$ *x villin cre*$^{+}$ mice could be indicative of increased inflammatory monocyte infiltration, it could also be a result of Th17 cells switching from CCR6+ to CCR2+ cell. This may explain why there is a dramatic increase in *Ccr2* and *Ccr6* expression in the intestine at day 9 with undetectable spinal cord *Ccr6* and increased *Ccr2.*

As previously mentioned, it may likely be the case that Th17 cells and other intestinal cells are not physically migrating into the CNS at all, but rather contributing to disease more indirectly via the bystander effect as discussed above. Our data leave open the possibility that cytokines, bacterial products and metabolites (316, 331), and other inflammatory mediators can be going from the intestine to the circulation and CNS. More locally, these factors can also act on the enteric nerves and affect disease in that way (246).

These studies offer many future directions exploring other possibilities by which intestinal IL-17RA signaling could be contributing to neuroinflammation. As previously mentioned, bacterial metabolites can play a large role in disease development and could be altered due to the commensal dysbiosis in the gut specific knockouts. Alterations in the intestinal microbiome and microbial-derived SCFAs have been known to influence the intestinal Treg population (332). As such, characterization of the Treg population in *Il17ra*$^{fl/fl}$ *x villin cre*$^{+}$ mice may be important as well, especially since shifts in the balance of Tregs/Th17 have been linked to microbiome-mediated effects on EAE (311–313). In terms of microbial product release into circulation, there

is no baseline defect in intestinal barrier integrity in *Il17ra*$^{fl/fl}$ *x villin cre*$^{+}$ mice. However, the barrier may be compromised after disease induction based on preliminary assessment of intestinal tight junction related genes (Figure 3-9). Increased permeability would allow for enhanced release of bacterial products including TLR ligands and SCFAs.

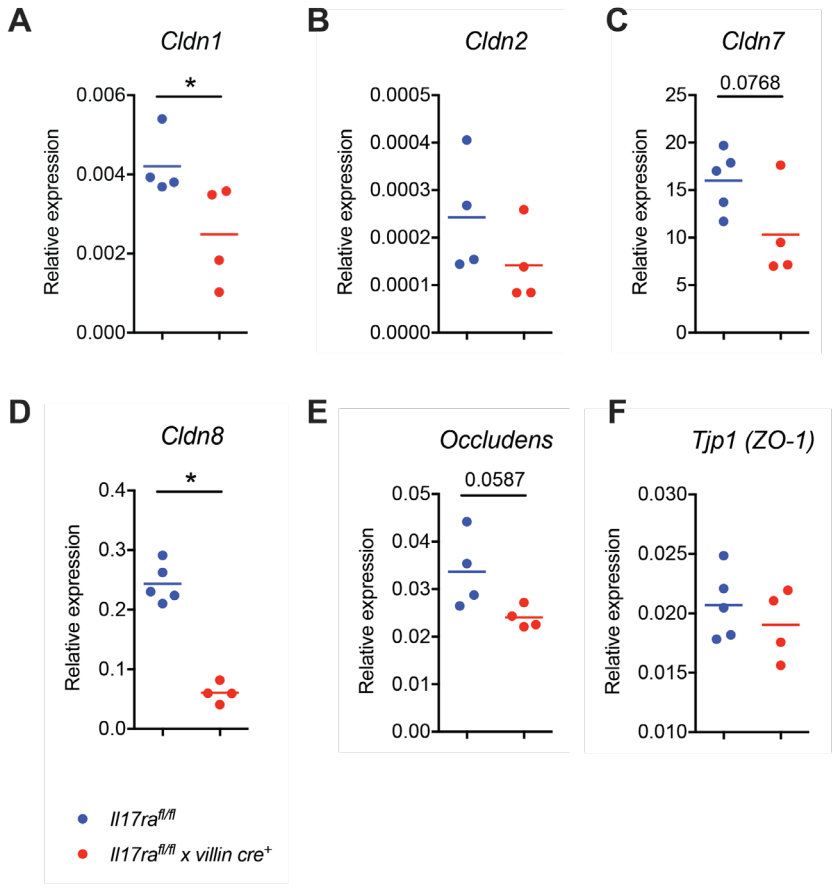

Figure 3-9. Terminal ileum tight junction protein gene expression at day 9 post EAE immunization.

Terminal ileum expression of *Claudin 1 (Cldn1)* (A), *Claudin 2 (Cldn2)* (B), *Claudin 7 (Cldn7)* (C), *Claudin 8 (Cldn8)* (D), *Occludens* (E), and *Tight junction protein 1 (Tjp1)/ Zona Occludens 1 (ZO-1)* (F) as measured by qRT-PCR.

In addition to the intestinal barrier integrity, assessment of the integrity of the BBB in *Il17ra*$^{fl/fl}$ *x villin cre*$^{+}$ mice is critical, as there may not only be increased release and migration of cells and immune mediators into the circulation due to intestinal barrier defects but increased accessibility to the CNS due to BBB compromise. Finally, a more thorough investigation of pathogenic Th17 cells in the context of EAE in *Il17ra*$^{fl/fl}$ *x villin cre*$^{+}$ mice would be informative. Identifying their tissue of origin, what factors induce them (i.e. IL-23), and which cells ultimately migrate into the CNS will provide additional mechanistic insight into how intestinal Th17 signaling can contribute to MS immunopathology.

In summary, these studies support a novel protective role of intestinal Th17 signaling in autoimmune neuroinflammation. We show that mice with disrupted intestinal IL-17RA exhibited earlier EAE onset and increased EAE severity. The data suggest that disease exacerbation may be due to microbiome-mediated increases in pathogenic Th17 responses that promote CNS infiltration and worsened neuroinflammation. While more studies are necessary to validate these findings, this work elucidates potential mechanisms by which intestinal Th17 signaling and its relationship with the microbiome contribute to MS and other autoimmune pathologies. Moreover, it exposes novel therapeutic avenues targeting the gut-brain axis to ultimately improve patient health.

3.5 Working Model

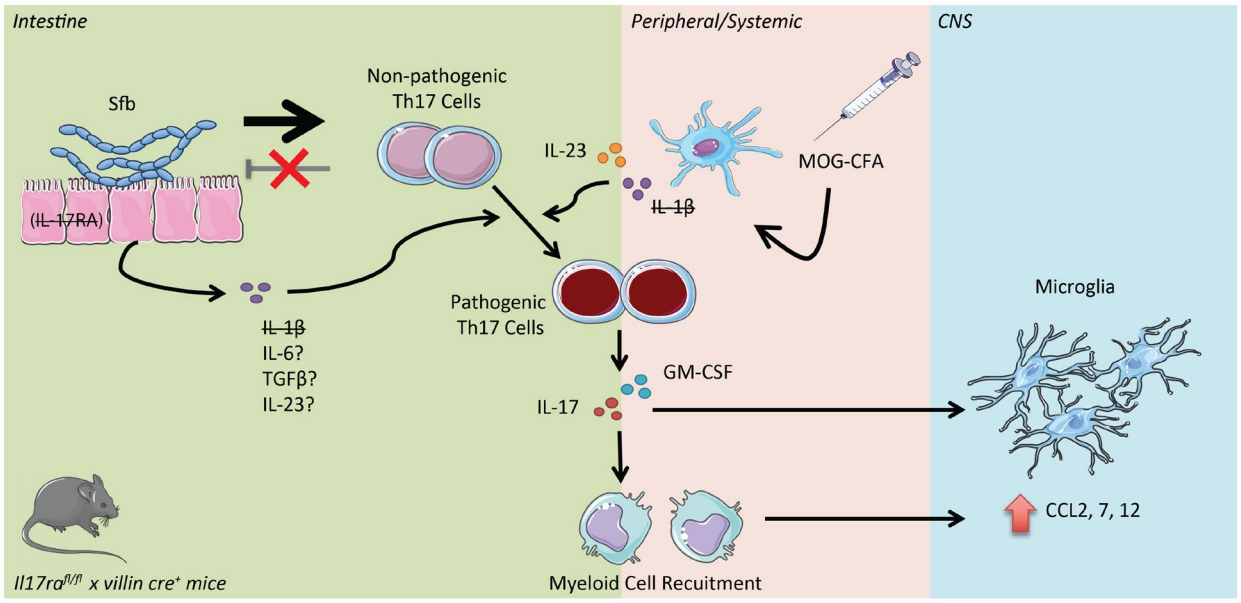

Figure 3-10. Working Model

In *Il17ra*$^{fl/fl}$ *x villin cre*$^{+}$ mice, where IL-17RA signaling is knocked out specifically in the intestinal epithelium, there was intestinal overgrowth of Sfb due to the lack of Th17-mediated regulation. Because of the reciprocal regulatory relationship between Th17 cells and Sfb, Sfb overgrowth induced intestinal IL-17 and increased non-pathogenic Th17 cells. We hypothesize that the cytokine response to immunization with myelin oligodendrocyte glycoprotein (MOG) in Complete Freund's adjuvant (CFA) partnered with microbiome-mediated cytokine changes promoted a switch from non-pathogenic to pathogenic Th17 cells that double produce IL-17 and GM-CSF. These two cytokines can then act systemically in a non-specific fashion to promote blood brain barrier weakening, recruitment and activation of myeloid cells, and chemokine release in the CNS to enhance bystander lymphocyte infiltration to ultimately exacerbate neuroinflammation.

4.0 Overall Conclusions & Future Directions

These dissertation studies investigated the role of intestinal Type 17 signaling and the microbiome in extra-intestinal pathologies, specifically focusing on the gut-liver and gut-brain axes. Both studies utilized in *Il17ra*$^{fl/fl}$ *x villin cre*$^{+}$ mice to knockout IL-17RA signaling in the intestinal epithelium, uncoupling intestinal IL-17RA signaling from systemic signaling to reveal novel protective roles. In mouse models of liver and neuroinflammation, these works demonstrated how disruption of intestinal Th17 signaling and subsequent alterations in the intestinal microbiome were capable of exacerbating disease at distal sites.

In the gut-liver axis, abrogation of intestinal IL-17RA was sufficient to worsen disease in a Con A mouse model of T cell-mediated hepatitis. More specifically, naïve *Il17ra*$^{fl/fl}$ *x villin cre*$^{+}$ mice exhibited microbiome dysbiosis and increased translocation of bacterial products (CpG DNA) to the liver, driving hepatic IL-18 production. Upon disease induction, absence of enteric IL-17RA signaling exacerbated hepatitis and hepatocyte cell death. IL-18 was necessary for disease exacerbation and associated with increased activated hepatic lymphocytes based on *Ifng* and *Fasl* expression. From these studies, we concluded that intestinal IL-17R regulated the translocation of TLR9 ligands and constrained susceptibility to hepatitis. These data connect enteric Th17 signaling and the microbiome in hepatitis, with broader implications on the effects of impaired intestinal immunity and subsequent release of microbial products observed in other extra-intestinal pathologies.

In the gut-brain axis, perturbation of intestinal IL-17RA was sufficient to worsen disease in the experimental autoimmune encephalomyelitis (EAE) mouse model of multiple sclerosis. Our data suggested that *Il17ra*$^{fl/fl}$ *x villin cre*$^{+}$ mice, which have higher Sfb levels, exhibited earlier EAE

onset and increased EAE incidence and severity as compared to littermate *Il17ra*$^{fl/fl}$ controls. Treatment with vancomycin ameliorated disease, suggesting that the phenotype was microbiome-dependent. Disease exacerbation was accompanied by systemic increases in IL-17 and GM-CSF responses. In addition, preliminary data indicated that *Il17ra*$^{fl/fl}$ *x villin cre*$^{+}$ mice had increased intestinal expression of *Csf2, Ccr2,* and *Ccr6* and increased spinal cord expression of *Nos2* immediately prior to disease onset. Together, this suggested that there could be increased migration into the CNS of *Il17ra*$^{fl/fl}$ *x villin cre*$^{+}$ mice, contributing to exacerbated disease. These studies elucidated how dysregulation of enteric IL-17R signaling and the commensal microbiota may contribute to the pathogenesis of MS and other autoimmune conditions. Moreover, it provides insight into novel therapeutic strategies targeting the gut-brain axis.

Together, both studies emphasize the importance of examining intestinal Th17 immunity in extra-intestinal diseases and mucosal immunity in general. It reaffirms the concept that mucosal immunity is critical in disease protection, and that when it fails or is disrupted, systemic immunity is affected. Specific to liver and neuroinflammation, many patients with Th17-associated diseases including multiple sclerosis and autoimmune hepatitis present with intestinal symptoms even early in the disease course. While this may be only a consequence rather than a cause, our studies argue for a potential role of the intestine in perpetuating further disease development and exacerbation. Previous research has shown that the intestine is a major regulator of Th17 signaling (322). Our work has demonstrated that intestinal Th17 signaling can contribute to extra-intestinal disease via its regulation of the microbiome and downstream release of cytokines, chemokines, and other inflammatory mediators. This link between intestinal Th17 immunity and extra-intestinal disease is supported by other work detailing intestinal Th17 downstream effects in other organs. McAleer et al. showed that in pulmonary *Aspergillus fumigatus* infection, gastrointestinal delivery of Reg3γ

conferred protection in an IL-22 dependent manner (333). Moreover, these Th17-induced antimicrobial peptides can also have effects on chemotactic activity and TLR responsiveness (334), adding to the potential systemic effects on health and disease. Ultimately, our studies support the idea that intestinal Th17 signaling is capable of affecting extra-intestinal disease through various mechanisms. What is especially interesting about these dissertation studies is that while there are parallels between the two mechanisms exacerbating hepatitis and neuroinflammation in *Il17ra*$^{fl/fl}$ *x villin cre*$^{+}$ mice, each model actually implicates different aspects of Th17 cells and the microbiome.

In each model, it appears that different Th17 cytokines are playing a role in disease exacerbation. One reason for this may be the differences in IL-17RA signaling in the small versus large intestine. As such, it would be helpful to isolate the various intestinal segments and evaluate immunologic changes as well as alterations in the microbiome within each segment. Based on the data, the EAE phenotype is likely connected at least in-part to small intestinal IL-17RA signaling given the effect of Sfb overgrowth (predominantly in the terminal ileum) in the EAE model. Our working model in EAE suggests an increase in pathogenic Th17 cells that are double producing GM-CSF and IL-17. This was seen in the intestine as well as in systemic responses during *ex vivo* stimulations. Both of these cytokines may then contribute to CNS immune infiltration and recruitment to exacerbate neuroinflammation via chemokine release, effects on myeloid cells, and disruption of the BBB. Conversely, IL-17RA signaling in the large intestine may have more of an effect in the hepatitis phenotype relative to the EAE phenotype due to the role of the colon in the enterohepatic circulation. During hepatitis, disease in *Il17ra*$^{fl/fl}$ *x villin cre*$^{+}$ mice was more so driven by general Th17 control of the microbiome and subsequent IL-18 release discussed in more detail below. Our data in *Nlrc4*^{mut}*Il18bp*$^{-/-}$ mice, which have increased intestinal IL-18 production

and decreased systemic regulation of IL-18, also suggested a role of intestinal IL-18 in disease exacerbation. *Il17ra*$^{fl/fl}$ *x villin cre*$^{+}$ mice do have an increase in intestinal IL-18 as well as IL-22 (48). These data align with evidence showing that IL-22 can drive IL-18 production by intestinal epithelial cells (161). The elevated IL-18 in *Il17ra*$^{fl/fl}$ *x villin cre*$^{+}$ mice then enhanced liver inflammation by promoting lymphocyte activation as measured by *Ifng* and cell death through Fas-FasL. While it was not investigated, the elevated IL-18 in *Il17ra*$^{fl/fl}$ *x villin cre*$^{+}$ mice could be influencing EAE exacerbation as well. Indeed, there was increased IL-18 in the CSF and serum of MS patients with active MRI lesions. In mice, however, IL-18 deficiency had no effect while knockout of IL-18Rα was protective against EAE (335, 336). Taken together, our data highlight the different mechanisms by which intestinal Th17 cells and subsequent Th17 related cytokines can influence disease in different organs. Moreover, it prompts further investigation of intestinal Th17 signaling in extra-intestinal diseases.

Based on antibiotic and cohousing studies, disrupted intestinal IL-17 signaling mediated its effects on hepatitis and neuroinflammation through the intestinal microbiota. The intestinal microbiota has been previously implicated in both the Con A and EAE. Indeed, in both models, germ-free mice exhibit ameliorated disease (178, 313). *Il17ra*$^{fl/fl}$ *x villin cre*$^{+}$ mice have an altered intestinal microbiome as previously described (48). Our data suggested that different bacteria within the *Il17ra*$^{fl/fl}$ *x villin cre*$^{+}$ microbiota are contributing to each disease model. In EAE, vancomycin, which targets gram-positive bacteria, ameliorated disease. Based on the literature, it is likely that the disease inciting bacteria in EAE was gram-positive bacteria, Sfb. There is a large Sfb overgrowth in *Il17ra*$^{fl/fl}$ *x villin cre*$^{+}$ mice due to the loss of Th17 control (48), and monocolonization with Sfb into germ-free mice was sufficient to exacerbate disease as compared to germ-free mice (313). Conversely, in Con A hepatitis, vancomycin had no effect on disease in

Il17ra$^{fl/fl}$ *x villin cre*$^{+}$ mice, while neomycin, which targets gram negative bacteria, ameliorated disease. This effectively shifted the focus away from Sfb within the Con A model and also suggested that intestinal IL-17RA signaling controlled more than Sfb. This is not surprising as the mechanisms by which Th17 cells control Sfb, such as sIgA and AMPs, are also applicable to other bacteria residing close to the intestinal epithelium. Indeed, we have evidence showing general bacterial overgrowth in the fecal content of *Il17ra*$^{fl/fl}$ *x villin cre*$^{+}$ mice with enrichment for IgA-bacteria. The fact that different bacteria within the same organism are exacerbating different diseases provides further support that the effect of the microbiome is contextual. For example, the Sfb-mediated IL-17 responses in *Il17ra*$^{fl/fl}$ *x villin cre*$^{+}$ mice may be detrimental in EAE but protective in a setting of fungal infection (337). Still within *Il17ra*$^{fl/fl}$ *x villin cre*$^{+}$ mice, gram-negative bacteria mediated IL-18 elevations, which exacerbated hepatitis but may prove beneficial in colitis (160). This challenges the concept of a "healthy" microbiome, as the various bacteria within one host's microbiome may be protective or detrimental depending on the disease process and co-existing microbial community.

Beyond the specific bacteria, our data have demonstrated a role for bacterial product translocation in disease exacerbation. In *Il17ra*$^{fl/fl}$ *x villin cre*$^{+}$ mice, translocation of CpG DNA from the gut to the liver promoted local hepatic IL-18 production and exacerbated disease. While systemic increases in bacterial products were not seen at the naïve state, it is possible that disease progression both in Con A and EAE may have compromised the intestinal barrier to release bacterial products into the circulation. Though there are some conflicting reports, TLR2, TLR4 and TLR9 have all been implicated in EAE (319, 338, 339) and could have an effect on disease in *Il17ra*$^{fl/fl}$ *x villin cre*$^{+}$ mice. Our data may also have implications on other illnesses with "leaky gut" and increased bacterial translocation. With regards to the translocation of TLR ligands, much

of the focus has been on LPS. For example, in HIV/AIDS, emphasis has been placed on leakage of LPS across the gut barrier causing wasting and chronic inflammation (181). Our data suggests extra-intestinal TLR9 ligand dissemination is regulated by intestinal IL-17R signaling and may therefore be another underlying mechanism in HIV/AIDS liver dysfunction (244). Our data also raise the possibility that intestinal Th17 dysregulation and subsequent bacterial translocation may also contribute neurological manifestations in HIV/AIDS. More broadly, our work reveals potential immune consequences of the subclinical bacteremia observed in many patients.

With regards to future directions, it would be important to look beyond TLR ligands and address the potential role of bacterial metabolites, such as SCFAs, in *Il17ra*$^{fl/fl}$ *x villin cre*$^{+}$ disease exacerbation. It is likely that alterations in the intestinal microbiota within *Il17ra*$^{fl/fl}$ *x villin cre*$^{+}$ mice may have resulted in changes in the intestinal metabolome. SCFAs have been shown to have a wide range of immunologic functions including Treg induction, myeloid cell regulation, and inhibition of histone deacetylases (78, 79, 340, 341). The enhanced immune responses to *ex vivo* stimulation in both the Con A and EAE projects suggested that there may be epigenetic modifications in gut-specific knockout mice such that the splenocytes and hepatic mononuclear cells are primed to secrete more inflammatory cytokines in response to even non-specific stimuli such as anti-CD3/CD28. Moreover, *ex vivo* treatment with bromodomain extra-terminal protein inhibitors abrogated the enhanced liver IFNγ response, further supporting an epigenetic contribution.

It would also advance the work to identify specific bacterial genera or species exacerbating Con A and EAE in *Il17ra*$^{fl/fl}$ *x villin cre*$^{+}$ mice. In EAE, vancomycin treatment partnered with the existing literature on Sfb in EAE focused the attention on Sfb. However, as seen in within the Con A project, *Il17ra*$^{fl/fl}$ *x villin cre*$^{+}$ mice exhibit an overall bacterial overgrowth. As such, it is possible

that additional bacteria beyond Sfb may be contributing to disease. Indeed, in the work monocolonizing germ-free mice with Sfb, EAE severity in Sfb-monocolonized mice did not reach the same level as conventional SPF mice (313). This suggested that other bacteria and microbial metabolites beyond Sfb contributed to disease or that Sfb requires other bacteria to exert its effects. To that end, following up on the elevated IgA-unbound bacteria in *Il17ra*$^{fl/fl}$ *x villin cre*$^{+}$ mice (detailed within the Gut-Liver Axis Chapter) may assist in identifying contributing bacteria in both the EAE and Con A models. To tailor the assay to identify the bacterial culprits in the EAE work, quantification of IgA-bound and unbound bacteria can be done after vancomycin treatment to determine if there is selective depletion of either subset. In addition, for both projects, the IgA bound and unbound fractions can be sorted via magnetic separation (194), sequenced, and analyzed for potential differences between *Il17ra*$^{fl/fl}$ *x villin cre*$^{+}$ mice and littermate floxed controls. That being said, the possibility still remains that it is not a specific bacterium, but rather changes in bacterial behavior or bacterial overgrowth of many species that could be enhancing disease.

Overall, these dissertation studies have numerous therapeutic implications. It emphasizes that diseases are very often multifactorial, involving not just the target organ but other aspects of the body and immune system. As such, treatment of disease should reflect this multisystem involvement. Specifically in MS and hepatitis, our work raises intestinal Th17 signaling and the intestinal microbiome as therapeutic considerations when designing therapies. While IL-17 has been shown to be detrimental in both disease types, it is possible that global IL-17A blockade may have adverse effects on intestinal Th17 signaling with subsequent microbiome alterations and proinflammatory effects. Indeed, “gastrointestinal disorders” was one of the organ system groupings with adverse side effects in response to Secukinumab, the humanized anti-IL-17A monoclonal antibody approved for psoriasis (342). To address these potentially adverse effects,

our data support the investigation of combination therapy in these diseases. Partnering IL-17 neutralization with blockade of other potentially pathogenic cytokines including IL-18 in hepatitis or GM-CSF in neuroinflammation may prove more effective.

Our work also suggests the microbiome as a therapeutic target in these diseases. While the targeting the microbiome is unlikely to be a cure-all for these diseases, these dissertation studies demonstrate that it may be a exacerbating factor in disease development. Our data suggest the role of specific subtypes of bacteria in disease exacerbation. Based on our data with IgA-unbound bacteria enrichment potentially exacerbating hepatitis, a possible future therapy may be administration of secretory IgA specific to inciting bacteria in that particular disease state. As such, identification of bacteria detrimental in specific diseases can undoubtedly advance the field, particularly if the work becomes translatable to patients and proves helpful in disease management. However, an important caveat is that many previous studies have also defined other differences in the intestinal microbiota in patients and mouse models of these diseases. For example, in hepatitis, our work implicates a gram-negative bacteria in disease exacerbation and showed that eliminating gram-positive bacteria had no effect in *Il17ra*$^{fl/fl}$ *x villin cre*$^{+}$ mice. Another hepatitis mouse model using a different genetic background implicated a gram-positive bacterium (179). In MS, a meta-analysis of the literature detailing the intestinal microbiome of patients with relapsing-remitting MS described multiple different bacteria that were altered in patients with RRMS patients as compared to controls (310). This study noted that many of these described differences were not shared among all of the reports (310). The variation in the "relevant" bacterial strains in disease highlight the biological differences observed in the microbiome, demonstrate the importance of performing studies to show cause as opposed to association, and stress the significance of gene-

environment interaction, as these microbiota changes may stem from the genetic predisposition of the host.

This type of variation certainly impacts the approach to targeting the microbiome in patients. For interventions such as fecal microbiota transfer, it would be important to consider the genetic predisposition of the host as well as what may be detrimental or beneficial in that specific health/disease state. Moreover, transferring of bacterial communities without first creating a niche may impede the success of the beneficial bacterial strain. Even then, the genetic predisposition of the host may prevent the more permanent establishment of the microbial communities of interest. Because of these challenges, it would be helpful to also go beyond identifying specific target strains and elucidate the mechanism by which these different bacteria contribute to disease. Doing so would then open up more therapeutic targets. For example, it may be more efficacious, though not necessarily sustained, to focus microbiota-related treatments to immunogenic bacterial products such as SCFAs. Overall, our studies partnered with those previously performed underline the role of the microbiome in extra-intestinal disease and the promising therapeutic avenue of targeting the microbiota.

In summary, these dissertation studies demonstrate how disruption of intestinal Th17 signaling and subsequent effects on the microbiome can exacerbate liver- and neuro-inflammation. The mechanisms by which this occurs further elucidate potential therapeutic targets in hepatitis and MS and have broader implications in mucosal immunity and the gut-brain and gut-liver axes.

Bibliography

1. Rouvier, E., M. F. Luciani, M. G. Mattéi, F. Denizot, and P. Golstein. 1993. CTLA-8, cloned from an activated T cell, bearing AU-rich messenger RNA instability sequences, and homologous to a herpesvirus saimiri gene. *J. Immunol.* 150: 5445–5456.

2. Yao, Z., W. C. Fanslow, M. F. Seldin, A. M. Rousseau, S. L. Painter, M. R. Comeau, J. I. Cohen, and M. K. Spriggs. 1995. Herpesvirus Saimiri encodes a new cytokine, IL-17, which binds to a novel cytokine receptor. *Immunity* 3: 811–821.

3. Gaffen, S. L., R. Jain, A. V. Garg, and D. J. Cua. 2014. The IL-23-IL-17 immune axis: from mechanisms to therapeutic testing. *Nat. Rev. Immunol.* 14: 585–600.

4. Zhou, L., I. I. Ivanov, R. Spolski, R. Min, K. Shenderov, T. Egawa, D. E. Levy, W. J. Leonard, and D. R. Littman. 2007. IL-6 programs T(H)-17 cell differentiation by promoting sequential engagement of the IL-21 and IL-23 pathways. *Nat. Immunol.* 8: 967–974.

5. Ghoreschi, K., A. Laurence, X.-P. Yang, C. M. Tato, M. J. McGeachy, J. E. Konkel, H. L. Ramos, L. Wei, T. S. Davidson, N. Bouladoux, J. R. Grainger, Q. Chen, Y. Kanno, W. T. Watford, H.-W. Sun, G. Eberl, E. M. Shevach, Y. Belkaid, D. J. Cua, W. Chen, and J. J. O'Shea. 2010. Generation of pathogenic T(H)17 cells in the absence of TGF-β signalling. *Nature* 467: 967–971.

6. Nurieva, R., X. O. Yang, G. Martinez, Y. Zhang, A. D. Panopoulos, L. Ma, K. Schluns, Q. Tian, S. S. Watowich, A. M. Jetten, and C. Dong. 2007. Essential autocrine regulation by IL-21 in the generation of inflammatory T cells. *Nature* 448: 480–483.

7. Korn, T., E. Bettelli, W. Gao, A. Awasthi, A. Jäger, T. B. Strom, M. Oukka, and V. K. Kuchroo. 2007. IL-21 initiates an alternative pathway to induce proinflammatory T(H)17 cells. *Nature* 448: 484–487.

8. Cua, D. J., J. Sherlock, Y. Chen, C. A. Murphy, B. Joyce, B. Seymour, L. Lucian, W. To, S. Kwan, T. Churakova, S. Zurawski, M. Wiekowski, S. A. Lira, D. Gorman, R. A. Kastelein, and J. D. Sedgwick. 2003. Interleukin-23 rather than interleukin-12 is the critical cytokine for autoimmune inflammation of the brain. *Nature* 421: 744–748.

9. Veldhoen, M., R. J. Hocking, C. J. Atkins, R. M. Locksley, and B. Stockinger. 2006. TGFbeta in the context of an inflammatory cytokine milieu supports de novo differentiation of IL-17-producing T cells. *Immunity* 24: 179–189.

10. Weaver, C. T., L. E. Harrington, P. R. Mangan, M. Gavrieli, and K. M. Murphy. 2006. Th17: an effector CD4 T cell lineage with regulatory T cell ties. *Immunity* 24: 677–688.

11. Yang, X. O., A. D. Panopoulos, R. Nurieva, S. H. Chang, D. Wang, S. S. Watowich, and C. Dong. 2007. STAT3 regulates cytokine-mediated generation of inflammatory helper T cells. *J. Biol. Chem.* 282: 9358–9363.

12. Kolls, J. K., and A. Lindén. 2004. Interleukin-17 family members and inflammation. *Immunity* 21: 467–476.

13. Ouyang, W., J. K. Kolls, and Y. Zheng. 2008. The biological functions of T helper 17 cell effector cytokines in inflammation. *Immunity* 28: 454–467.

14. Ivanov, I. I., B. S. McKenzie, L. Zhou, C. E. Tadokoro, A. Lepelley, J. J. Lafaille, D. J. Cua, and D. R. Littman. 2006. The orphan nuclear receptor RORgammat directs the differentiation program of proinflammatory IL-17+ T helper cells. *Cell* 126: 1121–1133.

15. Gaffen, S. L. 2009. Structure and signalling in the IL-17 receptor family. *Nat. Rev. Immunol.* 9: 556–567.

16. Gaffen, S. L. 2008. An overview of IL-17 function and signaling. *Cytokine* 43: 402–407.

17. Liang, S. C., A. J. Long, F. Bennett, M. J. Whitters, R. Karim, M. Collins, S. J. Goldman, K. Dunussi-Joannopoulos, C. M. M. Williams, J. F. Wright, and L. A. Fouser. 2007. An IL-17F/A heterodimer protein is produced by mouse Th17 cells and induces airway neutrophil recruitment. *J. Immunol.* 179: 7791–7799.

18. Khader, S. A., S. L. Gaffen, and J. K. Kolls. 2009. Th17 cells at the crossroads of innate and adaptive immunity against infectious diseases at the mucosa. *Mucosal Immunol.* 2: 403–411.

19. Chan, Y. R., J. S. Liu, D. A. Pociask, M. Zheng, T. A. Mietzner, T. Berger, T. W. Mak, M. C. Clifton, R. K. Strong, P. Ray, and J. K. Kolls. 2009. Lipocalin 2 is required for pulmonary host defense against Klebsiella infection. *J. Immunol.* 182: 4947–4956.

20. Datta, S., M. Novotny, P. G. Pavicic, C. Zhao, T. Herjan, J. Hartupee, and T. Hamilton. 2010. IL-17 regulates CXCL1 mRNA stability via an AUUUA/tristetraprolin-independent sequence. *J. Immunol.* 184: 1484–1491.

21. Herjan, T., P. Yao, W. Qian, X. Li, C. Liu, K. Bulek, D. Sun, W.-P. Yang, J. Zhu, A. He, J. A. Carman, S. C. Erzurum, H. D. Lipshitz, P. L. Fox, T. A. Hamilton, and X. Li. 2013. HuR is required for IL-17-induced Act1-mediated CXCL1 and CXCL5 mRNA stabilization. *J. Immunol.* 191: 640–649.

22. Amatya, N., J. A. Cruz, F. Aggor, A. Garg, A. J. Berman, U. Atasoy, and S. L. Gaffen. 2018. Arid5a orchestrates IL-17-mediated inflammation through post-transcriptional control of mRNA. *The Journal of Immunology* .

23. Majumder, S., N. Amatya, S. Revu, C. V. Jawale, D. Wu, N. Rittenhouse, A. Menk, S. Kupul, F. Du, I. Raphael, A. Bhattacharjee, U. Siebenlist, T. W. Hand, G. M. Delgoffe, A. C. Poholek, S. L. Gaffen, P. S. Biswas, and M. J. McGeachy. 2019. IL-17 metabolically reprograms activated fibroblastic reticular cells for proliferation and survival. *Nat. Immunol.* 20: 534–545.

24. Batten, M., J. Li, S. Yi, N. M. Kljavin, D. M. Danilenko, S. Lucas, J. Lee, F. J. de Sauvage, and N. Ghilardi. 2006. Interleukin 27 limits autoimmune encephalomyelitis by suppressing the development of interleukin 17-producing T cells. *Nat. Immunol.* 7: 929–936.

25. Stumhofer, J. S., A. Laurence, E. H. Wilson, E. Huang, C. M. Tato, L. M. Johnson, A. V. Villarino, Q. Huang, A. Yoshimura, D. Sehy, C. J. M. Saris, J. J. O'Shea, L. Hennighausen, M. Ernst, and C. A. Hunter. 2006. Interleukin 27 negatively regulates the development of interleukin 17-producing T helper cells during chronic inflammation of the central nervous system. *Nat. Immunol.* 7: 937–945.

26. Stritesky, G. L., N. Yeh, and M. H. Kaplan. 2008. IL-23 promotes maintenance but not commitment to the Th17 lineage. *J. Immunol.* 181: 5948–5955.

27. El-Behi, M., B. Ciric, H. Dai, Y. Yan, M. Cullimore, F. Safavi, G.-X. Zhang, B. N. Dittel, and A. Rostami. 2011. The encephalitogenicity of T(H)17 cells is dependent on IL-1- and IL-23-induced production of the cytokine GM-CSF. *Nat. Immunol.* 12: 568–575.

28. Lee, Y., A. Awasthi, N. Yosef, F. J. Quintana, S. Xiao, A. Peters, C. Wu, M. Kleinewietfeld, S. Kunder, D. A. Hafler, R. A. Sobel, A. Regev, and V. K. Kuchroo. 2012. Induction and molecular signature of pathogenic TH17 cells. *Nat. Immunol.* 13: 991–999.

29. McGeachy, M. J., Y. Chen, C. M. Tato, A. Laurence, B. Joyce-Shaikh, W. M. Blumenschein, T. K. McClanahan, J. J. O'Shea, and D. J. Cua. 2009. The interleukin 23 receptor is essential for the terminal differentiation of interleukin 17-producing effector T helper cells in vivo. *Nat. Immunol.* 10: 314–324.

30. Lee, Y., and V. Kuchroo. 2015. Defining the functional states of Th17 cells [version 1; peer review: 3 approved]. *F1000Res.* 4.

31. Yasuda, K., Y. Takeuchi, and K. Hirota. 2019. The pathogenicity of Th17 cells in autoimmune diseases. *Semin Immunopathol* 41: 283–297.

32. Sender, R., S. Fuchs, and R. Milo. 2016. Revised estimates for the number of human and bacteria cells in the body. *PLoS Biol.* 14: e1002533.

33. Round, J. L., and S. K. Mazmanian. 2009. The gut microbiota shapes intestinal immune responses during health and disease. *Nat. Rev. Immunol.* 9: 313–323.

34. Macpherson, A. J., E. Slack, M. B. Geuking, and K. D. McCoy. 2009. The mucosal firewalls against commensal intestinal microbes. *Semin Immunopathol* 31: 145–149.

35. Belkaid, Y., and T. W. Hand. 2014. Role of the microbiota in immunity and inflammation. *Cell* 157: 121–141.

36. Atarashi, K., T. Tanoue, M. Ando, N. Kamada, Y. Nagano, S. Narushima, W. Suda, A. Imaoka, H. Setoyama, T. Nagamori, E. Ishikawa, T. Shima, T. Hara, S. Kado, T. Jinnohara, H. Ohno, T. Kondo, K. Toyooka, E. Watanabe, S.-I. Yokoyama, S. Tokoro, H. Mori, Y. Noguchi, H. Morita, I. I. Ivanov, T. Sugiyama, G. Nuñez, J. G. Camp, M. Hattori, Y. Umesaki, and K. Honda. 2015. Th17 cell induction by adhesion of microbes to intestinal epithelial cells. *Cell* 163: 367–380.

37. Parks, O. B., D. A. Pociask, Z. Hodzic, J. K. Kolls, and M. Good. 2015. Interleukin-22 Signaling in the Regulation of Intestinal Health and Disease. *Front. Cell Dev. Biol.* 3: 85.

38. Schreiber, F., J. M. Arasteh, and T. D. Lawley. 2015. Pathogen Resistance Mediated by IL-22 Signaling at the Epithelial-Microbiota Interface. *J. Mol. Biol.* 427: 3676–3682.

39. Wolk, K., S. Kunz, E. Witte, M. Friedrich, K. Asadullah, and R. Sabat. 2004. IL-22 increases the innate immunity of tissues. *Immunity* 21: 241–254.

40. Lee, J. S., C. M. Tato, B. Joyce-Shaikh, M. F. Gulen, C. Cayatte, Y. Chen, W. M. Blumenschein, M. Judo, G. Ayanoglu, T. K. McClanahan, X. Li, and D. J. Cua. 2015. Interleukin-23-Independent IL-17 Production Regulates Intestinal Epithelial Permeability. *Immunity* 43: 727–738.

41. Wang, Y., J. B. Mumm, R. Herbst, R. Kolbeck, and Y. Wang. 2017. IL-22 Increases Permeability of Intestinal Epithelial Tight Junctions by Enhancing Claudin-2 Expression. *J. Immunol.* 199: 3316–3325.

42. Sugimoto, K., A. Ogawa, E. Mizoguchi, Y. Shimomura, A. Andoh, A. K. Bhan, R. S. Blumberg, R. J. Xavier, and A. Mizoguchi. 2008. IL-22 ameliorates intestinal inflammation in a mouse model of ulcerative colitis. *J. Clin. Invest.* 118: 534–544.

43. Lindemans, C. A., M. Calafiore, A. M. Mertelsmann, M. H. O'Connor, J. A. Dudakov, R. R. Jenq, E. Velardi, L. F. Young, O. M. Smith, G. Lawrence, J. A. Ivanov, Y.-Y. Fu, S. Takashima, G. Hua, M. L. Martin, K. P. O'Rourke, Y.-H. Lo, M. Mokry, M. Romera-Hernandez, T. Cupedo, L. Dow, E. E. Nieuwenhuis, N. F. Shroyer, C. Liu, R. Kolesnick, M. R. M. van den Brink, and A. M. Hanash. 2015. Interleukin-22 promotes intestinal-stem-cell-mediated epithelial regeneration. *Nature* 528: 560–564.

44. Mukherjee, S., and L. V. Hooper. 2015. Antimicrobial defense of the intestine. *Immunity* 42: 28–39.

45. Ouellette, A. J. 2011. Paneth cell α-defensins in enteric innate immunity. *Cell Mol. Life Sci.* 68: 2215–2229.

46. Salzman, N. H., D. Ghosh, K. M. Huttner, Y. Paterson, and C. L. Bevins. 2003. Protection against enteric salmonellosis in transgenic mice expressing a human intestinal defensin. *Nature* 422: 522–526.

47. Salzman, N. H., K. Hung, D. Haribhai, H. Chu, J. Karlsson-Sjöberg, E. Amir, P. Teggatz, M. Barman, M. Hayward, D. Eastwood, M. Stoel, Y. Zhou, E. Sodergren, G. M. Weinstock, C. L. Bevins, C. B. Williams, and N. A. Bos. 2010. Enteric defensins are essential regulators of intestinal microbial ecology. *Nat. Immunol.* 11: 76–83.

48. Kumar, P., L. Monin, P. Castillo, W. Elsegeiny, W. Horne, T. Eddens, A. Vikram, M. Good, A. A. Schoenborn, K. Bibby, R. C. Montelaro, D. W. Metzger, A. S. Gulati, and J. K. Kolls. 2016. Intestinal Interleukin-17 Receptor Signaling Mediates Reciprocal Control of the Gut Microbiota and Autoimmune Inflammation. *Immunity* 44: 659–671.

49. Cash, H. L., C. V. Whitham, and L. V. Hooper. 2006. Refolding, purification, and characterization of human and murine RegIII proteins expressed in Escherichia coli. *Protein Expr. Purif.* 48: 151–159.

50. Christa, L., F. Carnot, M. T. Simon, F. Levavasseur, M. G. Stinnakre, C. Lasserre, D. Thepot, B. Clement, E. Devinoy, and C. Brechot. 1996. HIP/PAP is an adhesive protein expressed in hepatocarcinoma, normal Paneth, and pancreatic cells. *Am. J. Physiol.* 271: G993-1002.

51. Cash, H. L., C. V. Whitham, C. L. Behrendt, and L. V. Hooper. 2006. Symbiotic bacteria direct expression of an intestinal bactericidal lectin. *Science* 313: 1126–1130.

52. McAleer, J. P., N. L. H. Nguyen, K. Chen, P. Kumar, D. M. Ricks, M. Binnie, R. A. Armentrout, D. A. Pociask, A. Hein, A. Yu, A. Vikram, K. Bibby, Y. Umesaki, A. Rivera, D. Sheppard, W. Ouyang, L. V. Hooper, and J. K. Kolls. 2016. Pulmonary th17 antifungal immunity is regulated by the gut microbiome. *J. Immunol.* 197: 97–107.

53. Johansen, F. E., and C. S. Kaetzel. 2011. Regulation of the polymeric immunoglobulin receptor and IgA transport: new advances in environmental factors that stimulate pIgR expression and its role in mucosal immunity. *Mucosal Immunol.* 4: 598–602.

54. Cao, A. T., S. Yao, B. Gong, C. O. Elson, and Y. Cong. 2012. Th17 cells upregulate polymeric Ig receptor and intestinal IgA and contribute to intestinal homeostasis. *J. Immunol.* 189: 4666–4673.

55. Reikvam, D. H., M. Derrien, R. Islam, A. Erofeev, V. Grcic, A. Sandvik, P. Gaustad, L. A. Meza-Zepeda, F. L. Jahnsen, H. Smidt, and F.-E. Johansen. 2012. Epithelial-microbial crosstalk in polymeric Ig receptor deficient mice. *Eur. J. Immunol.* 42: 2959–2970.

56. Suzuki, K., B. Meek, Y. Doi, M. Muramatsu, T. Chiba, T. Honjo, and S. Fagarasan. 2004. Aberrant expansion of segmented filamentous bacteria in IgA-deficient gut. *Proc. Natl. Acad. Sci. USA* 101: 1981–1986.

57. Le Chatelier, E., T. Nielsen, J. Qin, E. Prifti, F. Hildebrand, G. Falony, M. Almeida, M. Arumugam, J.-M. Batto, S. Kennedy, P. Leonard, J. Li, K. Burgdorf, N. Grarup, T. Jørgensen, I. Brandslund, H. B. Nielsen, A. S. Juncker, M. Bertalan, F. Levenez, N. Pons, S. Rasmussen, S. Sunagawa, J. Tap, S. Tims, E. G. Zoetendal, S. Brunak, K. Clément, J. Doré, M. Kleerebezem, K. Kristiansen, P. Renault, T. Sicheritz-Ponten, W. M. de Vos, J.-D. Zucker, J. Raes, T. Hansen, MetaHIT consortium, P. Bork, J. Wang, S. D. Ehrlich, and O. Pedersen. 2013. Richness of human gut microbiome correlates with metabolic markers. *Nature* 500: 541–546.

58. Valdes, A. M., J. Walter, E. Segal, and T. D. Spector. 2018. Role of the gut microbiota in nutrition and health. *BMJ* 361: k2179.

59. Zhao, L., F. Zhang, X. Ding, G. Wu, Y. Y. Lam, X. Wang, H. Fu, X. Xue, C. Lu, J. Ma, L. Yu, C. Xu, Z. Ren, Y. Xu, S. Xu, H. Shen, X. Zhu, Y. Shi, Q. Shen, W. Dong, R. Liu, Y. Ling, Y. Zeng, X. Wang, Q. Zhang, J. Wang, L. Wang, Y. Wu, B. Zeng, H. Wei, M. Zhang, Y. Peng, and C. Zhang. 2018. Gut bacteria selectively promoted by dietary fibers alleviate type 2 diabetes. *Science* 359: 1151–1156.

60. Ivanov, I. I., K. Atarashi, N. Manel, E. L. Brodie, T. Shima, U. Karaoz, D. Wei, K. C. Goldfarb, C. A. Santee, S. V. Lynch, T. Tanoue, A. Imaoka, K. Itoh, K. Takeda, Y. Umesaki, K. Honda, and D. R. Littman. 2009. Induction of intestinal Th17 cells by segmented filamentous bacteria. *Cell* 139: 485–498.

61. Ochoa-Repáraz, J., D. W. Mielcarz, L. E. Ditrio, A. R. Burroughs, S. Begum-Haque, S. Dasgupta, D. L. Kasper, and L. H. Kasper. 2010. Central nervous system demyelinating disease protection by the human commensal Bacteroides fragilis depends on polysaccharide A expression. *J. Immunol.* 185: 4101–4108.

62. Atarashi, K., T. Tanoue, K. Oshima, W. Suda, Y. Nagano, H. Nishikawa, S. Fukuda, T. Saito, S. Narushima, K. Hase, S. Kim, J. V. Fritz, P. Wilmes, S. Ueha, K. Matsushima, H. Ohno, B. Olle, S. Sakaguchi, T. Taniguchi, H. Morita, M. Hattori, and K. Honda. 2013. Treg induction by a rationally selected mixture of Clostridia strains from the human microbiota. *Nature* 500: 232–236.

63. Mazmanian, S. K., J. L. Round, and D. L. Kasper. 2008. A microbial symbiosis factor prevents intestinal inflammatory disease. *Nature* 453: 620–625.

64. Mazmanian, S. K., C. H. Liu, A. O. Tzianabos, and D. L. Kasper. 2005. An immunomodulatory molecule of symbiotic bacteria directs maturation of the host immune system. *Cell* 122: 107–118.

65. Kriegel, M. A., E. Sefik, J. A. Hill, H.-J. Wu, C. Benoist, and D. Mathis. 2011. Naturally transmitted segmented filamentous bacteria segregate with diabetes protection in nonobese diabetic mice. *Proc. Natl. Acad. Sci. USA* 108: 11548–11553.

66. Xu, M., Y. Yang, M. Pokrovskii, C. Galan, and D. R. Littman. 2016. Abstract A080: Balance of commensal bacteria specific Th17 and RORγt^{+} Treg cells in intestinal homeostasis and inflammation. *Cancer Immunol Res* 4: A080–A080.

67. Ansaldo, E., L. C. Slayden, K. L. Ching, M. A. Koch, N. K. Wolf, D. R. Plichta, E. M. Brown, D. B. Graham, R. J. Xavier, J. J. Moon, and G. M. Barton. 2019. Akkermansia muciniphila induces intestinal adaptive immune responses during homeostasis. *Science* 364: 1179–1184.

68. Galán, J. E. 2001. Salmonella interactions with host cells: type III secretion at work. *Annu. Rev. Cell Dev. Biol.* 17: 53–86.

69. Belkaid, Y., and O. J. Harrison. 2017. Homeostatic immunity and the microbiota. *Immunity* 46: 562–576.

70. Krieg, A. M. 2002. CpG motifs in bacterial DNA and their immune effects. *Annu. Rev. Immunol.* 20: 709–760.

71. Zhang, H., D. W. Niesel, J. W. Peterson, and G. R. Klimpel. 1998. Lipoprotein release by bacteria: potential factor in bacterial pathogenesis. *Infect. Immun.* 66: 5196–5201.

72. Schwechheimer, C., and M. J. Kuehn. 2015. Outer-membrane vesicles from Gram-negative bacteria: biogenesis and functions. *Nat. Rev. Microbiol.* 13: 605–619.

73. Chelakkot, C., Y. Choi, D.-K. Kim, H. T. Park, J. Ghim, Y. Kwon, J. Jeon, M.-S. Kim, Y.-K. Jee, Y. S. Gho, H.-S. Park, Y.-K. Kim, and S. H. Ryu. 2018. Akkermansia muciniphila-derived extracellular vesicles influence gut permeability through the regulation of tight junctions. *Exp Mol Med* 50: e450.

74. Shen, Y., M. L. Giardino Torchia, G. W. Lawson, C. L. Karp, J. D. Ashwell, and S. K. Mazmanian. 2012. Outer membrane vesicles of a human commensal mediate immune regulation and disease protection. *Cell Host Microbe* 12: 509–520.

75. Hickey, C. A., K. A. Kuhn, D. L. Donermeyer, N. T. Porter, C. Jin, E. A. Cameron, H. Jung, G. E. Kaiko, M. Wegorzewska, N. P. Malvin, R. W. P. Glowacki, G. C. Hansson, P. M. Allen, E. C. Martens, and T. S. Stappenbeck. 2015. Colitogenic Bacteroides thetaiotaomicron Antigens Access Host Immune Cells in a Sulfatase-Dependent Manner via Outer Membrane Vesicles. *Cell Host Microbe* 17: 672–680.

76. Maslowski, K. M., A. T. Vieira, A. Ng, J. Kranich, F. Sierro, D. Yu, H. C. Schilter, M. S. Rolph, F. Mackay, D. Artis, R. J. Xavier, M. M. Teixeira, and C. R. Mackay. 2009. Regulation of inflammatory responses by gut microbiota and chemoattractant receptor GPR43. *Nature* 461: 1282–1286.

77. El Kaoutari, A., F. Armougom, J. I. Gordon, D. Raoult, and B. Henrissat. 2013. The abundance and variety of carbohydrate-active enzymes in the human gut microbiota. *Nat. Rev. Microbiol.* 11: 497–504.

78. Rooks, M. G., and W. S. Garrett. 2016. Gut microbiota, metabolites and host immunity. *Nat. Rev. Immunol.* 16: 341–352.

79. Furusawa, Y., Y. Obata, S. Fukuda, T. A. Endo, G. Nakato, D. Takahashi, Y. Nakanishi, C. Uetake, K. Kato, T. Kato, M. Takahashi, N. N. Fukuda, S. Murakami, E. Miyauchi, S. Hino, K. Atarashi, S. Onawa, Y. Fujimura, T. Lockett, J. M. Clarke, D. L. Topping, M. Tomita, S. Hori, O. Ohara, T. Morita, H. Koseki, J. Kikuchi, K. Honda, K. Hase, and H. Ohno. 2013. Commensal microbe-derived butyrate induces the differentiation of colonic regulatory T cells. *Nature* 504: 446–450.

80. Trompette, A., E. S. Gollwitzer, K. Yadava, A. K. Sichelstiel, N. Sprenger, C. Ngom-Bru, C. Blanchard, T. Junt, L. P. Nicod, N. L. Harris, and B. J. Marsland. 2014. Gut microbiota metabolism of dietary fiber influences allergic airway disease and hematopoiesis. *Nat. Med.* 20: 159–166.

81. Castillo, P. A. C., and T. W. Hand. 2018. A little fiber goes a long way. *Immunity* 48: 844–846.

82. Trompette, A., E. S. Gollwitzer, C. Pattaroni, I. C. Lopez-Mejia, E. Riva, J. Pernot, N. Ubags, L. Fajas, L. P. Nicod, and B. J. Marsland. 2018. Dietary Fiber Confers Protection against Flu by Shaping Ly6c- Patrolling Monocyte Hematopoiesis and CD8+ T Cell Metabolism. *Immunity* 48: 992–1005.e8.

83. Desai, M. S., A. M. Seekatz, N. M. Koropatkin, N. Kamada, C. A. Hickey, M. Wolter, N. A. Pudlo, S. Kitamoto, N. Terrapon, A. Muller, V. B. Young, B. Henrissat, P. Wilmes, T. S. Stappenbeck, G. Núñez, and E. C. Martens. 2016. A Dietary Fiber-Deprived Gut Microbiota Degrades the Colonic Mucus Barrier and Enhances Pathogen Susceptibility. *Cell* 167: 1339–1353.e21.

84. de Aguiar Vallim, T. Q., E. J. Tarling, and P. A. Edwards. 2013. Pleiotropic roles of bile acids in metabolism. *Cell Metab.* 17: 657–669.

85. Dowling, R. H. 1972. The enterohepatic circulation. *Gastroenterology* 62: 122–140.

86. Ridlon, J. M., D. J. Kang, P. B. Hylemon, and J. S. Bajaj. 2014. Bile acids and the gut microbiome. *Curr. Opin. Gastroenterol.* 30: 332–338.

87. Wahlström, A., S. I. Sayin, H.-U. Marschall, and F. Bäckhed. 2016. Intestinal Crosstalk between Bile Acids and Microbiota and Its Impact on Host Metabolism. *Cell Metab.* 24: 41–50.

88. Macpherson, A. J., M. Heikenwalder, and S. C. Ganal-Vonarburg. 2016. The Liver at the Nexus of Host-Microbial Interactions. *Cell Host Microbe* 20: 561–571.

89. Sorg, J. A., and A. L. Sonenshein. 2008. Bile salts and glycine as cogerminants for Clostridium difficile spores. *J. Bacteriol.* 190: 2505–2512.

90. Kempski, J., L. Brockmann, N. Gagliani, and S. Huber. 2017. TH17 Cell and Epithelial Cell Crosstalk during Inflammatory Bowel Disease and Carcinogenesis. *Front. Immunol.* 8: 1373.

91. Guéry, L., and S. Hugues. 2015. Th17 cell plasticity and functions in cancer immunity. *Biomed Res. Int.* 2015: 314620.

92. Franzosa, E. A., A. Sirota-Madi, J. Avila-Pacheco, N. Fornelos, H. J. Haiser, S. Reinker, T. Vatanen, A. B. Hall, H. Mallick, L. J. McIver, J. S. Sauk, R. G. Wilson, B. W. Stevens, J. M. Scott, K. Pierce, A. A. Deik, K. Bullock, F. Imhann, J. A. Porter, A. Zhernakova, J. Fu, R. K. Weersma, C. Wijmenga, C. B. Clish, H. Vlamakis, C. Huttenhower, and R. J. Xavier. 2019. Gut microbiome structure and metabolic activity in inflammatory bowel disease. *Nat. Microbiol.* 4: 293–305.

93. Tilg, H., T. E. Adolph, R. R. Gerner, and A. R. Moschen. 2018. The intestinal microbiota in colorectal cancer. *Cancer Cell* 33: 954–964.

94. Hernández-Chirlaque, C., C. J. Aranda, B. Ocón, F. Capitán-Cañadas, M. Ortega-González, J. J. Carrero, M. D. Suárez, A. Zarzuelo, F. Sánchez de Medina, and O. Martínez-Augustin. 2016. Germ-free and Antibiotic-treated Mice are Highly Susceptible to Epithelial Injury in DSS Colitis. *J. Crohns Colitis* 10: 1324–1335.

95. Uronis, J. M., M. Mühlbauer, H. H. Herfarth, T. C. Rubinas, G. S. Jones, and C. Jobin. 2009. Modulation of the intestinal microbiota alters colitis-associated colorectal cancer susceptibility. *PLoS One* 4: e6026.

96. Abdel-Moneim, A., H. H. Bakery, and G. Allam. 2018. The potential pathogenic role of IL-17/Th17 cells in both type 1 and type 2 diabetes mellitus. *Biomed. Pharmacother.* 101: 287–292.

97. Wang, M., F. Chen, J. Wang, Z. Zeng, Q. Yang, and S. Shao. 2018. Th17 and Treg lymphocytes in obesity and Type 2 diabetic patients. *Clin. Immunol.* 197: 77–85.

98. Lafdil, F., A. M. Miller, S. H. Ki, and B. Gao. 2010. Th17 cells and their associated cytokines in liver diseases. *Cell Mol Immunol* 7: 250–254.

99. Henao-Mejia, J., E. Elinav, C. A. Thaiss, P. Licona-Limon, and R. A. Flavell. 2013. Role of the intestinal microbiome in liver disease. *J. Autoimmun.* 46: 66–73.

100. Van Herck, M. A., J. Weyler, W. J. Kwanten, E. L. Dirinck, B. Y. De Winter, S. M. Francque, and L. Vonghia. 2019. The Differential Roles of T Cells in Non-alcoholic Fatty Liver Disease and Obesity. *Front. Immunol.* 10: 82.

101. Rau, M., A.-K. Schilling, J. Meertens, I. Hering, J. Weiss, C. Jurowich, T. Kudlich, H. M. Hermanns, H. Bantel, N. Beyersdorf, and A. Geier. 2016. Progression from Nonalcoholic Fatty Liver to Nonalcoholic Steatohepatitis Is Marked by a Higher Frequency of Th17 Cells in the Liver and an Increased Th17/Resting Regulatory T Cell Ratio in Peripheral Blood and in the Liver. *J. Immunol.* 196: 97–105.

102. Henao-Mejia, J., E. Elinav, C. Jin, L. Hao, W. Z. Mehal, T. Strowig, C. A. Thaiss, A. L. Kau, S. C. Eisenbarth, M. J. Jurczak, J.-P. Camporez, G. I. Shulman, J. I. Gordon, H. M. Hoffman, and R. A. Flavell. 2012. Inflammasome-mediated dysbiosis regulates progression of NAFLD and obesity. *Nature* 482: 179–185.

103. Lin, R., L. Zhou, J. Zhang, and B. Wang. 2015. Abnormal intestinal permeability and microbiota in patients with autoimmune hepatitis. *Int J Clin Exp Pathol* 8: 5153–5160.

104. Aly, A. M., A. Adel, A. O. El-Gendy, T. M. Essam, and R. K. Aziz. 2016. Gut microbiome alterations in patients with stage 4 hepatitis C. *Gut Pathog* 8: 42.

105. Zhao, L., Y. Tang, Z. You, Q. Wang, S. Liang, X. Han, D. Qiu, J. Wei, Y. Liu, L. Shen, X. Chen, Y. Peng, Z. Li, and X. Ma. 2011. Interleukin-17 contributes to the pathogenesis of autoimmune hepatitis through inducing hepatic interleukin-6 expression. *PLoS One* 6: e18909.

106. Shin, E.-C., P. S. Sung, and S.-H. Park. 2016. Immune responses and immunopathology in acute and chronic viral hepatitis. *Nat. Rev. Immunol.* 16: 509–523.

107. Ye, Y., X. Xie, J. Yu, L. Zhou, H. Xie, G. Jiang, X. Yu, W. Zhang, J. Wu, and S. Zheng. 2010. Involvement of Th17 and Th1 effector responses in patients with Hepatitis B. *J. Clin. Immunol.* 30: 546–555.

108. Chen, J., Y. Wei, J. He, G. Cui, Y. Zhu, C. Lu, Y. Ding, R. Xue, L. Bai, T. Uede, L. Li, and H. Diao. 2014. Natural killer T cells play a necessary role in modulating of immune-mediated liver injury by gut microbiota. *Sci. Rep.* 4: 7259.

109. Dapito, D. H., A. Mencin, G.-Y. Gwak, J.-P. Pradere, M.-K. Jang, I. Mederacke, J. M. Caviglia, H. Khiabanian, A. Adeyemi, R. Bataller, J. H. Lefkowitch, M. Bower, R. Friedman, R. B. Sartor, R. Rabadan, and R. F. Schwabe. 2012. Promotion of hepatocellular carcinoma by the intestinal microbiota and TLR4. *Cancer Cell* 21: 504–516.

110. Cirera, I., T. M. Bauer, M. Navasa, J. Vila, L. Grande, P. Taurá, J. Fuster, J. C. García-Valdecasas, A. Lacy, M. J. Suárez, A. Rimola, and J. Rodés. 2001. Bacterial translocation of enteric organisms in patients with cirrhosis. *J. Hepatol.* 34: 32–37.

111. Cait, A., M. R. Hughes, F. Antignano, J. Cait, P. A. Dimitriu, K. R. Maas, L. A. Reynolds, L. Hacker, J. Mohr, B. B. Finlay, C. Zaph, K. M. McNagny, and W. W. Mohn. 2018. Microbiome-driven allergic lung inflammation is ameliorated by short-chain fatty acids. *Mucosal Immunol.* 11: 785–795.

112. Frati, F., C. Salvatori, C. Incorvaia, A. Bellucci, G. Di Cara, F. Marcucci, and S. Esposito. 2018. The role of the microbiome in asthma: the gut–lung axis. *Int. J. Mol. Sci.* 20.

113. Nanzer, A. M., E. S. Chambers, K. Ryanna, D. F. Richards, C. Black, P. M. Timms, A. R. Martineau, C. J. Griffiths, C. J. Corrigan, and C. M. Hawrylowicz. 2013. Enhanced production of IL-17A in patients with severe asthma is inhibited by 1α,25-dihydroxyvitamin D3 in a glucocorticoid-independent fashion. *J. Allergy Clin. Immunol.* 132: 297–304.e3.

114. Alcorn, J. F., C. R. Crowe, and J. K. Kolls. 2010. TH17 cells in asthma and COPD. *Annu. Rev. Physiol.* 72: 495–516.

115. Chambers, E. S., A. M. Nanzer, P. E. Pfeffer, D. F. Richards, P. M. Timms, A. R. Martineau, C. J. Griffiths, C. J. Corrigan, and C. M. Hawrylowicz. 2015. Distinct endotypes of steroid-resistant asthma characterized by IL-17A(high) and IFN-γ(high) immunophenotypes: Potential benefits of calcitriol. *J. Allergy Clin. Immunol.* 136: 628–637.e4.

116. McKinley, L., J. F. Alcorn, A. Peterson, R. B. Dupont, S. Kapadia, A. Logar, A. Henry, C. G. Irvin, J. D. Piganelli, A. Ray, and J. K. Kolls. 2008. TH17 cells mediate steroid-resistant airway inflammation and airway hyperresponsiveness in mice. *J. Immunol.* 181: 4089–4097.

117. Crowe, C. R., K. Chen, D. A. Pociask, J. F. Alcorn, C. Krivich, R. I. Enelow, T. M. Ross, J. L. Witztum, and J. K. Kolls. 2009. Critical role of IL-17RA in immunopathology of influenza infection. *J. Immunol.* 183: 5301–5310.

118. Tesmer, L. A., S. K. Lundy, S. Sarkar, and D. A. Fox. 2008. Th17 cells in human disease. *Immunol. Rev.* 223: 87–113.

119. Luger, D., P. B. Silver, J. Tang, D. Cua, Z. Chen, Y. Iwakura, E. P. Bowman, N. M. Sgambellone, C.-C. Chan, and R. R. Caspi. 2008. Either a Th17 or a Th1 effector response can drive autoimmunity: conditions of disease induction affect dominant effector category. *J. Exp. Med.* 205: 799–810.

120. Ke, Y., K. Liu, G.-Q. Huang, Y. Cui, H. J. Kaplan, H. Shao, and D. Sun. 2009. Anti-inflammatory role of IL-17 in experimental autoimmune uveitis. *J. Immunol.* 182: 3183–3190.

121. Horai, R., C. R. Zárate-Bladés, P. Dillenburg-Pilla, J. Chen, J. L. Kielczewski, P. B. Silver, Y. Jittayasothorn, C.-C. Chan, H. Yamane, K. Honda, and R. R. Caspi. 2015. Microbiota-Dependent Activation of an Autoreactive T Cell Receptor Provokes Autoimmunity in an Immunologically Privileged Site. *Immunity* 43: 343–353.

122. Horai, R., and R. R. Caspi. 2019. Microbiome and autoimmune uveitis. *Front. Immunol.* 10: 232.

123. Matusevicius, D., P. Kivisäkk, B. He, N. Kostulas, V. Ozenci, S. Fredrikson, and H. Link. 1999. Interleukin-17 mRNA expression in blood and CSF mononuclear cells is augmented in multiple sclerosis. *Mult. Scler.* 5: 101–104.

124. Lock, C., G. Hermans, R. Pedotti, A. Brendolan, E. Schadt, H. Garren, A. Langer-Gould, S. Strober, B. Cannella, J. Allard, P. Klonowski, A. Austin, N. Lad, N. Kaminski, S. J. Galli, J. R. Oksenberg, C. S. Raine, R. Heller, and L. Steinman. 2002. Gene-microarray analysis of multiple sclerosis lesions yields new targets validated in autoimmune encephalomyelitis. *Nat. Med.* 8: 500–508.

125. Hofstetter, H. H., S. M. Ibrahim, D. Koczan, N. Kruse, A. Weishaupt, K. V. Toyka, and R. Gold. 2005. Therapeutic efficacy of IL-17 neutralization in murine experimental autoimmune encephalomyelitis. *Cell Immunol.* 237: 123–130.

126. Gonzalez-García, I., Y. Zhao, S. Ju, Q. Gu, L. Liu, J. K. Kolls, and B. Lu. 2009. IL-17 signaling-independent central nervous system autoimmunity is negatively regulated by TGF-beta. *J. Immunol.* 182: 2665–2671.

127. Mir, G. H., M. A. Henkel, M. J. Maggio, K. Ramani, D. B. Stolz, P. S. Biswas, and M. J. McGeachy. 2016. BACE1: a novel player in the pathogenesis of Th17 cells in EAE. *The Journal of Immunology* .

128. Chen, J., N. Chia, K. R. Kalari, J. Z. Yao, M. Novotna, M. M. Paz Soldan, D. H. Luckey, E. V. Marietta, P. R. Jeraldo, X. Chen, B. G. Weinshenker, M. Rodriguez, O. H. Kantarci, H. Nelson, J. A. Murray, and A. K. Mangalam. 2016. Multiple sclerosis patients have a distinct gut microbiota compared to healthy controls. *Sci. Rep.* 6: 28484.

129. Cekanaviciute, E., B. B. Yoo, T. F. Runia, J. W. Debelius, S. Singh, C. A. Nelson, R. Kanner, Y. Bencosme, Y. K. Lee, S. L. Hauser, E. Crabtree-Hartman, I. K. Sand, M. Gacias, Y. Zhu, P. Casaccia, B. A. C. Cree, R. Knight, S. K. Mazmanian, and S. E. Baranzini. 2017. Gut bacteria from multiple sclerosis patients modulate human T cells and exacerbate symptoms in mouse models. *Proc. Natl. Acad. Sci. USA* 114: 10713–10718.

130. Abdel-Misih, S. R. Z., and M. Bloomston. 2010. Liver anatomy. *Surg Clin North Am* 90: 643–653.

131. Poisson, J., S. Lemoinne, C. Boulanger, F. Durand, R. Moreau, D. Valla, and P.-E. Rautou. 2017. Liver sinusoidal endothelial cells: Physiology and role in liver diseases. *J. Hepatol.* 66: 212–227.

132. Manwaring, W. H., and W. Fritschen. 1923. Study of Microbic-Tissue Affinity by Perfusion Methods. *The Journal of Immunology* .

133. Shetty, S., P. F. Lalor, and D. H. Adams. 2018. Liver sinusoidal endothelial cells - gatekeepers of hepatic immunity. *Nat. Rev. Gastroenterol. Hepatol.* 15: 555–567.

134. Tsuchida, T., and S. L. Friedman. 2017. Mechanisms of hepatic stellate cell activation. *Nat. Rev. Gastroenterol. Hepatol.* 14: 397–411.

135. Fujita, T., and S. Narumiya. 2016. Roles of hepatic stellate cells in liver inflammation: a new perspective. *Inflamm. Regen.* 36: 1.

136. Schneiderhan, W., A. Schmid-Kotsas, J. Zhao, A. Grünert, A. Nüssler, H. Weidenbach, A. Menke, R. M. Schmid, G. Adler, and M. G. Bachem. 2001. Oxidized low-density lipoproteins bind to the scavenger receptor, CD36, of hepatic stellate cells and stimulate extracellular matrix synthesis. *Hepatology* 34: 729–737.

137. Ganesan, L. P., S. Mohanty, J. Kim, K. R. Clark, J. M. Robinson, and C. L. Anderson. 2011. Rapid and efficient clearance of blood-borne virus by liver sinusoidal endothelium. *PLoS Pathog.* 7: e1002281.

138. Gäbele, E., M. Mühlbauer, C. Dorn, T. S. Weiss, M. Froh, B. Schnabl, R. Wiest, J. Schölmerich, F. Obermeier, and C. Hellerbrand. 2008. Role of TLR9 in hepatic stellate cells and experimental liver fibrosis. *Biochem. Biophys. Res. Commun.* 376: 271–276.

139. Limmer, A., J. Ohl, C. Kurts, H. G. Ljunggren, Y. Reiss, M. Groettrup, F. Momburg, B. Arnold, and P. A. Knolle. 2000. Efficient presentation of exogenous antigen by liver endothelial cells to CD8+ T cells results in antigen-specific T-cell tolerance. *Nat. Med.* 6: 1348–1354.

140. Lohse, A. W., P. A. Knolle, K. Bilo, A. Uhrig, C. Waldmann, M. Ibe, E. Schmitt, G. Gerken, and K. H. Meyer Zum Büschenfelde. 1996. Antigen-presenting function and B7 expression of murine sinusoidal endothelial cells and Kupffer cells. *Gastroenterology* 110: 1175–1181.

141. Viñas, O., R. Bataller, P. Sancho-Bru, P. Ginès, C. Berenguer, C. Enrich, J. M. Nicolás, G. Ercilla, T. Gallart, J. Vives, V. Arroyo, and J. Rodés. 2003. Human hepatic stellate cells show features of antigen-presenting cells and stimulate lymphocyte proliferation. *Hepatology* 38: 919–929.

142. Thomson, A. W., and P. A. Knolle. 2010. Antigen-presenting cell function in the tolerogenic liver environment. *Nat. Rev. Immunol.* 10: 753–766.

143. Krenkel, O., and F. Tacke. 2017. Liver macrophages in tissue homeostasis and disease. *Nat. Rev. Immunol.* 17: 306–321.

144. Hildebrand, F., W. J. Hubbard, M. A. Choudhry, M. Frink, H.-C. Pape, S. L. Kunkel, and I. H. Chaudry. 2006. Kupffer cells and their mediators: the culprits in producing distant organ damage after trauma-hemorrhage. *Am. J. Pathol.* 169: 784–794.

145. Ala, A., A. P. Dhillon, and H. J. Hodgson. 2003. Role of cell adhesion molecules in leukocyte recruitment in the liver and gut. *Int J Exp Pathol* 84: 1–16.

146. Schwabe, R. F., E. Seki, and D. A. Brenner. 2006. Toll-like receptor signaling in the liver. *Gastroenterology* 130: 1886–1900.

147. Jiang, W., R. Sun, R. Zhou, H. Wei, and Z. Tian. 2009. TLR-9 activation aggravates concanavalin A-induced hepatitis via promoting accumulation and activation of liver CD4+ NKT cells. *J. Immunol.* 182: 3768–3774.

148. Tay, S. S., Y. C. Wong, B. Roediger, F. Sierro, B. Lu, D. M. McDonald, C. M. McGuffog, N. J. Meyer, I. E. Alexander, I. A. Parish, W. R. Heath, W. Weninger, G. A. Bishop, J. R. Gamble, G. W. McCaughan, P. Bertolino, and D. G. Bowen. 2014. Intrahepatic activation of naive CD4+ T cells by liver-resident phagocytic cells. *J. Immunol.* 193: 2087–2095.

149. Winau, F., G. Hegasy, R. Weiskirchen, S. Weber, C. Cassan, P. A. Sieling, R. L. Modlin, R. S. Liblau, A. M. Gressner, and S. H. E. Kaufmann. 2007. Ito cells are liver-resident antigen-presenting cells for activating T cell responses. *Immunity* 26: 117–129.

150. Holz, L. E., J. E. Prier, D. Freestone, T. M. Steiner, K. English, D. N. Johnson, V. Mollard, A. Cozijnsen, G. M. Davey, D. I. Godfrey, K. Yui, L. K. Mackay, M. H. Lahoud, I. Caminschi, G. I. McFadden, P. Bertolino, D. Fernandez-Ruiz, and W. R. Heath. 2018. CD8+ T Cell Activation Leads to Constitutive Formation of Liver Tissue-Resident Memory T Cells that Seed a Large and Flexible Niche in the Liver. *Cell Rep.* 25: 68–79.e4.

151. Gao, B., S. Radaeva, and O. Park. 2009. Liver natural killer and natural killer T cells: immunobiology and emerging roles in liver diseases. *J. Leukoc. Biol.* 86: 513–528.

152. Heaver, S. L., E. L. Johnson, and R. E. Ley. 2018. Sphingolipids in host-microbial interactions. *Curr. Opin. Microbiol.* 43: 92–99.

153. Biburger, M., and G. Tiegs. 2005. Alpha-galactosylceramide-induced liver injury in mice is mediated by TNF-alpha but independent of Kupffer cells. *J. Immunol.* 175: 1540–1550.

154. Goodier, M. R., and M. Londei. 2000. Lipopolysaccharide stimulates the proliferation of human CD56+CD3- NK cells: a regulatory role of monocytes and IL-10. *J. Immunol.* 165: 139–147.

155. Kanevskiy, L. M., W. G. Telford, A. M. Sapozhnikov, and E. I. Kovalenko. 2013. Lipopolysaccharide induces IFN-γ production in human NK cells. *Front. Immunol.* 4: 11.

156. Vanderkerken, K., L. Bouwens, N. Van Rooijen, K. Van den Berg, M. Baekeland, and E. Wisse. 1995. The role of Kupffer cells in the differentiation process of hepatic natural killer cells. *Hepatology* 22: 283–290.

157. Jo, E.-K., J. K. Kim, D.-M. Shin, and C. Sasakawa. 2016. Molecular mechanisms regulating NLRP3 inflammasome activation. *Cell Mol Immunol* 13: 148–159.

158. Khare, S., A. Dorfleutner, N. B. Bryan, C. Yun, A. D. Radian, L. de Almeida, Y. Rojanasakul, and C. Stehlik. 2012. An NLRP7-containing inflammasome mediates recognition of microbial lipopeptides in human macrophages. *Immunity* 36: 464–476.

159. Seki, E., H. Tsutsui, H. Nakano, N. Tsuji, K. Hoshino, O. Adachi, K. Adachi, S. Futatsugi, K. Kuida, O. Takeuchi, H. Okamura, J. Fujimoto, S. Akira, and K. Nakanishi. 2001. Lipopolysaccharide-induced IL-18 secretion from murine Kupffer cells independently of myeloid differentiation factor 88 that is critically involved in induction of production of IL-12 and IL-1beta. *J. Immunol.* 166: 2651–2657.

160. Dinarello, C. A., D. Novick, S. Kim, and G. Kaplanski. 2013. Interleukin-18 and IL-18 binding protein. *Front. Immunol.* 4: 289.

161. Muñoz, M., C. Eidenschenk, N. Ota, K. Wong, U. Lohmann, A. A. Kühl, X. Wang, P. Manzanillo, Y. Li, S. Rutz, Y. Zheng, L. Diehl, N. Kayagaki, M. van Lookeren-Campagne, O. Liesenfeld, M. Heimesaat, and W. Ouyang. 2015. Interleukin-22 induces interleukin-18 expression from epithelial cells during intestinal infection. *Immunity* 42: 321–331.

162. Belkaya, S., E. Michailidis, C. B. Korol, M. Kabbani, A. Cobat, P. Bastard, Y. S. Lee, N. Hernandez, S. Drutman, Y. P. de Jong, E. Vivier, J. Bruneau, V. Béziat, B. Boisson, L. Lorenzo-Diaz, S. Boucherit, M. Sebagh, E. Jacquemin, J.-F. Emile, L. Abel, C. M. Rice, E. Jouanguy, and J.-L. Casanova. 2019. Inherited IL-18BP deficiency in human fulminant viral hepatitis. *J. Exp. Med.* .

163. Kojima, H., Y. Aizawa, Y. Yanai, K. Nagaoka, M. Takeuchi, T. Ohta, H. Ikegami, M. Ikeda, and M. Kurimoto. 1999. An essential role for NF-kappa B in IL-18-induced IFN-gamma expression in KG-1 cells. *J. Immunol.* 162: 5063–5069.

164. Gutzmer, R., K. Langer, S. Mommert, M. Wittmann, A. Kapp, and T. Werfel. 2003. Human dendritic cells express the IL-18R and are chemoattracted to IL-18. *J. Immunol.* 171: 6363–6371.

165. Enoksson, S. L., E. K. Grasset, T. Hägglöf, N. Mattsson, Y. Kaiser, S. Gabrielsson, T. L. McGaha, A. Scheynius, and M. C. I. Karlsson. 2011. The inflammatory cytokine IL-18 induces self-reactive innate antibody responses regulated by natural killer T cells. *Proc. Natl. Acad. Sci. USA* 108: E1399-407.

166. Weinstock, J. V., A. Blum, A. Metwali, D. Elliott, and R. Arsenescu. 2003. IL-18 and IL-12 signal through the NF-kappa B pathway to induce NK-1R expression on T cells. *J. Immunol.* 170: 5003–5007.

167. Yoo, J. K., H. Kwon, L.-Y. Khil, L. Zhang, H.-S. Jun, and J.-W. Yoon. 2005. IL-18 induces monocyte chemotactic protein-1 production in macrophages through the phosphatidylinositol 3-kinase/Akt and MEK/ERK1/2 pathways. *J. Immunol.* 175: 8280–8286.

168. Kang, M.-J., R. J. Homer, A. Gallo, C. G. Lee, K. A. Crothers, S. J. Cho, C. Rochester, H. Cain, G. Chupp, H. J. Yoon, and J. A. Elias. 2007. IL-18 is induced and IL-18 receptor alpha plays a critical role in the pathogenesis of cigarette smoke-induced pulmonary emphysema and inflammation. *J. Immunol.* 178: 1948–1959.

169. Subleski, J. J., V. L. Hall, J. M. Weiss, J. R. Ortaldo, and R. H. Wiltrout. 2007. Differential modulation of NK and NKT cells in the liver and spleen following IL-18 + IL-12 treatment of mice (98.9). *The Journal of Immunology* .

170. Okamoto, I., K. Kohno, T. Tanimoto, H. Ikegami, and M. Kurimoto. 1999. Development of CD8+ effector T cells is differentially regulated by IL-18 and IL-12. *J. Immunol.* 162: 3202–3211.

171. Bachmann, M., J. Pfeilschifter, and H. Mühl. 2018. A Prominent Role of Interleukin-18 in Acetaminophen-Induced Liver Injury Advocates Its Blockage for Therapy of Hepatic Necroinflammation. *Front. Immunol.* 9: 161.

172. Tsutsui, H., K. Nakanishi, K. Matsui, K. Higashino, H. Okamura, Y. Miyazawa, and K. Kaneda. 1996. IFN-gamma-inducing factor up-regulates Fas ligand-mediated cytotoxic activity of murine natural killer cell clones. *J. Immunol.* 157: 3967–3973.

173. Sattler, A., C. Dang-Heine, P. Reinke, and N. Babel. 2015. IL-15 dependent induction of IL-18 secretion as a feedback mechanism controlling human MAIT-cell effector functions. *Eur. J. Immunol.* 45: 2286–2298.

174. Faubion, W. A., and G. J. Gores. 1999. Death receptors in liver biology and pathobiology. *Hepatology* 29: 1–4.

175. Kakinuma, C., K. Takagaki, T. Yatomi, N. Nakamura, S. Nagata, A. Uemura, and Y. Shibutani. 1999. Acute toxicity of an anti-Fas antibody in mice. *Toxicol. Pathol.* 27: 412–420.

176. Wajant, H. 2002. The Fas signaling pathway: more than a paradigm. *Science* 296: 1635–1636.

177. Tripathi, A., J. Debelius, D. A. Brenner, M. Karin, R. Loomba, B. Schnabl, and R. Knight. 2018. The gut-liver axis and the intersection with the microbiome. *Nat. Rev. Gastroenterol. Hepatol.* 15: 397–411.

178. Celaj, S., M. W. Gleeson, J. Deng, G. A. O'Toole, T. H. Hampton, M. F. Toft, H. G. Morrison, M. L. Sogin, J. Putra, A. A. Suriawinata, and J. D. Gorham. 2014. The microbiota regulates susceptibility to Fas-mediated acute hepatic injury. *Lab. Invest.* 94: 938–949.

179. Manfredo Vieira, S., M. Hiltensperger, V. Kumar, D. Zegarra-Ruiz, C. Dehner, N. Khan, F. R. C. Costa, E. Tiniakou, T. Greiling, W. Ruff, A. Barbieri, C. Kriegel, S. S. Mehta, J. R. Knight, D. Jain, A. L. Goodman, and M. A. Kriegel. 2018. Translocation of a gut pathobiont drives autoimmunity in mice and humans. *Science* 359: 1156–1161.

180. Llopis, M., A. M. Cassard, L. Wrzosek, L. Boschat, A. Bruneau, G. Ferrere, V. Puchois, J. C. Martin, P. Lepage, T. Le Roy, L. Lefèvre, B. Langelier, F. Cailleux, A. M. González-Castro, S. Rabot, F. Gaudin, H. Agostini, S. Prévot, D. Berrebi, D. Ciocan, C. Jousse, S. Naveau, P. Gérard, and G. Perlemuter. 2016. Intestinal microbiota contributes to individual susceptibility to alcoholic liver disease. *Gut* 65: 830–839.

181. Brenchley, J. M., D. A. Price, T. W. Schacker, T. E. Asher, G. Silvestri, S. Rao, Z. Kazzaz, E. Bornstein, O. Lambotte, D. Altmann, B. R. Blazar, B. Rodriguez, L. Teixeira-Johnson, A. Landay, J. N. Martin, F. M. Hecht, L. J. Picker, M. M. Lederman, S. G. Deeks, and D. C. Douek. 2006. Microbial translocation is a cause of systemic immune activation in chronic HIV infection. *Nat. Med.* 12: 1365–1371.

182. Pan, C., Y. Gu, W. Zhang, Y. Zheng, L. Peng, H. Deng, Y. Chen, L. Chen, S. Chen, M. Zhang, and Z. Gao. 2012. Dynamic changes of lipopolysaccharide levels in different phases of acute on chronic hepatitis B liver failure. *PLoS One* 7: e49460.

183. Yan, A. W., and B. Schnabl. 2012. Bacterial translocation and changes in the intestinal microbiome associated with alcoholic liver disease. *World J Hepatol* 4: 110–118.

184. Li, W., T. Amet, Y. Xing, J. Lan, S. Liangpunsakul, P. Puri, P. Kamath, A. Sanyal, V. Shah, S. Radaeva, D. Crabb, N. Chalasani, and A. Yu. 2017. Enhanced susceptibility to alcohol-induced bacterial translocation, immune activation, and persistent inflammation in patients with alcoholic hepatitis: a prospective observational study. *The Journal of Immunology* .

185. Lemmers, A., C. Moreno, T. Gustot, R. Maréchal, D. Degré, P. Demetter, P. de Nadai, A. Geerts, E. Quertinmont, V. Vercruysse, O. Le Moine, and J. Devière. 2009. The interleukin-17 pathway is involved in human alcoholic liver disease. *Hepatology* 49: 646–657.

186. Nagata, T., L. McKinley, J. J. Peschon, J. F. Alcorn, S. J. Aujla, and J. K. Kolls. 2008. Requirement of IL-17RA in Con A induced hepatitis and negative regulation of IL-17 production in mouse T cells. *J. Immunol.* 181: 7473–7479.

187. Hammerich, L., F. Heymann, and F. Tacke. 2011. Role of IL-17 and Th17 cells in liver diseases. *Clin Dev Immunol* 2011: 345803.

188. Crispe, I. N. 2012. IL-17 in liver injury: an inflammatory issue? *Immunol. Cell Biol.* 90: 369–370.

189. Shih, V. F.-S., J. Cox, N. M. Kljavin, H. S. Dengler, M. Reichelt, P. Kumar, L. Rangell, J. K. Kolls, L. Diehl, W. Ouyang, and N. Ghilardi. 2014. Homeostatic IL-23 receptor signaling limits Th17 response through IL-22-mediated containment of commensal microbiota. *Proc. Natl. Acad. Sci. USA* 111: 13942–13947.

190. Kolls, J. K., P. B. McCray, and Y. R. Chan. 2008. Cytokine-mediated regulation of antimicrobial proteins. *Nat. Rev. Immunol.* 8: 829–835.

191. Zheng, M., W. Horne, J. P. McAleer, D. Pociask, T. Eddens, M. Good, B. Gao, and J. K. Kolls. 2016. Therapeutic Role of Interleukin 22 in Experimental Intra-abdominal Klebsiella pneumoniae Infection in Mice. *Infect. Immun.* 84: 782–789.

192. Croswell, A., E. Amir, P. Teggatz, M. Barman, and N. H. Salzman. 2009. Prolonged impact of antibiotics on intestinal microbial ecology and susceptibility to enteric Salmonella infection. *Infect. Immun.* 77: 2741–2753.

193. Caporaso, J. G., C. L. Lauber, W. A. Walters, D. Berg-Lyons, J. Huntley, N. Fierer, S. M. Owens, J. Betley, L. Fraser, M. Bauer, N. Gormley, J. A. Gilbert, G. Smith, and R. Knight. 2012. Ultra-high-throughput microbial community analysis on the Illumina HiSeq and MiSeq platforms. *ISME J.* 6: 1621–1624.

194. Gopalakrishna, K. P., B. R. Macadangdang, M. B. Rogers, J. T. Tometich, B. A. Firek, R. Baker, J. Ji, A. H. P. Burr, C. Ma, M. Good, M. J. Morowitz, and T. W. Hand. 2019. Maternal IgA protects against the development of necrotizing enterocolitis in preterm infants. *Nat. Med.* 25: 1110–1115.

195. Schloss, P. D., S. L. Westcott, T. Ryabin, J. R. Hall, M. Hartmann, E. B. Hollister, R. A. Lesniewski, B. B. Oakley, D. H. Parks, C. J. Robinson, J. W. Sahl, B. Stres, G. G. Thallinger, D. J. Van Horn, and C. F. Weber. 2009. Introducing mothur: open-source, platform-independent, community-supported software for describing and comparing microbial communities. *Appl. Environ. Microbiol.* 75: 7537–7541.

196. Tarabichi, Y., K. Li, S. Hu, C. Nguyen, X. Wang, D. Elashoff, K. Saira, B. Frank, M. Bihan, E. Ghedin, B. A. Methé, and J. C. Deng. 2015. The administration of intranasal live attenuated influenza vaccine induces changes in the nasal microbiota and nasal epithelium gene expression profiles. *Microbiome* 3: 74.

197. Edgar, R., M. Domrachev, and A. E. Lash. 2002. Gene Expression Omnibus: NCBI gene expression and hybridization array data repository. *Nucleic Acids Res.* 30: 207–210.

198. Tiegs, G., J. Hentschel, and A. Wendel. 1992. A T cell-dependent experimental liver injury in mice inducible by concanavalin A. *J. Clin. Invest.* 90: 196–203.

199. Blaschitz, C., and M. Raffatellu. 2010. Th17 cytokines and the gut mucosal barrier. *J. Clin. Immunol.* 30: 196–203.

200. Yi, A. K., J. H. Chace, J. S. Cowdery, and A. M. Krieg. 1996. IFN-gamma promotes IL-6 and IgM secretion in response to CpG motifs in bacterial DNA and oligodeoxynucleotides. *J. Immunol.* 156: 558–564.

201. Hartmann, G., G. J. Weiner, and A. M. Krieg. 1999. CpG DNA: a potent signal for growth, activation, and maturation of human dendritic cells. *Proc. Natl. Acad. Sci. USA* 96: 9305–9310.

202. Gupta, S., M. P. Gould, J. DeVecchio, D. H. Canaday, J. J. Auletta, and F. P. Heinzel. 2006. CpG-induced IFNgamma expands TLR4-specific IL-18 responses in vivo. *Cell Immunol.* 243: 75–82.

203. Wang, H.-X., M. Liu, S.-Y. Weng, J.-J. Li, C. Xie, H.-L. He, W. Guan, Y.-S. Yuan, and J. Gao. 2012. Immune mechanisms of Concanavalin A model of autoimmune hepatitis. *World J. Gastroenterol.* 18: 119–125.

204. Nishikage, T., S. Seki, S. Toyabe, T. Abo, Y. Kagata, T. Iwai, and H. Hiraide. 1999. Inhibition of concanavalin A-induced hepatic injury of mice by bacterial lipopolysaccharide via the induction of IL-6 and the subsequent reduction of IL-4: the cytokine milieu of concanavalin A hepatitis. *J. Hepatol.* 31: 18–26.

205. Mizuhara, H., M. Uno, N. Seki, M. Yamashita, M. Yamaoka, T. Ogawa, K. Kaneda, T. Fujii, H. Senoh, and H. Fujiwara. 1996. Critical involvement of interferon gamma in the pathogenesis of T-cell activation-associated hepatitis and regulatory mechanisms of interleukin-6 for the manifestations of hepatitis. *Hepatology* 23: 1608–1615.

206. Tagawa, Y., K. Sekikawa, and Y. Iwakura. 1997. Suppression of concanavalin A-induced hepatitis in IFN-gamma(-/-) mice, but not in TNF-alpha(-/-) mice: role for IFN-gamma in activating apoptosis of hepatocytes. *J. Immunol.* 159: 1418–1428.

207. Kaplanski, G. 2018. Interleukin-18: Biological properties and role in disease pathogenesis. *Immunol. Rev.* 281: 138–153.

208. Weiss, E. S., C. Girard-Guyonvarc'h, D. Holzinger, A. A. de Jesus, Z. Tariq, J. Picarsic, E. J. Schiffrin, D. Foell, A. A. Grom, S. Ammann, S. Ehl, T. Hoshino, R. Goldbach-Mansky, C. Gabay, and S. W. Canna. 2018. Interleukin-18 diagnostically distinguishes and pathogenically promotes human and murine macrophage activation syndrome. *Blood* 131: 1442–1455.

209. Morel, J. C., C. C. Park, P. Kumar, and A. E. Koch. 2001. Interleukin-18 induces rheumatoid arthritis synovial fibroblast CXC chemokine production through NFkappaB activation. *Lab. Invest.* 81: 1371–1383.

210. Nakamura, K., H. Okamura, K. Nagata, T. Komatsu, and T. Tamura. 1993. Purification of a factor which provides a costimulatory signal for gamma interferon production. *Infect. Immun.* 61: 64–70.

211. Fujita, T., K. Soontrapa, Y. Ito, K. Iwaisako, C. S. Moniaga, M. Asagiri, M. Majima, and S. Narumiya. 2016. Hepatic stellate cells relay inflammation signaling from sinusoids to parenchyma in mouse models of immune-mediated hepatitis. *Hepatology* 63: 1325–1339.

212. Carpino, G., A. Franchitto, S. Morini, S. G. Corradini, M. Merli, and E. Gaudio. 2004. Activated hepatic stellate cells in liver cirrhosis. A morphologic and morphometrical study. *Ital J Anat Embryol* 109: 225–238.

213. Szabo, G., S. Bala, J. Petrasek, and A. Gattu. 2010. Gut-liver axis and sensing microbes. *Dig. Dis.* 28: 737–744.

214. Dobashi, H., S. Seki, Y. Habu, T. Ohkawa, S. Takeshita, H. Hiraide, and I. Sekine. 1999. Activation of mouse liver natural killer cells and NK1.1(+) T cells by bacterial superantigen-primed Kupffer cells. *Hepatology* 30: 430–436.

215. Tagawa, Y., S. Kakuta, and Y. Iwakura. 1998. Involvement of Fas/Fas ligand system-mediated apoptosis in the development of concanavalin A-induced hepatitis. *Eur. J. Immunol.* 28: 4105–4113.

216. Tsutsui, H., N. Kayagaki, K. Kuida, H. Nakano, N. Hayashi, K. Takeda, K. Matsui, S. Kashiwamura, T. Hada, S. Akira, H. Yagita, H. Okamura, and K. Nakanishi. 1999. Caspase-1-independent, Fas/Fas ligand-mediated IL-18 secretion from macrophages causes acute liver injury in mice. *Immunity* 11: 359–367.

217. Seino, K., N. Kayagaki, K. Takeda, K. Fukao, K. Okumura, and H. Yagita. 1997. Contribution of Fas ligand to T cell-mediated hepatic injury in mice. *Gastroenterology* 113: 1315–1322.

218. Lafdil, F., H. Wang, O. Park, W. Zhang, Y. Moritoki, S. Yin, X. Y. Fu, M. E. Gershwin, Z.-X. Lian, and B. Gao. 2009. Myeloid STAT3 inhibits T cell-mediated hepatitis by regulating T helper 1 cytokine and interleukin-17 production. *Gastroenterology* 137: 2125–35.e1.

219. Yan, S., L. Wang, N. Liu, Y. Wang, and Y. Chu. 2012. Critical role of interleukin-17/interleukin-17 receptor axis in mediating Con A-induced hepatitis. *Immunol. Cell Biol.* 90: 421–428.

220. Zenewicz, L. A., G. D. Yancopoulos, D. M. Valenzuela, A. J. Murphy, M. Karow, and R. A. Flavell. 2007. Interleukin-22 but not interleukin-17 provides protection to hepatocytes during acute liver inflammation. *Immunity* 27: 647–659.

221. Boursier, J., and A. M. Diehl. 2015. Implication of gut microbiota in nonalcoholic fatty liver disease. *PLoS Pathog.* 11: e1004559.

222. Leung, D. H., and D. Yimlamai. 2017. The intestinal microbiome and paediatric liver disease. *Lancet Gastroenterol. Hepatol.* 2: 446–455.

223. Bouladoux, N., J. A. Hall, J. R. Grainger, L. M. dos Santos, M. G. Kann, V. Nagarajan, D. Verthelyi, and Y. Belkaid. 2012. Regulatory role of suppressive motifs from commensal DNA. *Mucosal Immunol.* 5: 623–634.

224. Winter, S. E., and A. J. Bäumler. 2014. Why related bacterial species bloom simultaneously in the gut: principles underlying the “Like will to like” concept. *Cell Microbiol.* 16: 179–184.

225. Zhang, H., Q. Gong, J. Li, X. Kong, L. Tian, L. Duan, J. Tong, F. Song, M. Fang, F. Zheng, P. Xiong, Z. Tan, and F. Gong. 2010. CpG ODN pretreatment attenuates concanavalin A-induced hepatitis in mice. *Int. Immunopharmacol.* 10: 79–85.

226. Levy, M., C. A. Thaiss, D. Zeevi, L. Dohnalová, G. Zilberman-Schapira, J. A. Mahdi, E. David, A. Savidor, T. Korem, Y. Herzig, M. Pevsner-Fischer, H. Shapiro, A. Christ, A. Harmelin, Z. Halpern, E. Latz, R. A. Flavell, I. Amit, E. Segal, and E. Elinav. 2015. Microbiota-Modulated Metabolites Shape the Intestinal Microenvironment by Regulating NLRP6 Inflammasome Signaling. *Cell* 163: 1428–1443.

227. Nowarski, R., R. Jackson, N. Gagliani, M. R. de Zoete, N. W. Palm, W. Bailis, J. S. Low, C. C. D. Harman, M. Graham, E. Elinav, and R. A. Flavell. 2015. Epithelial IL-18 Equilibrium Controls Barrier Function in Colitis. *Cell* 163: 1444–1456.

228. Faggioni, R., R. C. Cattley, J. Guo, S. Flores, H. Brown, M. Qi, S. Yin, D. Hill, S. Scully, C. Chen, D. Brankow, J. Lewis, C. Baikalov, H. Yamane, T. Meng, F. Martin, S. Hu, T. Boone, and G. Senaldi. 2001. IL-18-binding protein protects against lipopolysaccharide-induced lethality and prevents the development of Fas/Fas ligand-mediated models of liver disease in mice. *J. Immunol.* 167: 5913–5920.

229. Pinkoski, M. J., T. Brunner, D. R. Green, and T. Lin. 2000. Fas and Fas ligand in gut and liver. *Am. J. Physiol. Gastrointest. Liver Physiol.* 278: G354-66.

230. Hammam, O., O. Mahmoud, M. Zahran, S. Aly, K. Hosny, A. Helmy, and A. Anas. 2012. The role of fas/fas ligand system in the pathogenesis of liver cirrhosis and hepatocellular carcinoma. *Hepat Mon* 12: e6132.

231. Tagami, A., H. Ohnishi, H. Moriwaki, M. Phillips, and R. D. Hughes. 2003. Fas-mediated apoptosis in acute alcoholic hepatitis. *Hepatogastroenterology* 50: 443–448.

232. Guicciardi, M. E., and G. J. Gores. 2006. Fasl and fas in liver homeostasis and hepatic injuries. In *Fas Signaling* Springer US, Boston, MA. 103–117.

233. Elinav, E., T. Strowig, A. L. Kau, J. Henao-Mejia, C. A. Thaiss, C. J. Booth, D. R. Peaper, J. Bertin, S. C. Eisenbarth, J. I. Gordon, and R. A. Flavell. 2011. NLRP6 inflammasome regulates colonic microbial ecology and risk for colitis. *Cell* 145: 745–757.

234. Ma, C., M. Han, B. Heinrich, Q. Fu, Q. Zhang, M. Sandhu, D. Agdashian, M. Terabe, J. A. Berzofsky, V. Fako, T. Ritz, T. Longerich, C. M. Theriot, J. A. McCulloch, S. Roy, W. Yuan, V. Thovarai, S. K. Sen, M. Ruchirawat, F. Korangy, X. W. Wang, G. Trinchieri, and T. F. Greten. 2018. Gut microbiome-mediated bile acid metabolism regulates liver cancer via NKT cells. *Science* 360.

235. Tsikrikoni, A., D. S. Kyriakou, E. I. Rigopoulou, M. G. Alexandrakis, K. Zachou, F. Passam, and G. N. Dalekos. 2005. Markers of cell activation and apoptosis in bone marrow mononuclear cells of patients with autoimmune hepatitis type 1 and primary biliary cirrhosis. *J. Hepatol.* 42: 393–399.

236. Fox, C. K., A. Furtwaengler, R. R. Nepomuceno, O. M. Martinez, and S. M. Krams. 2001. Apoptotic pathways in primary biliary cirrhosis and autoimmune hepatitis. *Liver* 21: 272–279.

237. Ogawa, S., K. Sakaguchi, A. Takaki, K. Shiraga, T. Sawayama, H. Mouri, M. Miyashita, N. Koide, and T. Tsuji. 2000. Increase in CD95 (Fas/APO-1)-positive CD4+ and CD8+ T cells in peripheral blood derived from patients with autoimmune hepatitis or chronic hepatitis C with autoimmune phenomena. *J. Gastroenterol. Hepatol.* 15: 69–75.

238. Hussain, M. J., A. Mustafa, H. Gallati, A. P. Mowat, G. Mieli-Vergani, and D. Vergani. 1994. Cellular expression of tumour necrosis factor-alpha and interferon-gamma in the liver biopsies of children with chronic liver disease. *J. Hepatol.* 21: 816–821.

239. Yamano, T., T. Higashi, K. Nouso, H. Nakatsukasa, K. Kariyama, E. Yumoto, Y. Kobayashi, K. Yamamoto, H. Iwagaki, T. Yagi, T. Tanimoto, M. Kurimoto, N. Tanaka, and T. Tsuji. 2000. Serum interferon-gamma-inducing factor/IL-18 levels in primary biliary cirrhosis. *Clin. Exp. Immunol.* 122: 227–231.

240. Zeremski, M., L. M. Petrovic, L. Chiriboga, Q. B. Brown, H. T. Yee, M. Kinkhabwala, I. M. Jacobson, R. Dimova, M. Markatou, and A. H. Talal. 2008. Intrahepatic levels of CXCR3-associated chemokines correlate with liver inflammation and fibrosis in chronic hepatitis C. *Hepatology* 48: 1440–1450.

241. Sharma, A., A. Chakraborti, A. Das, R. K. Dhiman, and Y. Chawla. 2009. Elevation of interleukin-18 in chronic hepatitis C: implications for hepatitis C virus pathogenesis. *Immunology* 128: e514-22.

242. Kimura, K., K. Ando, E. Tomita, H. Ohnishi, T. Ishikawa, S. Kakumu, Y. Muto, and H. Moriwaki. 1999. Elevated intracellular IFN-γ levels in circulating CD8 + lymphocytes in patients with fulminant hepatitis. *J. Hepatol.* 31: 579–583.

243. Shinoda, M., G. Wakabayashi, M. Shimazu, H. Saito, K. Hoshino, M. Tanabe, Y. Morikawa, S. Endo, H. Ishii, and M. Kitajima. 2006. Increased serum and hepatic tissue levels of interleukin-18 in patients with fulminant hepatic failure. *J. Gastroenterol. Hepatol.* 21: 1731–1736.

244. Chamroonkul, N., and M. B. Bansal. 2019. HIV and the liver. *Nat. Rev. Gastroenterol. Hepatol.* 16: 1–2.

245. Tansey, E. M. 2006. Pavlov at home and abroad: His role in international physiology. *Auton Neurosci* 125: 1–11.

246. Powell, N., M. M. Walker, and N. J. Talley. 2017. The mucosal immune system: master regulator of bidirectional gut-brain communications. *Nat. Rev. Gastroenterol. Hepatol.* 14: 143–159.

247. Benakis, C., D. Brea, S. Caballero, G. Faraco, J. Moore, M. Murphy, G. Sita, G. Racchumi, L. Ling, E. G. Pamer, C. Iadecola, and J. Anrather. 2016. Commensal microbiota affects ischemic stroke outcome by regulating intestinal γδ T cells. *Nat. Med.* 22: 516–523.

248. Dendrou, C. A., L. Fugger, and M. A. Friese. 2015. Immunopathology of multiple sclerosis. *Nat. Rev. Immunol.* 15: 545–558.

249. Compston, A., and A. Coles. 2008. Multiple sclerosis. *Lancet* 372: 1502–1517.

250. Wallin, M. T., W. J. Culpepper, J. D. Campbell, L. M. Nelson, A. Langer-Gould, R. A. Marrie, G. R. Cutter, W. E. Kaye, L. Wagner, H. Tremlett, S. L. Buka, P. Dilokthornsakul, B. Topol, L. H. Chen, N. G. LaRocca, and US Multiple Sclerosis Prevalence Workgroup. 2019. The prevalence of MS in the United States: A population-based estimate using health claims data. *Neurology* 92: e1029–e1040.

251. GBD 2015 Neurological Disorders Collaborator Group. 2017. Global, regional, and national burden of neurological disorders during 1990-2015: a systematic analysis for the Global Burden of Disease Study 2015. *Lancet Neurol.* 16: 877–897.

252. Evans, C., S.-G. Beland, S. Kulaga, C. Wolfson, E. Kingwell, J. Marriott, M. Koch, N. Makhani, S. Morrow, J. Fisk, J. Dykeman, N. Jetté, T. Pringsheim, and R. A. Marrie. 2013. Incidence and prevalence of multiple sclerosis in the Americas: a systematic review. *Neuroepidemiology* 40: 195–210.

253. Culpepper, W. J., R. A. Marrie, A. Langer-Gould, M. T. Wallin, J. D. Campbell, L. M. Nelson, W. E. Kaye, L. Wagner, H. Tremlett, L. H. Chen, S. Leung, C. Evans, S. Yao, N. G. LaRocca, and United States Multiple Sclerosis Prevalence Workgroup (MSPWG). 2019. Validation of an algorithm for identifying MS cases in administrative health claims datasets. *Neurology* 92: e1016–e1028.

254. Alonso, A., and M. A. Hernán. 2008. Temporal trends in the incidence of multiple sclerosis: a systematic review. *Neurology* 71: 129–135.

255. Goodin, D. S. 2014. The epidemiology of multiple sclerosis: insights to disease pathogenesis. *Handb Clin Neurol* 122: 231–266.

256. Lincoln, M. R., A. Montpetit, M. Z. Cader, J. Saarela, D. A. Dyment, M. Tiislar, V. Ferretti, P. J. Tienari, A. D. Sadovnick, L. Peltonen, G. C. Ebers, and T. J. Hudson. 2005. A predominant role for the HLA class II region in the association of the MHC region with multiple sclerosis. *Nat. Genet.* 37: 1108–1112.

257. Willer, C. J., D. A. Dyment, N. J. Risch, A. D. Sadovnick, G. C. Ebers, and Canadian Collaborative Study Group. 2003. Twin concordance and sibling recurrence rates in multiple sclerosis. *Proc. Natl. Acad. Sci. USA* 100: 12877–12882.

258. Thompson, A. J., B. L. Banwell, F. Barkhof, W. M. Carroll, T. Coetzee, G. Comi, J. Correale, F. Fazekas, M. Filippi, M. S. Freedman, K. Fujihara, S. L. Galetta, H. P. Hartung, L. Kappos, F. D. Lublin, R. A. Marrie, A. E. Miller, D. H. Miller, X. Montalban, E. M. Mowry, P. S. Sorensen, M. Tintoré, A. L. Traboulsee, M. Trojano, B. M. J. Uitdehaag, S. Vukusic, E. Waubant, B. G. Weinshenker, S. C. Reingold, and J. A. Cohen. 2018. Diagnosis of multiple sclerosis: 2017 revisions of the McDonald criteria. *Lancet Neurol.* 17: 162–173.

259. Langer-Gould, A., R. A. Popat, S. M. Huang, K. Cobb, P. Fontoura, M. K. Gould, and L. M. Nelson. 2006. Clinical and demographic predictors of long-term disability in patients with relapsing-remitting multiple sclerosis: a systematic review. *Arch. Neurol.* 63: 1686–1691.

260. Swanton, J., K. Fernando, and D. Miller. 2014. Early prognosis of multiple sclerosis. *Handb Clin Neurol* 122: 371–391.

261. Bergamaschi, R. 2007. Prognostic factors in multiple sclerosis. *Int Rev Neurobiol* 79: 423–447.

262. Finkelsztejn, A., J. B. B. Brooks, F. M. Paschoal, and Y. D. Fragoso. 2011. What can we really tell women with multiple sclerosis regarding pregnancy? A systematic review and meta-analysis of the literature. *BJOG* 118: 790–797.

263. Shah, N. M., A. A. Herasimtschuk, A. Boasso, A. Benlahrech, D. Fuchs, N. Imami, and M. R. Johnson. 2017. Changes in T Cell and Dendritic Cell Phenotype from Mid to Late Pregnancy Are Indicative of a Shift from Immune Tolerance to Immune Activation. *Front. Immunol.* 8: 1138.

264. Kay, A. W., J. Fukuyama, N. Aziz, C. L. Dekker, S. Mackey, G. E. Swan, M. M. Davis, S. Holmes, and C. A. Blish. 2014. Enhanced natural killer-cell and T-cell responses to influenza A virus during pregnancy. *Proc. Natl. Acad. Sci. USA* 111: 14506–14511.

265. Koren, O., J. K. Goodrich, T. C. Cullender, A. Spor, K. Laitinen, H. K. Bäckhed, A. Gonzalez, J. J. Werner, L. T. Angenent, R. Knight, F. Bäckhed, E. Isolauri, S. Salminen, and R. E. Ley. 2012. Host remodeling of the gut microbiome and metabolic changes during pregnancy. *Cell* 150: 470–480.

266. Galea, I., N. Ward-Abel, and C. Heesen. 2015. Relapse in multiple sclerosis. *BMJ* 350: h1765.

267. Brown, J. W. L., A. Coles, D. Horakova, E. Havrdova, G. Izquierdo, A. Prat, M. Girard, P. Duquette, M. Trojano, A. Lugaresi, R. Bergamaschi, P. Grammond, R. Alroughani, R. Hupperts, P. McCombe, V. Van Pesch, P. Sola, D. Ferraro, F. Grand'Maison, M. Terzi, J. Lechner-Scott, S. Flechter, M. Slee, V. Shaygannejad, E. Pucci, F. Granella, V. Jokubaitis, M. Willis, C. Rice, N. Scolding, A. Wilkins, O. R. Pearson, T. Ziemssen, M. Hutchinson, K. Harding, J. Jones, C. McGuigan, H. Butzkueven, T. Kalincik, N. Robertson, and MSBase Study Group. 2019. Association of Initial Disease-Modifying Therapy With Later Conversion to Secondary Progressive Multiple Sclerosis. *JAMA* 321: 175–187.

268. Chun, J., and H.-P. Hartung. 2010. Mechanism of action of oral fingolimod (FTY720) in multiple sclerosis. *Clin Neuropharmacol* 33: 91–101.

269. Kappos, L., E.-W. Radue, P. O'Connor, C. Polman, R. Hohlfeld, P. Calabresi, K. Selmaj, C. Agoropoulou, M. Leyk, L. Zhang-Auberson, P. Burtin, and FREEDOMS Study Group. 2010. A placebo-controlled trial of oral fingolimod in relapsing multiple sclerosis. *N. Engl. J. Med.* 362: 387–401.

270. Havrdova, E., D. Horakova, and I. Kovarova. 2015. Alemtuzumab in the treatment of multiple sclerosis: key clinical trial results and considerations for use. *Ther Adv Neurol Disord* 8: 31–45.

271. Hu, Y., M. J. Turner, J. Shields, M. S. Gale, E. Hutto, B. L. Roberts, W. M. Siders, and J. M. Kaplan. 2009. Investigation of the mechanism of action of alemtuzumab in a human CD52 transgenic mouse model. *Immunology* 128: 260–270.

272. Coles, A. J., C. L. Twyman, D. L. Arnold, J. A. Cohen, C. Confavreux, E. J. Fox, H.-P. Hartung, E. Havrdova, K. W. Selmaj, H. L. Weiner, T. Miller, E. Fisher, R. Sandbrink, S. L. Lake, D. H. Margolin, P. Oyuela, M. A. Panzara, D. A. S. Compston, and CARE-MS II investigators. 2012. Alemtuzumab for patients with relapsing multiple sclerosis after disease-modifying therapy: a randomised controlled phase 3 trial. *Lancet* 380: 1829–1839.

273. Mazdeh, M., S. Hosseini, M. Taheri, and S. Ghafouri-Fard. 2018. The effect of natalizumab on disability score and relapse rate of multiple sclerosis patients: a prospective cohort study. *Clin. Transl. Med.* 7: 38.

274. Brandstadter, R., and I. Katz Sand. 2017. The use of natalizumab for multiple sclerosis. *Neuropsychiatr. Dis. Treat.* 13: 1691–1702.

275. Polman, C. H., P. W. O'Connor, E. Havrdova, M. Hutchinson, L. Kappos, D. H. Miller, J. T. Phillips, F. D. Lublin, G. Giovannoni, A. Wajgt, M. Toal, F. Lynn, M. A. Panzara, A. W. Sandrock, and AFFIRM Investigators. 2006. A randomized, placebo-controlled trial of natalizumab for relapsing multiple sclerosis. *N. Engl. J. Med.* 354: 899–910.

276. Ziemssen, T., and W. Schrempf. 2007. Glatiramer Acetate: Mechanisms of Action in Multiple Sclerosis. In *The Neurobiology of Multiple Sclerosis*. International Review of Neurobiology vol. 79. Elsevier. 537–570.

277. Comi, G., M. Filippi, J. S. Wolinsky, and European/Canadian Glatiramer Acetate Study Group. 2001. European/Canadian multicenter, double-blind, randomized, placebo-controlled study of the effects of glatiramer acetate on magnetic resonance imaging-measured disease activity and burden in patients with relapsing multiple sclerosis. *Ann. Neurol.* 49: 290–297.

278. Comi, G., V. Martinelli, M. Rodegher, L. Moiola, O. Bajenaru, A. Carra, I. Elovaara, F. Fazekas, H. P. Hartung, J. Hillert, J. King, S. Komoly, C. Lubetzki, X. Montalban, K. M. Myhr, M. Ravnborg, P. Rieckmann, D. Wynn, C. Young, M. Filippi, and PreCISe study group. 2009. Effect of glatiramer acetate on conversion to clinically definite multiple sclerosis in patients with clinically isolated syndrome (PreCISe study): a randomised, double-blind, placebo-controlled trial. *Lancet* 374: 1503–1511.

279. Kieseier, B. C. 2011. The mechanism of action of interferon-β in relapsing multiple sclerosis. *CNS Drugs* 25: 491–502.

280. Kasper, L. H., and A. T. Reder. 2014. Immunomodulatory activity of interferon-beta. *Ann Clin Transl Neurol* 1: 622–631.

281. 1993. Interferon beta-1b is effective in relapsing-remitting multiple sclerosis. I. Clinical results of a multicenter, randomized, double-blind, placebo-controlled trial. The IFNB Multiple Sclerosis Study Group. *Neurology* 43: 655–661.

282. Montalban, X., S. L. Hauser, L. Kappos, D. L. Arnold, A. Bar-Or, G. Comi, J. de Seze, G. Giovannoni, H.-P. Hartung, B. Hemmer, F. Lublin, K. W. Rammohan, K. Selmaj, A. Traboulsee, A. Sauter, D. Masterman, P. Fontoura, S. Belachew, H. Garren, N. Mairon, P. Chin, J. S. Wolinsky, and ORATORIO Clinical Investigators. 2017. Ocrelizumab versus Placebo in Primary Progressive Multiple Sclerosis. *N. Engl. J. Med.* 376: 209–220.

283. Giovannoni, G., G. Comi, S. Cook, K. Rammohan, P. Rieckmann, P. Soelberg Sørensen, P. Vermersch, P. Chang, A. Hamlett, B. Musch, S. J. Greenberg, and CLARITY Study Group. 2010. A placebo-controlled trial of oral cladribine for relapsing multiple sclerosis. *N. Engl. J. Med.* 362: 416–426.

284. Kappos, L., A. Bar-Or, B. A. C. Cree, R. J. Fox, G. Giovannoni, R. Gold, P. Vermersch, D. L. Arnold, S. Arnould, T. Scherz, C. Wolf, E. Wallström, F. Dahlke, and EXPAND Clinical Investigators. 2018. Siponimod versus placebo in secondary progressive multiple sclerosis (EXPAND): a double-blind, randomised, phase 3 study. *Lancet* 391: 1263–1273.

285. Wilson, E. H., W. Weninger, and C. A. Hunter. 2010. Trafficking of immune cells in the central nervous system. *J. Clin. Invest.* 120: 1368–1379.

286. Engelhardt, B., and R. M. Ransohoff. 2012. Capture, crawl, cross: the T cell code to breach the blood-brain barriers. *Trends Immunol.* 33: 579–589.

287. Kivisäkk, P., B. Tucky, T. Wei, J. J. Campbell, and R. M. Ransohoff. 2006. Human cerebrospinal fluid contains CD4+ memory T cells expressing gut- or skin-specific trafficking determinants: relevance for immunotherapy. *BMC Immunol.* 7: 14.

288. Abbott, N. J., A. A. K. Patabendige, D. E. M. Dolman, S. R. Yusof, and D. J. Begley. 2010. Structure and function of the blood-brain barrier. *Neurobiol. Dis.* 37: 13–25.

289. Du, F., A. V. Garg, K. Kosar, S. Majumder, D. G. Kugler, G. H. Mir, M. Maggio, M. Henkel, A. Lacy-Hulbert, and M. J. McGeachy. 2016. Inflammatory Th17 Cells Express Integrin αvβ3 for Pathogenic Function. *Cell Rep.* 16: 1339–1351.

290. Barkalow, F. J., M. J. Goodman, M. E. Gerritsen, and T. N. Mayadas. 1996. Brain endothelium lack one of two pathways of P-selectin-mediated neutrophil adhesion. *Blood* 88: 4585–4593.

291. Hickey, W. F. 1991. Migration of hematogenous cells through the blood-brain barrier and the initiation of CNS inflammation. *Brain Pathol.* 1: 97–105.

292. Agrawal, S., P. Anderson, M. Durbeej, N. van Rooijen, F. Ivars, G. Opdenakker, and L. M. Sorokin. 2006. Dystroglycan is selectively cleaved at the parenchymal basement membrane at sites of leukocyte extravasation in experimental autoimmune encephalomyelitis. *J. Exp. Med.* 203: 1007–1019.

293. Babaloo, Z., M. R. Aliparasti, F. Babaiea, S. Almasi, B. Baradaran, and M. Farhoudi. 2015. The role of Th17 cells in patients with relapsing-remitting multiple sclerosis: interleukin-17A and interleukin-17F serum levels. *Immunol. Lett.* 164: 76–80.

294. Kebir, H., K. Kreymborg, I. Ifergan, A. Dodelet-Devillers, R. Cayrol, M. Bernard, F. Giuliani, N. Arbour, B. Becher, and A. Prat. 2007. Human TH17 lymphocytes promote blood-brain barrier disruption and central nervous system inflammation. *Nat. Med.* 13: 1173–1175.

295. Hu, Y., N. Ota, I. Peng, C. J. Refino, D. M. Danilenko, P. Caplazi, and W. Ouyang. 2010. IL-17RC is required for IL-17A- and IL-17F-dependent signaling and the pathogenesis of experimental autoimmune encephalomyelitis. *J. Immunol.* 184: 4307–4316.

296. Schraml, B. U., K. Hildner, W. Ise, W.-L. Lee, W. A.-E. Smith, B. Solomon, G. Sahota, J. Sim, R. Mukasa, S. Cemerski, R. D. Hatton, G. D. Stormo, C. T. Weaver, J. H. Russell, T. L. Murphy, and K. M. Murphy. 2009. The AP-1 transcription factor Batf controls T(H)17 differentiation. *Nature* 460: 405–409.

297. Carr, T. M., J. D. Wheaton, G. M. Houtz, and M. Ciofani. 2017. JunB promotes Th17 cell identity and restrains alternative CD4+ T-cell programs during inflammation. *Nat. Commun.* 8: 301.

298. Haak, S., A. L. Croxford, K. Kreymborg, F. L. Heppner, S. Pouly, B. Becher, and A. Waisman. 2009. IL-17A and IL-17F do not contribute vitally to autoimmune neuro-inflammation in mice. *J. Clin. Invest.* 119: 61–69.

299. Komiyama, Y., S. Nakae, T. Matsuki, A. Nambu, H. Ishigame, S. Kakuta, K. Sudo, and Y. Iwakura. 2006. IL-17 plays an important role in the development of experimental autoimmune encephalomyelitis. *J. Immunol.* 177: 566–573.

300. Chu, C. Q., S. Wittmer, and D. K. Dalton. 2000. Failure to suppress the expansion of the activated CD4 T cell population in interferon gamma-deficient mice leads to exacerbation of experimental autoimmune encephalomyelitis. *J. Exp. Med.* 192: 123–128.

301. Ferber, I. A., S. Brocke, C. Taylor-Edwards, W. Ridgway, C. Dinisco, L. Steinman, D. Dalton, and C. G. Fathman. 1996. Mice with a disrupted IFN-gamma gene are susceptible to the induction of experimental autoimmune encephalomyelitis (EAE). *J. Immunol.* 156: 5–7.

302. Sosa, R. A., C. Murphey, R. R. Robinson, and T. G. Forsthuber. 2015. IFN-γ ameliorates autoimmune encephalomyelitis by limiting myelin lipid peroxidation. *Proc. Natl. Acad. Sci. USA* 112: E5038-47.

303. Ponomarev, E. D., L. P. Shriver, K. Maresz, J. Pedras-Vasconcelos, D. Verthelyi, and B. N. Dittel. 2007. GM-CSF production by autoreactive T cells is required for the activation of microglial cells and the onset of experimental autoimmune encephalomyelitis. *J. Immunol.* 178: 39–48.

304. McQualter, J. L., R. Darwiche, C. Ewing, M. Onuki, T. W. Kay, J. A. Hamilton, H. H. Reid, and C. C. Bernard. 2001. Granulocyte macrophage colony-stimulating factor: a new putative therapeutic target in multiple sclerosis. *J. Exp. Med.* 194: 873–882.

305. Sutton, C., C. Brereton, B. Keogh, K. H. G. Mills, and E. C. Lavelle. 2006. A crucial role for interleukin (IL)-1 in the induction of IL-17-producing T cells that mediate autoimmune encephalomyelitis. *J. Exp. Med.* 203: 1685–1691.

306. Lévesque, S. A., A. Paré, B. Mailhot, V. Bellver-Landete, H. Kébir, M.-A. Lécuyer, J. I. Alvarez, A. Prat, J. P. de Rivero Vaccari, R. W. Keane, and S. Lacroix. 2016. Myeloid cell transmigration across the CNS vasculature triggers IL-1β-driven neuroinflammation during autoimmune encephalomyelitis in mice. *J. Exp. Med.* 213: 929–949.

307. Langrish, C. L., Y. Chen, W. M. Blumenschein, J. Mattson, B. Basham, J. D. Sedgwick, T. McClanahan, R. A. Kastelein, and D. J. Cua. 2005. IL-23 drives a pathogenic T cell population that induces autoimmune inflammation. *J. Exp. Med.* 201: 233–240.

308. Codarri, L., G. Gyülvészi, V. Tosevski, L. Hesske, A. Fontana, L. Magnenat, T. Suter, and B. Becher. 2011. RORγt drives production of the cytokine GM-CSF in helper T cells, which is essential for the effector phase of autoimmune neuroinflammation. *Nat. Immunol.* 12: 560–567.

309. Cosorich, I., G. Dalla-Costa, C. Sorini, R. Ferrarese, M. J. Messina, J. Dolpady, E. Radice, A. Mariani, P. A. Testoni, F. Canducci, G. Comi, V. Martinelli, and M. Falcone. 2017. High frequency of intestinal TH17 cells correlates with microbiota alterations and disease activity in multiple sclerosis. *Sci. Adv.* 3: e1700492.

310. van den Hoogen, W. J., J. D. Laman, and B. A. 't Hart. 2017. Modulation of multiple sclerosis and its animal model experimental autoimmune encephalomyelitis by food and gut microbiota. *Front. Immunol.* 8: 1081.

311. Ochoa-Repáraz, J., D. W. Mielcarz, L. E. Ditrio, A. R. Burroughs, D. M. Foureau, S. Haque-Begum, and L. H. Kasper. 2009. Role of gut commensal microflora in the development of experimental autoimmune encephalomyelitis. *J. Immunol.* 183: 6041–6050.

312. Yokote, H., S. Miyake, J. L. Croxford, S. Oki, H. Mizusawa, and T. Yamamura. 2008. NKT cell-dependent amelioration of a mouse model of multiple sclerosis by altering gut flora. *Am. J. Pathol.* 173: 1714–1723.

313. Lee, Y. K., J. S. Menezes, Y. Umesaki, and S. K. Mazmanian. 2011. Proinflammatory T-cell responses to gut microbiota promote experimental autoimmune encephalomyelitis. *Proc. Natl. Acad. Sci. USA* 108 Suppl 1: 4615–4622.

314. Koh, A., F. De Vadder, P. Kovatcheva-Datchary, and F. Bäckhed. 2016. From Dietary Fiber to Host Physiology: Short-Chain Fatty Acids as Key Bacterial Metabolites. *Cell* 165: 1332–1345.

315. Singh, N., A. Gurav, S. Sivaprakasam, E. Brady, R. Padia, H. Shi, M. Thangaraju, P. D. Prasad, S. Manicassamy, D. H. Munn, J. R. Lee, S. Offermanns, and V. Ganapathy. 2014. Activation of Gpr109a, receptor for niacin and the commensal metabolite butyrate, suppresses colonic inflammation and carcinogenesis. *Immunity* 40: 128–139.

316. Haghikia, A., S. Jörg, A. Duscha, J. Berg, A. Manzel, A. Waschbisch, A. Hammer, D.-H. Lee, C. May, N. Wilck, A. Balogh, A. I. Ostermann, N. H. Schebb, D. A. Akkad, D. A. Grohme, M. Kleinewietfeld, S. Kempa, J. Thöne, S. Demir, D. N. Müller, R. Gold, and R. A. Linker. 2015. Dietary fatty acids directly impact central nervous system autoimmunity via the small intestine. *Immunity* 43: 817–829.

317. Haghikia, A., A. Duscha, J. Berg, S. Jörg, N. Wilck, D. Müller, R. Linker, and R. Gold. 2016. Role of Fatty Acids in Multipe Sclerosis: Therapeutic Potential of Propionic Acid (P1.374). *Neurology* .

318. Reynolds, J. M., G. J. Martinez, Y. Chung, and C. Dong. 2012. Toll-like receptor 4 signaling in T cells promotes autoimmune inflammation. *Proc. Natl. Acad. Sci. USA* 109: 13064–13069.

319. Miranda-Hernandez, S., N. Gerlach, J. M. Fletcher, E. Biros, M. Mack, H. Körner, and A. G. Baxter. 2011. Role for MyD88, TLR2 and TLR9 but not TLR1, TLR4 or TLR6 in experimental autoimmune encephalomyelitis. *J. Immunol.* 187: 791–804.

320. Kleinschek, M. A., A. M. Owyang, B. Joyce-Shaikh, C. L. Langrish, Y. Chen, D. M. Gorman, W. M. Blumenschein, T. McClanahan, F. Brombacher, S. D. Hurst, R. A. Kastelein, and D. J. Cua. 2007. IL-25 regulates Th17 function in autoimmune inflammation. *J. Exp. Med.* 204: 161–170.

321. Benny Klimek, M. E., A. Sali, S. Rayavarapu, J. H. Van der Meulen, and K. Nagaraju. 2016. Effect of the IL-1 Receptor Antagonist Kineret® on Disease Phenotype in mdx Mice. *PLoS One* 11: e0155944.

322. Esplugues, E., S. Huber, N. Gagliani, A. E. Hauser, T. Town, Y. Y. Wan, W. O'Connor, A. Rongvaux, N. Van Rooijen, A. M. Haberman, Y. Iwakura, V. K. Kuchroo, J. K. Kolls, J. A. Bluestone, K. C. Herold, and R. A. Flavell. 2011. Control of TH17 cells occurs in the small intestine. *Nature* 475: 514–518.

323. Omenetti, S., C. Bussi, A. Metidji, A. Iseppon, S. Lee, M. Tolaini, Y. Li, G. Kelly, P. Chakravarty, S. Shoaie, M. G. Gutierrez, and B. Stockinger. 2019. The Intestine Harbors Functionally Distinct Homeostatic Tissue-Resident and Inflammatory Th17 Cells. *Immunity* 51: 77–89.e6.

324. Lee, H.-G., J.-U. Lee, D.-H. Kim, S. Lim, I. Kang, and J.-M. Choi. 2019. Pathogenic function of bystander-activated memory-like CD4+ T cells in autoimmune encephalomyelitis. *Nat. Commun.* 10: 709.

325. Jones, R. E., T. Kay, T. Keller, and D. Bourdette. 2003. Nonmyelin-specific T cells accelerate development of central nervous system APC and increase susceptibility to experimental autoimmune encephalomyelitis. *J. Immunol.* 170: 831–837.

326. Korn, T., J. Reddy, W. Gao, E. Bettelli, A. Awasthi, T. R. Petersen, B. T. Bäckström, R. A. Sobel, K. W. Wucherpfennig, T. B. Strom, M. Oukka, and V. K. Kuchroo. 2007. Myelin-specific regulatory T cells accumulate in the CNS but fail to control autoimmune inflammation. *Nat. Med.* 13: 423–431.

327. Jäger, A., V. Dardalhon, R. A. Sobel, E. Bettelli, and V. K. Kuchroo. 2009. Th1, Th17, and Th9 effector cells induce experimental autoimmune encephalomyelitis with different pathological phenotypes. *J. Immunol.* 183: 7169–7177.

328. Croxford, A. L., M. Lanzinger, F. J. Hartmann, B. Schreiner, F. Mair, P. Pelczar, B. E. Clausen, S. Jung, M. Greter, and B. Becher. 2015. The Cytokine GM-CSF Drives the Inflammatory Signature of CCR2+ Monocytes and Licenses Autoimmunity. *Immunity* 43: 502–514.

329. Kreutzberg, G. W. 1996. Microglia: a sensor for pathological events in the CNS. *Trends Neurosci.* 19: 312–318.

330. Kara, E. E., D. R. McKenzie, C. R. Bastow, C. E. Gregor, K. A. Fenix, A. D. Ogunniyi, J. C. Paton, M. Mack, D. R. Pombal, C. Seillet, B. Dubois, A. Liston, K. P. A. MacDonald, G. T. Belz, M. J. Smyth, G. R. Hill, I. Comerford, and S. R. McColl. 2015. CCR2 defines in vivo development and homing of IL-23-driven GM-CSF-producing Th17 cells. *Nat. Commun.* 6: 8644.

331. Rothhammer, V., D. M. Borucki, E. C. Tjon, M. C. Takenaka, C.-C. Chao, A. Ardura-Fabregat, K. A. de Lima, C. Gutiérrez-Vázquez, P. Hewson, O. Staszewski, M. Blain, L. Healy, T. Neziraj, M. Borio, M. Wheeler, L. L. Dragin, D. A. Laplaud, J. Antel, J. I. Alvarez, M. Prinz, and F. J. Quintana. 2018. Microglial control of astrocytes in response to microbial metabolites. *Nature* 557: 724–728.

332. Smith, P. M., M. R. Howitt, N. Panikov, M. Michaud, C. A. Gallini, M. Bohlooly-Y, J. N. Glickman, and W. S. Garrett. 2013. The microbial metabolites, short-chain fatty acids, regulate colonic Treg cell homeostasis. *Science* 341: 569–573.

333. McAleer, J., N. Nguyen, K. Chen, P. Kumar, D. Ricks, M. Binnie, R. Armentrout, D. Pociask, A. Hein, A. Yu, A. Vikram, K. Bibby, Y. Umesaki, A. Rivera, D. Sheppard, W. Ouyang, L. Hooper, and J. Kolls. Pulmonary Th17 fungal immunity is regulated by Regenerating islet-derived III-gamma and the gut microbiome. .

334. Gallo, R. L., and L. V. Hooper. 2012. Epithelial antimicrobial defence of the skin and intestine. *Nat. Rev. Immunol.* 12: 503–516.

335. Losy, J., and A. Niezgoda. 2001. IL-18 in patients with multiple sclerosis. *Acta Neurol. Scand.* 104: 171–173.

336. Gutcher, I., E. Urich, K. Wolter, M. Prinz, and B. Becher. 2006. Interleukin 18-independent engagement of interleukin 18 receptor-alpha is required for autoimmune inflammation. *Nat. Immunol.* 7: 946–953.

337. Conti, H. R., and S. L. Gaffen. 2015. IL-17-Mediated Immunity to the Opportunistic Fungal Pathogen Candida albicans. *J. Immunol.* 195: 780–788.

338. Marta, M., A. Andersson, M. Isaksson, O. Kämpe, and A. Lobell. 2008. Unexpected regulatory roles of TLR4 and TLR9 in experimental autoimmune encephalomyelitis. *Eur. J. Immunol.* 38: 565–575.

339. Paradis, A., S. Bernier, and N. Dumais. 2016. TLR4 induces CCR7-dependent monocytes transmigration through the blood-brain barrier. *J. Neuroimmunol.* 295–296: 12–17.

340. Maslowski, K. M., and C. R. Mackay. 2011. Diet, gut microbiota and immune responses. *Nat. Immunol.* 12: 5–9.

341. Dang, A. T., and B. J. Marsland. 2019. Microbes, metabolites, and the gut-lung axis. *Mucosal Immunol.* 12: 843–850.

342. van de Kerkhof, P. C. M., C. E. M. Griffiths, K. Reich, C. L. Leonardi, A. Blauvelt, T.-F. Tsai, Y. Gong, J. Huang, C. Papavassilis, and T. Fox. 2016. Secukinumab long-term safety experience: A pooled analysis of 10 phase II and III clinical studies in patients with moderate to severe plaque psoriasis. *J. Am. Acad. Dermatol.* 75: 83–98.e4.